



JACOBS
UNIVERSITY

**Organic matter and meiobenthos in submarine canyons of the
Iberian continental margin**

by

Rosa García Novoa

A thesis submitted in partial fulfilment
of the requirements for the degree of
Doctor of Philosophy

Approved, Thesis Committee

Prof. Laurenz Thomsen

Prof. Antje Boetius

Prof. Jelle Bijma

Dr. Dick Van Oevelen

July 2007

School of Engineering and Science

A mi gente

Todo pasa y todo queda,
pero lo nuestro es pasar,
pasar haciendo caminos,
caminos sobre el mar.

Nunca perseguí la gloria,
ni dejar en la memoria
de los hombres mi canción;
yo amo los mundos sutiles,
ingrávidos y gentiles,
como pompas de jabón.

Me gusta verlos pintarse
de sol y grana, volar
bajo el cielo azul, temblar
súbitamente y quebrarse...

Nunca perseguí la gloria.

Caminante, son tus huellas
el camino y nada más;
caminante, no hay camino,
se hace camino al andar.

Al andar se hace camino
y al volver la vista atrás
se ve la senda que nunca
se ha de volver a pisar.

Caminante no hay camino
sino estelas en la mar...

Hace algún tiempo en ese lugar
donde hoy los bosques se visten de espinos
se oyó la voz de un poeta gritar
"Caminante no hay camino,
se hace camino al andar..."

Golpe a golpe, verso a verso...

Murió el poeta lejos del hogar.
Le cubre el polvo de un país vecino.
Al alejarse le vieron llorar.
"Caminante no hay camino,
se hace camino al andar..."

Golpe a golpe, verso a verso...

Cuando el jilguero no puede cantar.
Cuando el poeta es un peregrino,
cuando de nada nos sirve rezar.
"Caminante no hay camino,
se hace camino al andar..."

Golpe a golpe, verso a verso.

Cantares,
Antonio Machado (1875-1939)

SUMMARY

This thesis aimed to investigate the sedimentary organic matter contents and diagenetic characteristics, as well as the composition of the meiofaunal assemblages in submarine canyons in comparison to adjacent open slopes. Moreover, two submarine canyons with oceanographically different regimes and their respective adjacent open slopes were compared in terms of the organic matter contents, diagenetic characteristics, deposition and bioturbation rates. Most of the studies on submarine canyons from the Iberian continental margin have addressed the geology, the physical oceanography and sedimentological processes from the canyons and surrounding areas, in order to investigate their role as transport mechanisms of sedimentary material from coastal regions to the deep ocean. Seldom and scattered studies have addressed biological and ecological processes in these environments. This thesis adds new information on the organic matter availability in two submarine canyons from the Iberian continental margin. It describes the meiofaunal composition of one of these canyons, and the ecological drivers of the meiofauna community. In addition, this study explains the influence of oceanographically different conditions in determining different sedimentary biogeochemical characteristics in two submarine canyons.

Chapter 1 gives a scientific framework to this thesis, sets the objectives and hypothesis to be tested, introduces the study area and describes the general methodology.

Chapter 2 describes the distribution of metazoan meiofauna and foraminiferal abundances, nematode biomass and nematode community structure along a depth gradient in the Nazaré canyon and adjacent slope in relation to the availability of the organic matter. Organic matter contents in the Nazaré canyon sediments were higher than on the adjacent slope

Summary

sediments, and the phytodetritus was fresher. Meiofauna appeared positively correlated to the phytodetritus content and freshness. However, despite the organic matter being more available in the canyon than on the adjacent open slope, the abundance of polychaetes, copepods, bivalves, nematodes, total metazoans, and nematode biomass were not always higher in the canyon. In some stations in the upper and middle canyon areas lower metazoan abundances occurred, and the numbers of living benthic foraminifers were minute. The reduced diversity and evenness of the nematode assemblages, and high K-dominance in this part of the canyon indicated high levels of environmental disturbance. Further, opportunistic non-selective deposit-feeding nematodes dominated. Altogether, it indicated that only few opportunistic species were able to survive in the upper and middle canyon areas.

Chapter 3 describes the spatial distribution of bioavailable organic matter in surface sediments along and across the Nazaré canyon, in comparison to the adjacent open slope. Furthermore, the passive biodeposition of fresh suspended particulate organic matter is assessed under strong bottom current conditions. The concentration of chlorophyll *a* (chl *a*), phaeopigments (phaeo), chloroplastic pigment equivalents (CPE) and total hydrolysable amino acids (THAA) decreased with increasing water depth, and were in general higher within the canyon (specially in the upper regions) than on the open slope. The concentrations were low on the canyon walls, increasing towards the canyon axis. The lability of the phytodetritus and bioavailable organic matter, as indicated by the chl *a*:phaeo ratio, degradation index (DI), asp:β-ala and glu:γ-aba ratios, was highest in the upper canyon with deeper canyon regions and the slope sharing similar low labilities. Across the canyon, the organic matter lability was similar. THAA:OM and chl *a*:OM ratios indicated that the quality of the bulk organic matter in the canyon and slope was similar, with lability decreasing with water depth. Bioavailable organic matter accumulates in the upper canyon regions, and its quality is diluted with refractory material from deeper regions transported by the flood tides. Ebb tides transport the upper canyon organic matter down canyon,

where it is dispersed across a bigger area under a more refractory state. Flume experiments demonstrate that arborescent foraminifera and polychaete pellet mounds, as found in the head of the canyon, enhance the deposition of phytodetritys under critical shear velocities.

Chapter 4 compares the Nazaré canyon and adjacent open slope in the Western Iberian Margin with the Cap de Creus canyon and respective adjacent open slope in the Gulf of Lions, in terms of several biogeochemical sedimentary characteristics. A novel approach was used, modelling chl *a* and ²¹⁰Pb sediment profiles simultaneously in a diagenetic model to estimate bioturbation rates, chl *a* and ²¹⁰Pb depositions and background concentrations. In addition, the model shows that the chl *a* decay rate as given by Sun et al. (1993) can be widely used. Both canyons and respective adjacent slopes differed in terms of biogeochemical sedimentary characteristics. The Gulf of Lion study area appeared to be less active in terms of depositions of organic matter and burial than the Western Iberian Margin. Corg and chl *a* contents, and chl *a* and ²¹⁰Pb background concentration were very low in the Cap de Creus canyon and adjacent slope, and elevated in the Nazaré canyon and slope sediments. Bioturbation rates were lower in the Gulf of Lions. Both canyons also showed different organic matter accumulation patterns. The biogeochemical characteristics in the Nazaré canyon indicated high rates of accumulation and burial of organic matter, while in the Cap de Creus they indicated low rates. These differences were attributed to the oceanographically different conditions prevailing in the Western Iberian Margin and Gulf of Lions.

Chapter 5 sums up the main conclusions of this thesis and present some perspectives.

The results here presented show that submarine canyons are complex ecosystems that function differently depending on the oceanography of the surrounding area. For instance, the Nazaré canyon in the Western Iberian Margin (Atlantic) accumulates and buries high amounts of organic matter. In contrast, the Cap de Creus in the Gulf of Lions (Mediterranean) do not. Furthermore, the refractory characteristics of the phytodetritus and

Summary

bioavailable organic matter can be higher in canyons, but not everywhere. The lability of the bulk organic matter in surface sediments of the Nazaré canyon is similar to that found on the open slope surface sediments. The meiofauna abundance distribution in the Nazaré canyon is patchy, and the assemblages show opportunistic characteristics, such as low diversity, high dominance and deposit feeding. This indicates that benthic communities in such environment may be in constant early stages of the recolonization process, due to the frequent disturbance of the sedimentary habitat.

ACKNOWLEDGEMENTS

This PhD work was supported by EUROSTRATAFORM project, EC contract EVK3-CT-2002-00079 funded by the European Commission, DG-XII, and the HERMES project, EC contract OCE-CT-2005-511234 funded by the European Commission's Sixth Framework Programme under the priority Sustainable Development, Global Change and Ecosystems. The Royal Netherlands Institute for Sea Research (NIOZ) provided ship time on RV 'Pelagia'.

First of all, I would like to thank my advisor Prof. Laurenz Thomsen for supporting my PhD studies at International University Bremen (IUB), and giving me the opportunity to work under the framework of EU funded programmes. It has been an instructive experience from which I have learnt a lot about science and its community. I would also like to thank my other thesis committee members at IUB, Prof. Antje Boetious and Prof. Jelle Bijma, for giving good advices during the preparation of the PhD proposal defence. I would like to thank my colleagues Torsten Behnke, Thomas Viergutz, Volker Karpen and Annika Moje whose efforts to solve the day-to-day technical problems in the OceanLab facilitated the work enormously, and Pedro Mendes for showing the work with Gust chambers. I'm very happy of the fresh girly atmosphere that Annika together with Jule Mawick and Daniella Meissner brought when they joined the geochemistry lab.

The MarMic research school from the Max Planck Institute for Marine Microbiology has contributed to my background skills with very interesting workshops and seminars.

This thesis wouldn't have been possible without the help, advice and encouragement of many people I have met on the way. The identification of nematodes to genus level was possible thanks to the microscopy room of Prof. Alexander Lerchl at IUB. The nematode biomass analysis was possible thanks

Acknowledgements

to the semiautomatic images system (analySIS®2.1) of the Deep Sea group at the Alfred Wegener Institute (AWI). Dr. Christiane Hasemann instructed me on the biomass analysis and shared nice tricks on nematode slides preparation. Dr. Karen von Juterzenka, Dr. Michael Klages and Dr. Thomas Soltwedel gave very useful advices before the starting of my first sampling trip. The amino acids extraction technique shared by Prof. Jack Middleburg and his student Sandra Vandewiele from Netherlands Institute of Ecology (NIOO-KNAW) was a great starting point for the work I did together with Annika, our chemical technician, on a later stage of my PhD. Sandra was very patient with my questions on amino acids extraction and HPLC. The successful calibration of the benthic flume at the OceanLab was possible thanks to the directions, guidelines and very comprehensive answers to my never ending questions provided by Dr. Luca van Duren from NIOO-KNAW and Dr. Michael Friedrichs from University of Rostock. The modelling work was possible thanks to the expertise provided by Dr. Karline Soetaert and Dr. Dick van Oevelen from NIOO-KNAW. They have been modelling gurus and I have learnt a lot from both of them over the period of time we have worked together. Karoliina Koho and Dr. Tanja Kouwenhoven from University of Utrecht have been a great deck working team in the two cruises we did together, and good critics of my first manuscript. Finally, Dr. Henko de Stigter and Dr. Eric Epping from NIOZ were always supportive and encouraging references. Henko's expertise in submarine canyons has been precious over the length of my work. Eric's comments on my research proposal encouraged me a lot during a difficult time. Further, he facilitated we conduct an in situ lander experiment on high and low quality carbon labelling. In the end, the lander didn't work on the canyon soupy sediments; otherwise I'm sure this thesis would have had an extra interesting chapter. In any case, I learned a lot of new things and had a good time. Henko and Eric's constructive critics have helped a lot to improve my work.

TABLE OF CONTENTS

SUMMARY	I
ACKNOWLEDGEMENTS.....	V
TABLE OF CONTENTS.....	VII
CHAPTER 1	1
GENERAL INTRODUCTION.....	1
<i>Organic matter and meiobenthos in submarine canyons of the Iberian continental margin</i>	<i>1</i>
<i>Study areas.....</i>	<i>6</i>
<i>Material and Methods.....</i>	<i>9</i>
Sampling	9
Considerations when determining organic matter availability for benthic fauna	11
<i>Literature cited.....</i>	<i>13</i>
CHAPTER 2	21
DISTRIBUTION OF MEIOBENTHOS IN THE NAZARÉ CANYON AND ADJACENT SLOPE (WESTERN IBERIAN MARGIN) IN RELATION TO SEDIMENTARY COMPOSITION	21
<i>Abstract.....</i>	<i>21</i>
<i>Introduction.....</i>	<i>22</i>
<i>Material and Methods.....</i>	<i>24</i>
Study area.....	24
Sampling	25
Grain-size analysis	26
Geochemical analysis.....	26
Meiofauna analysis	26
Data analysis	27
<i>Results</i>	<i>28</i>
Sediment granulometry	28
Geochemical characteristics of sediments	28
Meiofauna	30
Foraminifera.....	31
Metazoans	33
Nematode assemblage.....	36

Table of contents

Relationships between benthic meiofauna and geochemical parameters	41
<i>Discussion</i>	41
Meiofauna and organic matter levels	41
Distribution of meiofauna abundance and biomass	44
Nematode community structure	46
Conclusions	47
<i>Acknowledgements</i>	47
<i>Literature cited</i>	48
CHAPTER 3	53
BIOAVAILABLE ORGANIC MATTER IN SURFACE SEDIMENTS OF THE NAZARÉ CANYON AND ADJACENT SLOPE (WESTERN IBERIAN MARGIN).....	53
<i>Abstract</i>	53
<i>Introduction</i>	54
<i>Study area</i>	56
<i>Material and methods</i>	57
Sampling	57
Phytopigment analysis	58
Amino acid analysis	59
Statistical analysis	60
Flume experiments	60
<i>Results</i>	63
Phytopigments in surface sediments and amino acids in sediment aggregates.....	63
Lability of organic matter in surface sediments and sediment aggregates	66
Biodeposition of algae aggregates	69
<i>Discussion</i>	71
Organic matter and lability patterns	71
Biodeposition in the Nazaré canyon	74
Conclusions	75
<i>Acknowledgements</i>	76
<i>Literature cited</i>	76
CHAPTER 4	81
ORGANIC CONTENT, BIOTURBATION AND DEPOSITION RATES IN TWO CONTRASTING SUBMARINE CANYONS.....	81
<i>Abstract</i>	81
<i>Introduction</i>	82
<i>Study areas</i>	84
<i>Material and methods</i>	86
Sampling	86
Chlorophyll <i>a</i> and phaeopigment analysis	88

Organic carbon and nitrogen analysis	88
²¹⁰ Pb analysis	88
Sediment porosity	89
Diagenetic model	89
Model comparison and uncertainty analysis	92
Model solving and fitting	94
<i>Results</i>	95
Sediment composition	95
Model output	96
Bioturbation, chl a and ²¹⁰ Pb deposition rates, background concentrations and decay rates	104
<i>Discussion</i>	105
Model results	105
Patterns in the biogeochemical parameters	108
Conclusions	111
<i>Acknowledgements</i>	111
<i>Literature cited</i>	112
CHAPTER 5	119
CONCLUSIONS AND REMARKS	119
<i>Organic matter and meiobenthos in submarine canyons of the Iberian continental margin</i>	119
The Nazaré submarine canyon	120
Different oceanography and sedimentary biogeochemical characteristics in the Nazaré and Cap de Creus submarine canyons ..	122
<i>Perspectives</i>	123
APPENDIX I	125
OCEANLAB FLUME CALIBRATION	125
<i>OceanLab flume characteristics</i>	125
<i>Hydraulic calibration test</i>	127
Relation between belt motor settings and resulting flow speed	127
The response time to speed changes	128
Velocity profiles	129
Sidewalls effect	135
<i>Literature cited</i>	136
APPENDIX II	139
DEGRADATION INDEX CALCULATION	139
<i>Literature cited</i>	141

CHAPTER 1

General introduction

ORGANIC MATTER AND MEIOBENTHOS IN SUBMARINE CANYONS OF THE IBERIAN CONTINENTAL MARGIN

The particulate organic matter produced in the euphotic zone, when it finally settles on the sea floor, constitutes an important food source for deep-sea benthic communities (Gage & Tyler 1991). Particulate organic matter reaches the sea floor more or less transformed due to diagenetic processes occurring in the water column during transport. The amount and diagenetic characteristics of the organic matter that settles seem an important factor controlling benthic fauna in terms of abundance, biomass, diversity, and structuring the trophic composition of benthic communities (e.g. Pearson & Rosenberg 1978, Dauwe & Middelburg 1998, Flach & Thomsen 1998, Albertelli et al. 1999, Cartes et al. 2002, Flach et al. 2002, Grémare et al. 2002). The quantification of particulate organic matter and the organic matter diagenetic characteristics in continental margins is necessary to better understand patterns in benthic communities and ecosystem functioning.

Over the past 10-20 years, the understanding of the particulate matter transport from the shelves to the abyssal plains has been the core subject of several multidisciplinary programmes. In the Middle Atlantic Bight, the SEEP I experiment yielded indications of organic matter deposition on low energy slope areas (Biscaye et al. 1988); and the SEEP II experiment showed that only

a small proportion (<5%) of organic matter from the shelf was exported to the adjacent slopes, the rest being recycled by consumption on the shelf areas (Biscaye et al. 1994). The SEEP II experiment, and the OMEX I and II programmes in the Goban Spur and Iberian Margin gave evidence of off shelf organic matter transport to depths of 1000-2000 m (Biscaye et al. 1994, Van Weering et al. 1998, Van Weering & McCave 2002), although no clear depocentres with high carbon content were found. Studies on benthic faunal community of the Goban Spur showed that the benthic fauna species composition, abundance and biomass decreased with water depth and distance from shore, which was generally correlated to a decrease in the food availability (Flach & Thomsen 1998, Heip et al. 2001). Further, these studies indicated that the benthic fauna feeding strategies could give an indication of the quantity and quality of organic matter arriving at the sea floor, as well as of the flow conditions (Flach et al. 1998, Flach & Thomsen 1998, Flach et al. 2002). Thomsen & Gust (2000) revealed a two-layer sediment surface with the aggregate layer probably being transported through canyons on a regular basis. Thomsen (2002) postulated that the potential fast downslope mechanism transporting fresh phytodetritus to benthic communities in deep sea would thus be via canyons, but such processes have neither been observed nor searched for along the Iberian continental Margin off Vigo. A study in the Whittard Canyon adjacent to the Goban Spur area yielded indication for local enrichment of the canyon floor in comparison to the Goban Spur open slope, probably due to transport through the canyon (Duineveld et al. 2001). Faunal densities and biomasses in the canyon were found to be higher (Duineveld et al. 2001). OMEX II in the Iberian Margin (Schmidt et al. 2001, Epping et al. 2002, Van Weering et al. 2002) and ECOMARGE in the Gulf of Lions (Monaco et al. 1999, Durieu de Madron et al. 2000) pointed out the importance of submarine canyons as direct transport conduits of organic matter from the shelf to the deep ocean. The Nazaré canyon was identified as an area of higher sedimentary organic carbon content and relatively high biochemical activity since it traps part of the suspended particulate organic matter (Epping et al. 2002). Previous studies in submarine canyons have shown higher faunal densities and biomasses (e.g. Soetaert et al. 1991, Gage et al. 1995, Vetter &

Dayton 1998) and lower faunal diversities (e.g. Gage et al. 1995, Vetter & Dayton 1998) in canyons than in the adjacent abyssal plain, continental shelf or slope. These differences in the fauna communities have been attributed to the higher organic content observed in these systems (Soetaert et al. 1991, Gage et al. 1995, Duineveld et al. 2001). However, there are indications that not always fauna abundances are higher in canyons than adjacent areas (Maurer et al. 1994).

Studying gradients of increasing organic matter concentrations, Pearson & Rosenberg (1978) showed in their succession model that changes on macrofauna abundance, biomass and diversity occurred. Increasing organic matter concentrations produced an increase in macrofauna abundance, a decrease in individual biomass per species and in diversity. Furthermore, at a certain maximum in organic matter concentration, a peak on opportunistic species appeared. This is due to the colonization by r-selected organisms that can thrive in unstable or unpredictable environments (MacArthur & Wilson 1967) such as suboxic sediments in organic rich conditions. r-selected animal communities are characterised by few species of small body size and with short generation time. In stable or predictable environments organisms that predominate are K- selected. K- selected animal communities are typically very constant and close to the maximum the environment can withstand, organisms have the ability to compete successfully for limited resources, are large in body size and have longer generation time. Studies in the North Sea have shown that opportunistic subsurface deposit feeding fauna dominated in areas characterized by high amounts of low quality sedimentary organic matter; while more specialized suspension interface feeding fauna dominated in areas with lower amounts of high quality organic matter (Dauwe et al. 1998). Indeed, the compounds more commonly used to evaluate organic matter quality seem to correlate well with the benthic fauna. Nematode abundance and in some cases total meiofauna have been shown to positively correlated with sedimentary phytopigments, lipids, total hydrolysable amino acids (THAA), enzymatically hydrolysable amino acids (EHAA), organic carbon, nitrogen and sometimes carbohydrates (Albertelli et al. 1999, Grémare

et al. 2002, Riaux-Gobin et al. 2004). Nematode biomass also has been shown to positively correlate with the above parameters in addition to chlorophyll *a* and protein contents (Albertelli et al. 1999, Grémare et al. 2002). However, in some areas faunal abundance and biomass might not correlate with the above parameters (Cartes et al. 2002, Grémare et al. 2002), which indicate that in certain zones, other factors than organic matter quality might take over control on faunal communities at a higher level.

Apart from the amount and diagenetic characteristics of the organic matter reaching the deep sea floor, a complex combination of different factors such as the sediment granulometric characteristics, salinity, temperature, pH, redox potential, oxygen, H₂S, and pollutants also control benthic faunal abundance, biomass, size, species composition and spatial distribution in sediments (Giere 1993). Dissolved organic matter, bacteria, phyto-benthos, zoobenthos competition or predation are also associated with changes in benthic community structure (Giere 1993). Moreover, differences in organic matter supply rate (Flach & Thomsen 1998), or in nutrient richness of adjacent coastal zones (Gage & Tyler 1991, Aller et al. 2002) might be responsible for different faunal densities and biomasses values taken at similar depths in different geographical regions. The flow regime in continental margins also can affect benthic macrofauna communities. Suspension feeders have been shown to be more abundant where high water currents were measured (Flach et al. 1998) and macrofauna mean individual weight were negatively related to increasing flow velocities (Flach & Thomsen 1998). In addition, faunal communities by modifying their environment can exert control over a wide variety of other organism. For instance, high densities of suspension feeders by creating feeding pits, faecal pellets mounds and tube structures can locally change the flow regime and enhance the biodeposition of suspended particles (Jumars & Nowell 1984, Graf & Rosenberg 1997) making organic matter available for other organisms. These particles can be further transported, and eventually buried deep within the sediment by deposit feeding infauna through a process called bioturbation, that has a direct control on sediment biogeochemical reactions (Aller 2001). When trying to understand patterns in

benthic fauna communities in continental margins we have to bear all these processes in mind.

Recently, submarine canyons in continental margins have been identified as major transport systems of sedimentary organic matter from the shelf to the deep ocean (Durrieu de Madron 1994, Heussner et al. 1999, Puig & Palanques 1999, Mullenbach & Nittrouer 2000, Van Weering et al. 2002). The aim of Eurostrataform was to gain a better understanding of how sediment particles are transported from river mouths, across the shallow shelf and through submarine canyons, down to the deep sea. The current European program HERMES has identified submarine canyons as potential hotspots of biodiversity due to its complex hydrography, sedimentology, biogeochemistry and biology. HERMES is an international, interdisciplinary effort that brings together expertise in biodiversity, geology, sedimentology, physical oceanography, microbiology and biogeochemistry so that the generic relationship between biodiversity and ecosystem functioning can be understood.

This thesis is a contribution to the EU Eurostrataform and HERMES programmes with organic matter and meiofauna investigations in submarine canyons. Natural gradients of organic matter contents and diagenetic characteristics are found along down-slope depth gradients. Previous works indicated also interesting differences in organic matter availability in submarine canyons compared to the surrounding slope. Hence, the major objectives of this thesis are: 1) to quantify the particulate organic matter and diagenetic characteristics along a depth gradient in submarine canyon and adjacent open slopes sediments, as well as in cross canyon sections; 2) to characterise meiofaunal assemblages along a depth gradient in submarine canyons and adjacent slopes, as well as in cross canyon sections; 3) to carry out a flume experiment where the biodeposition produced by biogenic benthic structures will be assessed in terms of making phytodetritus available to other benthic fauna; 4) to compare two submarine canyons with oceanographically different conditions in terms of organic matter content, diagenetic characteristics, organic matter deposition and bioturbation.

This will allow testing the following hypotheses:

H1) The organic matter content and diagenetic characteristics are higher in submarine canyons than in the adjacent slopes.

H2) The organic matter content and diagenetic characteristics will decrease along a depth gradient in submarine canyons and adjacent slopes.

H3) The composition of meiofaunal assemblages changes significantly along a depth gradient in canyon ecosystems as well as between canyons and slopes at same depths, because of the differences in organic matter content and diagenetic characteristics.

H4) Benthic biogenic structures in submarine canyons can biodeposit fresh phytodetritus under high bottom flow conditions.

H5) Canyons with oceanographically different conditions will show differences in terms of organic matter content, diagenetic characteristics, organic matter deposition and bioturbation.

STUDY AREAS

This PhD thesis research was carried out in the Nazaré submarine canyon and adjacent slope at the western Iberian margin off Portugal, and in the Cap de Creus canyon and adjacent slope at the Gulf of Lions off Spain (Figure 1).

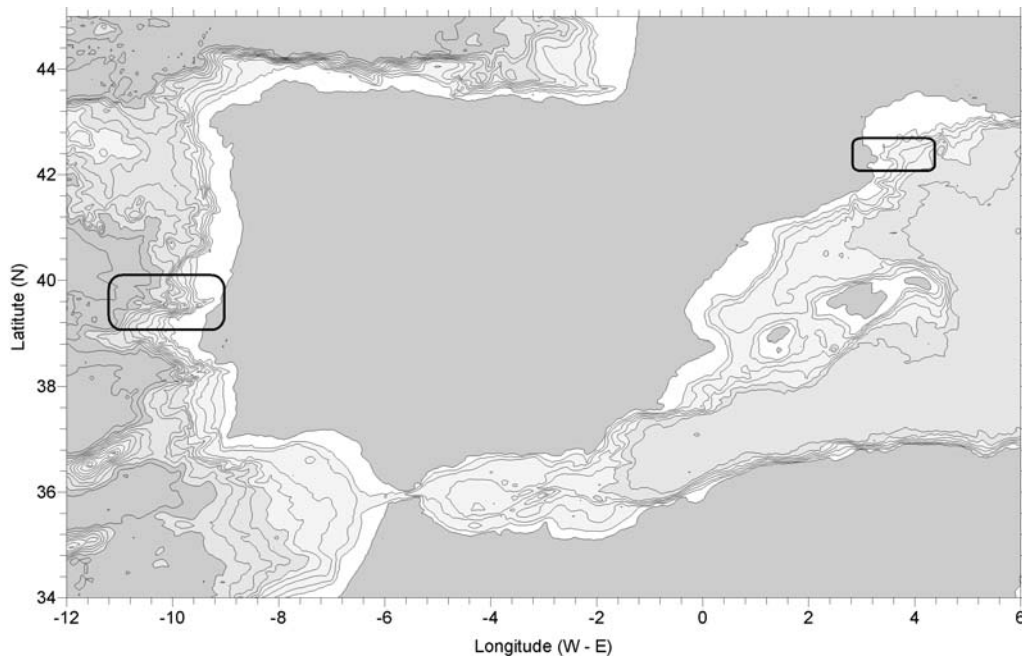


Fig. 1. Map showing the location of the study areas on the Iberian continental margin.

The Western Iberian margin is characterized by a relatively flat shelf ~ 50 km in width, with the shelf break defined by the ~ 200 m isobaths (Fiúza et al. 1998). The slope is steep and dissected by deep gullies and several canyons (Van Weering et al. 2002). The Nazaré canyon is the largest submarine canyon in this margin, and it is centred at $\sim 39^\circ\text{N}$ off Portugal. It intersects the entire continental margin, starting at depths of 50 m and reaching depths of 5000 m. Moreover, the Nazaré canyon is far away from any large river connection and steep cliffs with sparse vegetation characterize the adjacent coastal area. A detailed description of the geomorphology of the canyon has recently been updated by De Stigter et al. (2007). Summarizing, the Nazaré canyon can be divided in three main sections: a) the upper part of the canyon characterized by a sharp V-shaped valley deeply incised into the shelf and steep upper slope, which begins at ~ 50 m depths and descends to ~ 2700 m depth over a length of 70 km measured along the thalweg, b) the middle part of the canyon is a broad meandering valley, with terraced slopes and V-shaped valley axial channel. It is incised into the middle slope and descends from ~ 2700 m to ~ 4000 m depth over 50 km, c) the lower canyon is a flat floored valley incised into the lower continental slope. It very gently

descends from ~ 4000 m to ~ 5000 m depth over 100 km. While descending, the valley gradually increases in width from 3 km to 15 km at the mouth of the canyon. The mineralogical characteristics of the canyon floor and adjacent shelf have been recently described by Oliveira et al. (*in press*). Previous works have shown a strong signal of terrigenous sedimentary material in the canyon sediments (Epping et al. 2002, Van Weering et al. 2002).

The hydrography of the Iberian margin was characterized by Mazé et al. (1997) and Fiúza et al. (1998), which identified five main different water masses in an area between 40° to 41°N and 9°W to 11°W, above the Nazaré canyon study area. The North Atlantic Central Water (NACW) extends between a subsurface salinity maximum at depths ~ 100 m and a salinity minimum at water depths ~ 500 to 600 m. Bellow the NACW, the upper core and lower core of the Mediterranean Water (MW_U and MW_L) can be identified from ~ 600 to 1500 m by the strong thermohaline maximum. Bellow the MW various stages of mixing of the MW with the underlying North Atlantic Deep Water (NADW) can be identified, also known as Deep Intermediate Water (DIW). The NADW is characterized by very low temperatures (~ 2.5 °C) reaching ~ 5000 m water depths. Mazé et al. (1997) and Fiúza et al. (1998) described a northwards surface current reaching down to 250 m and transporting NACW, and a northward deeper current constituted by MW contouring the Portuguese continental slope. The shelf is dominated by a poleward current in winter and an equatorward current during summer that favour downwelling and coastal upwelling respectively (Vitorino et al. 2002).

The Gulf of Lions is characterized by a flat wide shelf that reaches ~ 70 km width (Berné et al. 2004) and narrows westwards to few kilometres close to the Cap de Creus canyon. The shelf break is situated at about 130 m depth and has a complex bathymetry due to the presence of an intricate network of submarine canyons that dissect the continental slope reaching depths of up to ~ 2500 m (Berné et al. 2004). The Gulf of Lions is influenced by the discharged of several rivers, being the Rhône River the larger one. The Cap de Creus canyon is located in the western part of the Gulf of Lions. It cuts the

shelf break at ~ 130 m reaching depths of ~ 2000 m. The canyon has been divided in four main geomorphologic regions (Degeest 2005): a) canyon head down to ~400 m characterized by coarse sands overlying consolidated muds, b) thalweg (excluding the canyon head) characterized by unconsolidated muds overlying coarser material, c) a southern flank characterized by coarse sands, gravel or consolidated muds and a field of giant furrows, and d) a steep northern flank characterized by higher accumulation than the southern flank.

The hydrography of the Gulf of Lions was described by Font (1987) and Millot (1987, 1990), and is characterized by three water masses: the water of Atlantic origin on the surface, the Levantine Intermediate Water (LIW) and the Deep Western Mediterranean Water (DWMW). Millot (1987, 1990) proposes three major water masses flow: the Liguro-Provençal current or Northern current formed by surface water of Atlantic origin that flows southwestwards following the continental slope, an intermediate depth LIW buoyancy flow mainly constrained by the topography, and a deep DWMW flow following the isobaths towards southeast. Another major hydrological characteristic of the Gulf of Lions is the cooling of shelf waters by cold northerly and northwesterly winds, forming dense shelf water that cascades down slope (Canals et al. 2006, Palanques et al. 2006). The circulation of water on the shelf is wind driven, predominantly flowing southwestwards (Millot 1990).

MATERIAL AND METHODS

Sampling

During 2004 and 2005, two cruises were undertaken as part of the Eurostratatform and HERMES programmes. Cruise 64PE225 was conducted from April 24th to May 24th 2004 and 64PE236 from April 28th to May 18th 2005. The Nazaré canyon study area was visited during both cruises, and the Cap de Creus study area was only visited during cruise 64PE225.

During cruise 64PE225 in 2004, the sampling strategy consisted in sampling the thalweg of the Nazaré and Cap de Creus canyon following a bathymetrical gradient. In addition, the respective adjacent open slopes were also sampled following at best the same bathymetrical gradient. This allowed having reference stations in the open slopes in order to make comparisons with the canyon stations at equivalent water depths, and compare different depths within the canyon and within the open slopes areas. During cruise 64PE236, the sampling strategy consisted in two transect across the Nazaré canyon. The cross sections were located where the canyon thalweg reaches 1000 m and 3000 m maximum depths. This allowed studding gradients across the canyon.

Sediment was sampled with the MUC 8+4 multiple corer developed by Oktopus GmbH. Two multiple corer casts were taken at each station in order to analyse sediment granulometry, ^{210}Pb activity, organic carbon, total carbon, total nitrogen, ammonia, nitrate, dissolved inorganic carbon, phosphate, phytopigments, amino acids, meiofauna and foraminifera. Each individual core was sectioned at discrete intervals with the help of the NIOZ slicing machine or by hand. During cruise 64PE225 sediments was also sampled with a box corer in order to obtain natural sediment with natural fauna to conduct and experiment in the flume in the laboratories at International University Bremen. Concise details in the number of replicates used for each analysis, the section intervals used to slice the cores, the handling of the samples until analysis, the different methodologies used for each analysis and the flume experiment are given in chapters 2, 3 and 4, and will not be repeated here. A detailed description of the flume and its calibration is given in Appendix I.

Note: Dr. Henko de Stigter from NIOZ, The Netherlands contributed with sediment granulometry and ^{210}Pb activity data for chapters 2 and 4. Dr. Eric Epping from NIOZ, The Netherlands contributed with organic carbon, total carbon and total nitrogen data for chapters 2 and 4. PhD student Karoliina Koho from Utrecht University, The Netherlands contributed with foraminifera abundance data for chapter 2. Phytopigments data, amino acids

data, meiofauna data and the flume experiment is my contribution to this thesis.

Considerations when determining organic matter availability for benthic fauna

Traditionally, most of the studies tackling the relationship between sedimentary organic matter and benthic fauna have utilised bulk indicators of sedimentary organic matter such as total organic matter, organic carbon and nitrogen (e.g. Graf 1992, Gage et al. 1995, Flach et al. 1998, Flach & Thomsen 1998, Pfannkuche et al. 1985, 1999, Duineveld et al. 2001, Heip et al. 2001, Flach et al. 2002). More recent studies have incorporated other parameters such as lipids, carbohydrates, pigments and amino acids (Albertelli et al. 1999, Cartes et al. 2002, Grémare et al. 2002, Riaux-Gobin et al. 2004), because the particulate organic matter (POM) available for benthic organism is rather heterogeneous in composition. This is due to the fact that most organic materials found in different environments are at some intermediate stage of the diagenetic process (Cowie & Hedges 1994). They often contain fresh material as well as older material. An important proportion of the sedimentary POM corresponds to refractory forms that cannot be absorbed by benthic organisms because of the characteristics of their digestive systems (Plante & Jumars 1992, Plante & Shriver 1998). Hence, rather than using bulk descriptors of sedimentary organic matter such as total organic matter, organic carbon and nitrogen to assess relationships between benthic fauna and sedimentary organics, it is better to try to assess the fraction of POM indeed available to benthic fauna. Amino acids, proteins, hexosamines, lipids, lignins, pigments and carbohydrates form the major fraction of analytically recognizable organic material in many natural samples. They are of diverse structure and intrinsic lability, and offer valuable comparative information on organic degradation processes (Cowie & Hedges 1992, 1994, Dauwe & Middelburg 1998). Information on the decomposition state of these organic compounds may be useful in identifying their availability or nutritional potential for organisms (Cowie & Hedges 1994). Selected pigments, lipids,

amino acids and lignins can be used as indicators of the organic matter degradation stage because during diagenesis they undergo preferential loss, for instance chlorophyll *a*, or preservation as is the case of lignins (Cowie & Hedges 1994, Dauwe & Middelburg 1998).

In this study, pigments and amino acids were chosen in order to describe the organic matter diagenetic characteristic in the submarine canyons under study.

Chlorophyll *a* concentrations are an indicator of water column phytoplankton biomass, while the concentrations of its degradation products (phaeopigments) are an indicator of the physiological status, detrital content and grazing processes in natural populations of phytoplankton (Mantoura & Llewellyn 1983). Therefore, the chlorophyll *a* versus phaeopigment concentrations in sediments has been used as a measure of the fresh organic matter from photosynthetic origin reaching the sea floor (Soltwedel et al. 2000, Levin et al. 2002). The pooled concentrations of chlorophyll *a* and phaeopigments are termed chloroplastic pigment equivalents (CPE) and indicate the amount of phytodetritus present in the environment (Thiel 1978).

Amino acids are the most labile biochemical compound and are critical to sustain microbial activity in marine environments (Keil et al. 2000). Amino acids compose the bulk of organic matter identifiable at molecular level in marine sediments (Wakeham et al. 1997). Changes of this uniform amino acid composition can be used to determine the decomposition stage of the organic matter, as for example, some amino acids and hexosamines become relatively enriched during degradation, whereas others are preferentially utilized (Dauwe & Middelburg 1998). The degradation index (DI) of Dauwe et al. (1999) is based on the distribution of the 14 commonly analysed protein amino acids in the organic matter of different marine origins. It summarises the subtle changes in the amino acid distribution into a value that ranges between 1.5 for labile phytoplankton and -2.2 for oxidized turbidite sediments where organic matter is stable on millennial timescales. Moreover, non-protein amino acids (β -alanine, α -amino butyric acid, γ - amino butyric acid and ornithine) are of diagenetic origin and generally absent in living

organisms (Cowie & Hedges 1992). When concentrations of these compounds are high it indicates enzymatic formation from the protein amino acids precursors, thus diagenetic alteration. The ratios between the protein amino acids precursors (e.g. glutamic and aspartic acids) to their respective degradation products (β -alanine and γ - amino butyric acid) can be used as a measure of the organic matter lability (Dauwe & Middelburg 1998), where low ratios indicate refractory material.

The methodologies used to extract pigments and amino acids from the sediment samples are given in detail in chapters 1, 2 and 3, and will not be repeated here. A table with the exact individual amino acid content for the Nazaré canyon and adjacent open slope sediments is given in Appendix 2.

LITERATURE CITED

- Albertelli G, Covazzi-Harriague A, Danovaro R, Fabiano M, Fraschetti S, Pusceddu A (1999) Differential responses of bacteria, meiofauna and macrofauna in a shelf area (Ligurian Sea, NW Mediterranean): role of food availability. *J Sea Res* 42:11-26
- Aller JY, Aller RC, Green MA (2002) Benthic faunal assemblages and carbon supply along the continental shelf/shelf break-slope off Cape Hatteras, North Carolina. *Deep-Sea Res Part II-Top Stud Oceanogr* 49:4599-4625
- Aller RC (2001) Transport and reactions in the bioirrigated zone. In: Boudreau BP, Jorgensen BB (eds) *The Benthic Boundary Layer Transport Processes and Biogeochemistry*. Oxford University Press, Oxford, p 269-301

- Berné S, Rabineau J, Flores JA, Sierro FJ (2004) The impact of Quaternary global change on strata formation: exploration on the shelf edge in the Northwestern Mediterranean sea. *Oceanogr* 17:92-103
- Biscaye, PE, Anderson, RF, Deck, BL (1988) Fluxes of particles and constituents to eastern United States continental slope and rise: SEEP-I. *Cont Shelf Res* 8:855-904
- Biscaye PE, Flagg CN, Falkowski PG (1994) The shelf edge exchange processes experiment, SEEP-II: an introduction to hypotheses, results and conclusions. *Deep-Sea Res Part II-Top Stud Oceanogr* 41 (2-3):231-252
- Canals M, Puig P, Durrieu de Madron X, Heussner S, Palanques A, Fabres J (2006) Flushing submarine canyons. *Nature* 444:354-357
- Cartes JE, Grémare A, Maynou F, Villora-Moreno S, Dinét A (2002) Bathymetric changes in the distributions of particulate organic matter and associated fauna along a deep-sea transect down the catalan sea slope (Northwestern Mediterranean). *Prog Oceanogr* 53:29-56
- Cowie GL, Hedges JI (1992) Sources and Reactivities of Amino-Acids in a Coastal Marine-Environment. *Limnol Oceanogr* 37:703-724
- Cowie GL, Hedges JI (1994) Biochemical indicators of diagenetic alteration in natural organic mixtures. *Nature* 369:304-307
- Dauwe B, Herman PMJ, Heip CHR (1998) Community structure and bioturbation potential of macrofauna at four North Sea stations with contrasting food supply. *Mar Ecol Prog Ser* 173:67-83
- Dauwe B, Middelburg JJ (1998) Amino acids and hexosamines as indicators of organic matter degradation state in North Sea sediments. *Limnol Oceanogr* 43:782-798
- Dauwe B, Middelburg JJ, Herman PMJ, Heip CHR (1999) Linking diagenetic alteration of amino acids and bulk organic matter reactivity. *Limnol Oceanogr* 44:1809-1814

- De Stigter HC, Boer W, De Jesus Mendes PA, Jesus CC, Thomsen L, Van den Bergh GD, Van Weering TCE (2007) Recent sediment transport and deposition in the Nazaré Canyon, Portuguese continental margin. *Mar Geol* (doi: 10.1016/j.margeo.2007.04.011)
- Degeest AM (2005) Cap de Creus canyon: a link between shelf and slope sediment dispersal systems in the western Gulf of Lion, France. MSc Thesis, Texas A&N University
- Duineveld G, Lavaleye M, Berghuis E, de Wilde P (2001) Activity and composition of the benthic fauna in the Whittard Canyon and the adjacent continental slope (NE Atlantic). *Oceanol Acta* 24:69-83
- Durrieu de Madron X (1994) Hydrography and Nepheloid Structures in the Grand-Rhone Canyon. *Cont Shelf Res* 14:457-477
- Durieux de Madron X, Abassi A, Heussner S, Monaco A, Aloisi JC, Radakovitch O, Giresse P, Buscail R, Kerherve P (2000) Particulate matter and organic carbon budgets for the Gulf of Lions (NW Mediterranean). *Oceanol Acta* 23 (6), 717-730
- Epping E, van der Zee C, Soetaert K, Helder W (2002) On the oxidation and burial of organic carbon in sediments of the Iberian margin and Nazare Canyon (NE Atlantic). *Prog Oceanogr* 52:399-431
- Fiúza AFG, Hamann M, Ambar I, Diaz del Rio G, Gonzalez N, Cabanas JM (1998) Water masses and their circulation off western Iberia during May 1993. *Deep-Sea Res Part II-Top Stud Oceanogr* 45:1127-1160
- Flach E, Lavaleye M, de Stigter H, Thomsen L (1998) Feeding types of the benthic community and particle transport across the slope of the NW European Continental Margin (Goban Spur). *Prog Oceanogr* 42:209-231
- Flach E, Muthumbi A, Heip CHR (2002) Meiofauna and macrofauna community structure in relation to sediment composition at the Iberian margin compared to the Goban Spur (NE Atlantic). *Prog Oceanogr* 52:433-457

Chapter 1

- Flach E, Thomsen L (1998) Do physical and chemical factors structure the macrobenthic community at a continental slope in the NE Atlantic? *Hydrobiol* 376:265-285
- Font J (1987) The path of the Levantine Intermediate Water to the Alboran sea. *Deep-Sea Res I* 34:1745-1755
- Gage JD, Lamont PA, Tyler PA (1995) Deep-Sea Macrobenthic Communities at Contrasting Sites Off Portugal, Preliminary-Results .1. Introduction and Diversity Comparisons. *Internationale Revue Der Gesamten Hydrobiologie* 80:235-250
- Gage JD, Tyler PA (1991) *Deep-sea biology: A natural history of organisms at the deep-sea floor*, Vol. Cambridge University Press, Cambridge
- Giere O (1993) *Meiobenthology: The Microscopic Fauna in Aquatic Sediments*, Vol. Springer-Verlag, Berlin
- Graf G (1992) Benthic pelagic coupling: A benthic view. *Oceanography and Mar Biol: An annual rev* 30:149-190
- Graf G, Rosenberg R (1997) Bioresuspension and biodeposition: A review. *J Mar Sys* 11:269-278
- Grémare A, Medernach L, de Bovee F, Amouroux JM, Vétion G, Albert P (2002) Relationships between sedimentary organics and benthic meiofauna on the continental shelf and the upper slope of the Gulf of Lion (NW Mediterranean). *Mar Ecol Prog Ser* 234:85-94
- Heip CHR, Duineveld G, Flach E, Graf G, Helder W, Herman PMJ, Lavaleye M, Middelburg JJ, Pfannkuche O, Soetaert K, Soltwedel T, de Stigter H, Thomsen L, Vanaverbeke J, de Wilde P (2001) The role of the benthic biota in sedimentary metabolism and sediment-water exchange processes in the Goban Spur area (NE Atlantic). *Deep-Sea Res Part II-Top Stud Oceanogr* 48:3223-3243
- Heussner S, Durrieu de Madron X, Radakovitch O, Beaufort L, Biscaye PE, Carbonne J, Delsaut N, Etcheber H, Monaco A (1999) Spatial and temporal patterns of downward particle fluxes on the continental slope

- of the Bay of Biscay (northeastern Atlantic). *Deep-Sea Res Part II-Top Stud Oceanogr* 46:2101-2146
- Jumars PA, Nowell ARM (1984) Effects of benthos on sediment transport: difficulties with functional grouping. *Cont Shelf Res* 3:115-130
- Keil RG, Tsamakis E, Hedges JI (2000) Early diagenesis of particulate amino acids in marine systems. In: Goodfriend GA, Collins MJ, Fogel ML, Macko SA, Wehmiller JF (eds) *Perspectives in Amino Acid and Protein Geochemistry*. Oxford University Press, New York
- Levin L, Gutierrez D, Rathburn A, Neira C, Sellanes J, Munoz P, Gallardo V, Salamanca M (2002) Benthic processes on the Peru margin: a transect across the oxygen minimum zone during the 1997-98 El Niño. *Prog Oceanogr* 53:1-27
- MacArthur RH, Wilson EO (1967) *The Theory of Island Biogeography*, Princeton University Press, New Jersey
- Mantoura RFC, Llewellyn CA (1983) The rapid determination of algal chlorophyll and carotenoid pigments and their breakdown products in natural waters by reverse-phase high-performance liquid chromatography. *Anal Chim Acta* 151:297-314
- Maurer D, Robertson G, Gerlinger T (1994) Comparison of Community Structure of Soft-Bottom Macrobenthos of the Newport Submarine Canyon, California and the Adjoining Shelf. *Internationale Revue Der Gesamten Hydrobiologie* 79:591-603
- Mazé JP, Arhan M, Mercier H (1997) Volume budget of the eastern boundary layer off the Iberian Peninsula. *Deep-Sea Res Part I-Oceanogr Res Pap* 44:1543-1574
- Millot C (1987) Circulation in the western Mediterranean Sea. *Oceanol Acta* 10:143-149
- Millot C (1990) The Gulf of Lions' hydrodynamics. *Cont Shelf Res* 10:885-894

Chapter 1

- Monaco A, Durieux de Madron X, Radakovitch O, Heussner S, Carbonne J (1999) Origin and variability of downward biogeochemical fluxes on the Rhone continental margin (NW Mediterranean). *Deep-Sea Res Part I-Oceanogr Res Pap* 46:1483-1511
- Mullenbach BL, Nittrouer CA (2000) Rapid deposition of fluvial sediment in the Eel Canyon, northern California. *Cont Shelf Res* 20:2191-2212
- Oliveira A, Santos AI, Rodrigues A, Vitorino J (in press) Sedimentary particle distribution and dynamics of the Nazaré canyon system and adjacent shelf (Portugal). *Mar Geol (Spec Iss)*
- Palanques A, Durrieu de Madron X, Puig P, Fabres J, Guillén J, Calafat A, Canals M, Heussner S, Bonnin J (2006) Suspended sediment fluxes and transport processes in the Gulf of Lions submarine canyons. The role of storms and dense water cascading. *Mar Geol* 236:43-61
- Pearson TH, Rosenberg R (1978) Macrobenthic succession in relation to a organic enrichment and pollution of the marine environment. *Oceanogr Mar Biol Ann Rev* 16:229-311
- Pfannkuche O (1985) The deep-sea meiofauna of the Porcupine Seabight and abyssal plain (NE Atlantic): population structure, distribution, standing stocks. *Oecol Acta* 8:343-353
- Pfannkuche O, Boetius A, Lochte K, Lundgreen U, Thiel H (1999) Responses of deep-sea benthos to sedimentation patterns in the North-East Atlantic in 1992. *Deep-Sea Res Part I-Oceanogr Res Pap* 46:573-596
- Plante CJ, Jumars PA (1992) The microbial environment of marine deposit feeders gets characterized via microelectrodes. *Microb Ecol* 23:257-277
- Plante CJ, Shrivvers AG (1998) Differential lysis of sedimentary bacteria by *Arenicola marina* L.: examination of cell wall structure and exopolymeric capsules as correlates. *J Exp Mar Biol Ecol* 229:35-52
- Puig P, Palanques A (1999) Temporal variability and composition of settling particle fluxes on the Barcelona continental margin (Northwestern Mediterranean). *J Mar Res* 56:639-654

- Riaux-Gobin C, Dinet A, Dugue G, Vetion G, Maria E, Grémare A (2004) Phytodetritus at the sediment-water interface, NW Mediterranean Basin: spatial repartition, living cells signatures, meiofaunal relationships. *Sci Mar* 68:7-21
- Schmidt S, de Stigter HC, Van Weering TCE (2001) Enhanced short-term sediment deposition within the Nazaré Canyon, North-East Atlantic. *Mar Geol* 173:55-67
- Soetaert K, Heip CHR, Vincx M (1991) The Meiobenthos Along a Mediterranean Deep-Sea Transect off Calvi (Corsica) and in an Adjacent Canyon. *Mar Ecol* 12:227-242
- Soltwedel T, Mokievsky V, Schewe I (2000) Benthic activity and biomass on the Yermak Plateau and in adjacent deep-sea regions northwest of Svalbard. *Deep-Sea Res Part I-Oceanogr Res Pap* 47:1761-1785
- Thiel H (1978) Benthos in upwelling regions. In: Boje R, Tomczak M (eds) *Upwelling ecosystems*. Springer-Verlag, Berlin, p 124-138
- Thomsen L, Gust G (2000) Sediment erosion thresholds and characteristics of resuspended aggregates on the western European continental margin. *Deep-Sea Res Part I-Oceanogr Res Pap* 47:1881-1897
- Thomsen L, van Weering T, Gust G (2002) Processes in the benthic boundary layer at the Iberian continental margin and their implication for carbon mineralization. *Prog Oceanogr* 52:315-329
- Van Weering TCE, Hall IR, de Stigter HC, McCave IN, Thomsen L (1998) Recent sediments, sediment accumulation and carbon burial at Goban Spur, NW European Continental Margin (47-50 degrees N). *Prog Oceanogr* 42:5-35
- Van Weering TCE, McCave IN (2002) Benthic processes and dynamics at the NW Iberian margin: an introduction. *Progr Oceanogr* 52:349-372
- Van Weering TCE, De Stigter HC, Boer W, De Haas H (2002) Recent sediment transport and accumulation on the NW Iberian margin. *Prog Oceanogr* 52:349-371

Chapter 1

Vetter EW, Dayton PK (1998) Macrofaunal communities within and adjacent to a detritus-rich submarine canyon system. *Deep-Sea Res Part II-Top Stud Oceanogr* 45:25-54

Vitorino J, Oliveira A, Jouanneau JM, Drago T (2002) Winter dynamics on the northern Portuguese shelf. Part 1: physical processes. *Prog Oceanogr* 52:29-153

Wakeham SG, Lee C, Hedges J, Hermes PJ, Peterson ML (1997) Molecular indicators of diagenetic status in marine organic matter. *Geochim Cosmochim Ac* 61:5363-5369

CHAPTER 2

Distribution of meiobenthos in the Nazaré canyon and adjacent slope (western Iberian Margin) in relation to sedimentary composition

ABSTRACT

Abundance of metazoan meiofauna and foraminifera, and biomass and community structure of nematodes were investigated in benthic zones along the Nazaré Canyon and adjacent continental slope in relation to concentration of organic matter and its suitability as a food source for the meiobenthos. The Nazaré canyon sediments were richer in organic carbon (Corg), total nitrogen, and phytopigments compared to the adjacent open slope. In addition, phytodetritus was fresher in the canyon sediment than on the slope (higher chlorophyll a: phaeopigments). Nevertheless, the abundance of polychaetes, copepods, bivalves, nematodes, total metazoans, and nematode biomass were not always higher in the canyon than on the adjacent open slope. Lower densities occurred in the upper and middle canyon, and living benthic foraminifers were significantly more abundant on the adjacent slope. The stations in the upper and middle canyon contained infinitesimal numbers of foraminifers. Reduced diversity and evenness and high K-dominance of the nematode assemblages in the upper part of the canyon indicated environmental stress, perhaps related to high Corg content

Published as: R. García, K.A. Koho, H.C. De Stigter, E. Epping, E. Koning, L. Thomsen (2007)
Distribution of meiobenthos in the Nazaré canyon and adjacent slope (western Iberian Margin) in relation to sedimentary composition. *Marine Ecology Progress Series* 340:207-220

and sediment disturbance. Non-selective deposit-feeders dominated the nematode assemblages of the upper and middle parts of the canyon, whereas a more diverse trophic structure was found in the deeper parts and the open slope. Conditions in the upper and middle areas of the Nazaré canyon are harsh, and only opportunistic organisms can survive there.

KEY WORDS: Nazaré canyon · Meiobenthos · Foraminifera · Sedimentary organic carbon · Physical disturbance

INTRODUCTION

Deep gullies and submarine canyons run perpendicular to the shoreline and can dissect the entire continental shelf and slope. Canyons can trap part of the suspended particulate organic matter transported along the continental margin, and serve as conduits for organic particles and sediments from the shelf and upper slope to the deep sea (Van Weering et al. 2002). Therefore, they represent areas of high sedimentary organic carbon content and relatively high biochemical activity (Epping et al. 2002). Furthermore, some submarine canyons are very unstable environments, since tidal currents, episodic slumps and turbidity flows periodically transport sediments and organic particles into the canyon system (Puig et al. 2004). Currents inside canyons can reach velocities of 2 m s^{-1} (Vetter & Dayton 1998).

In the Nazaré canyon, sediments and fine particles are actively transported in nepheloid layers, and high sedimentation rates occur especially in its upper and middle regions (Van Weering et al. 2002). In the canyon, detritus of terrigenous origin predominates over pelagic detritus, and there is a higher Corg content than in the open continental shelf and slope (Epping et al. 2002, Van Weering et al. 2002). Enhanced remineralization rates have been shown as a result of enrichment with Corg (Epping et al. 2002).

Meiofaunal communities are responsible for a significant amount of sediment remineralization and support significant trophic pathways (Leguerrier et al. 2003). According to Tietjen (1992), on average, bacteria comprise 86 %, macrofauna 7 % and meiofauna 5% of living carbon in deep-sea sediments. Hence, despite comprising a relatively minor component of the living carbon compared to bacteria, macro- and meiofauna play an important role in the total carbon turnover of deep-sea environments. The meiofauna communities in the Nazaré canyon have rarely been studied: a few records of metazoan meiobenthos are available for the Western Iberian Margin (see Soltwedel 2000, Flach et al. 2002), while Flach (2003) reported very high densities of meiofauna in the canyon at all depths.

Benthic animal communities from canyon systems can reflect the unstable and organically enriched conditions of these systems. Indeed, the fauna communities inhabiting submarine canyons have been found to differ in structure from those on adjacent abyssal plains, continental shelf, or slope. Faunal densities and biomasses in canyon systems have been found to be higher (e.g. Gage et al. 1995, Vetter & Dayton 1998, Duineveld et al. 2001) and faunal diversities lower (e.g. Gage et al. 1995, Vetter & Dayton 1998, Curdia et al. 2004) than in adjacent habitats. These differences in faunal structure have been attributed to the higher organic content of canyon systems (see Gage et al. 1995, Duineveld et al. 2001). However, there are indications that abundances can also be lower in canyons than in adjacent areas (see Maurer et al. 1994); this could be related to factors other than the high Corg content of these systems. In the Nazaré canyon, Flach (2003) reported lower numbers of macrofauna than on the Iberian continental slope. Polychaetes dominated the macrofauna in this canyon, and opportunistic polychaete communities occurred in regions with high organic matter content (Flach 2003, Curdia et al. 2004). Furthermore, macrofauna biomass in the canyon increases with increasing Corg fluxes (Flach 2003).

This study investigated changes in the composition of meiofaunal assemblages along a depth gradient in the Nazaré canyon and the adjacent open slope. Organic matter concentrations and lability were also studied to

investigate whether the content and freshness of the sedimentary organic matter in the canyon were the main driving factors controlling the meiobenthic community.

MATERIAL AND METHODS

Study area

The Nazaré canyon is the largest canyon on the Western Iberian Margin, and intersects the entire continental shelf (Vanney & Mougenot 1981). Inside the canyon there is a strong internal tide circulation of water, with velocities of up to 15 cm s^{-1} (Coelho et al. 2003). Sediment transported over the shelf and upper slope by alongshore currents is temporarily deposited in the very narrow upper and middle part of the canyon, until it is transported to the deep sea in nepheloid layers or flushed down canyon by turbidite currents (Van Weering et al. 2002, Garcia et al. 2003).

The hydrography of the shelf is dominated by a poleward current in winter and an equatorward current during summer (Vitorino et al. 2002, Coelho et al. 2003). The poleward current favours downwelling, while the equatorward current is generally associated with coastal upwelling, which triggers high primary production along the Iberian Margin (Vitorino et al. 2002).

The canyon is characterised by a well-stratified water column. North Atlantic Deep Water (NADW) with temperatures of 2 to 7°C and salinities of 34.8 to 35.6 ppm is present between depths of approximately 2000 and 3000 m water depths (Garcia et al. 2003). Between approximately 600 and 1500 m, Mediterranean water is present, with temperatures of 8 to 13°C and salinities of 35.8 to 36.2 ppm. Temperatures of 14 to 18°C and salinities of 35.4 to 35.8 ppm characterise the upper water layer.

Sampling

Sediment cores for meiofauna and physicochemical analyses were collected in May 2004 during Cruise 64PE225 of the RV 'Pelagia'. For this study we analysed data from 8 stations located along a depth gradient in the Nazaré canyon axis (S41, S26, S34, S24 and S22) and adjacent open slope (S39, S27 and S25) (Fig. 1).

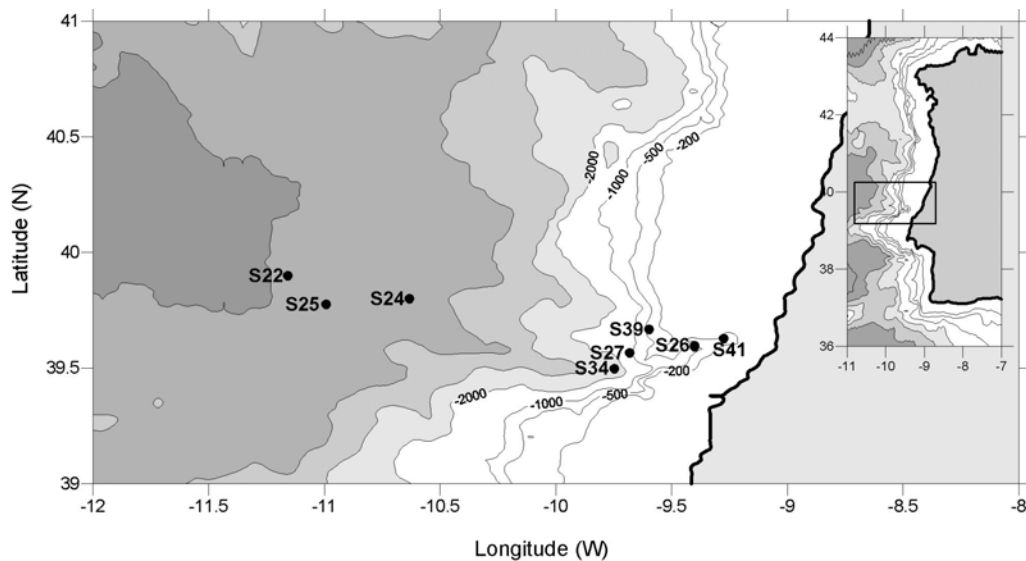


Fig. 1. Nazaré canyon showing stations sampled during cruise 64PE225

Sediment samples for physicochemical and faunal analyses were taken with the MUC 8+4 multiple corer developed by Oktopus GmbH. This corer has an array of eight 6 cm diameter and four 10 cm diameter coring tubes, 61 cm in length. For each station, three 10 cm multicorer tubes were used for metazoan analysis, one 10 cm tube for sedimentological analysis, three 6 cm tubes for phytopigment analysis, and one 6 cm tube for foraminifer analysis. From a second deployment, four 6 cm tubes were used for analysis of total and organic C and N. Cores were stored at in situ temperature in a temperature-controlled room and processed within 3 h of collection.

The sediment samples for phytopigment, total and organic C and N analysis were stored at -20°C until analysis; 4 to 6 replicate sub-cores were taken from the core tubes for metazoan analysis using 60 ml syringes with cut-

off anterior ends. These sediment samples were preserved in 4% buffered formaldehyde solution. The sediment samples from the core used for analysis of foraminifers were preserved in 96% ethanol solution with Rose Bengal. Only the upper 5 cm of the cores were used in this study.

Grain-size analysis

Sediment samples were freeze-dried, and then crumbled and mixed. Subsequently, ~100 mg of sediment was dispersed in water, applying ultrasound for mechanical dispersal but without addition of chemical dispersatives. The dispersed sediment was then introduced into a Coulter LS 230 laser particle-sizer for determination of particle size spectra.

Geochemical analysis

Phytodetritus input to the seafloor was assessed by fluorometric measurement of sediment-bound chlorophyll *a* (chl *a*) and phaeopigment (phaeo) concentrations following the method of Yentsch & Menzel (1963). Sediment samples were first freeze-dried and homogenised in a mortar. Pigments were subsequently extracted in 10 ml 90% acetone solution and measured in a Turner fluorometer following Shuman & Lorenzen (1975). The bulk of pigments measured with this method were termed “chloroplastic pigment equivalents”, CPE (Thiel 1978). Chl *a* versus phaeo concentrations were used to assess the fresh organic matter of photosynthetic origin that reached the seafloor.

Sediment total carbon, total nitrogen (TN) and Corg were measured using a ThermoFinnigan flash element analyser following the procedures described by Lohse et al. (2000).

Meiofauna analysis

In the laboratory, sediment samples for metazoan investigations were washed through a 48 µm sieve and metazoans were extracted using Ludox (colloidal silica polymer) diluted in water to a specific gravity of 1.209

(Ólafsson & Elmgren 1997). The metazoans were counted and identified to major taxa in a Petri dish under a stereomicroscope. All the nematodes were picked and put in a watch glass with a glycerine solution (5% glycerine, 5% pure ethanol and 90% distilled water). After 24 h at 50°C, the nematodes were mounted on micro-slides, using anhydrous glycerine as mounting medium, for identification to genus under a compound microscope. To estimate nematode biomasses, nematode length (excluding filiform tails) and width were measured by the semiautomatic images system (analySIS®2.1) at the Alfred Wegener Institute. Nematode volume and biomass (wet weights) were calculated using Andrassy's (1956) formulas. Nematode wet weights were then converted into carbon biomass assuming that 100% wet weight corresponds to 12.4% carbon weight (Jensen 1984). Nematode feeding types (1A, 1B, 2A and 2B) were determined after the classification provided by Wieser (1953).

Sediment samples for investigations of foraminifers were washed through 150 and 63 µm sieves. Only the 150 µm fraction was used for this study. Well-stained foraminifers were counted in a Petri dish under a stereomicroscope, and transferred to Chapman slides for identification. For the quantification of arborescent foraminifers (a type of branching agglutinant foraminifer), a standard minimum size of 1.5 ± 0.1 mm was adopted because these foraminifers can easily break apart when sorting. The estimate of total individuals thus included fragments of various sizes.

Data analysis

Shannon-Wiener diversity index H' (Krebs 1989), evenness J' (Pielou, 1969) and K -dominance curves (Lambhead et al. 1983) were calculated for the nematode assemblage at each site.

Univariate 2-way ANOVAs were used to investigate differences in faunal abundance, nematode biomass, diversity and evenness between the 2 locations (i.e. canyon vs. open slope) and between different water depths. A nested design was constructed with depth nested within location. A 1-sample Kolmogorov-Smirnov test was used to check the normality of the taxa counts,

nematode biomass data and ecological indices. The data was not normally distributed, and was therefore $\log_2(x + 1)$ -transformed prior to ANOVA analysis. To test for possible relationships between the various meiofaunal and geochemical parameters and for possible differences between the Nazaré canyon and the adjacent open slope, 2 non-parametric correlation analyses were performed; one with canyon data the other with open-slope data. The Kendall's tau statistic from the statistical package SPSS 12.0 was used, as this is extremely conservative, with a low number of measurements.

RESULTS

Sediment granulometry

Sediments in the canyon were predominantly muddy (silt and clay), except at Stns S26 and S34 (Table 1), where silt and clay comprised only about 50% of the sediment, with the other 50% consisting of sand, and the finer material occurring in the top centimetres. On the open slope, sediments became muddier with increasing water depth. In the shallow open-slope station (S39), about 35% of the sediment particles were silt and clay, whereas in the deepest open-slope station (S25) about 98% of the sediment particles were silt and clay.

Geochemical characteristics of sediments

The canyon sediments were organically enriched compared to the adjacent open slope (Table 1), containing higher CPE, a measure of phytodetritus content. The upper part of the canyon (Stns S41 and S26) had

Table1. Sediment granulometry (clay = <2 µm, silt = >2 to <63 µm, sand = >63 µm), concentrations of chloroplastic pigments equivalents (CPE), total nitrogen (TN), organic carbon (Corg), chlorophyll a: phaeopigment ratio (chl a:phaeo), and carbon to nitrogen molar ratio (C:N) for top 5 cm of sediment at each station as a function of water depth

Stn	Latitude (°N)	Longitude (°W)	Depth (m)	Clay (% Vol)	Silt (% Vol)	Sand (% Vol)	CPE (µg/5cm ³)	chl.a:phaeo	TN (%)	Corg (%)	C:N
Canyon											
S41	39°34.8'	9°09.9'	354	7.72	78.87	13.42	89.10	0.09	0.22	1.73	9.00
S26	39°35.9'	9°23.9'	1121	5.06	42.04	52.89	92.40	0.18	0.19	1.78	10.90
S34	39°30.0'	9°45.9'	2847	6.02	44.63	49.38	48.60	0.03	0.20	1.86	10.90
S24	39°48.0'	10°37.9'	4810	13.21	73.63	13.18	13.90	0.03	0.15	1.54	12.10
S22	39°53.9'	11°10.0'	4969	14.06	81.18	4.75	5.70	0.03	0.14	1.52	12.50
Open slope											
S39	39°39.9'	9°35.9'	300	4.89	29.58	65.54	22.30	0.02	0.04	0.30	8.50
S27	39°33.9'	9°40.9'	1000	15.31	71.32	13.36	9.40	0.03	0.13	1.02	8.90
S25	39°46.5'	10°59.9'	4798	23.62	75.21	1.18	1.70	0.02	0.09	0.54	7.00

the highest CPE values, which decreased with increasing water depth. Furthermore, the quality of the phytodetritus was highest in the upper part of the canyon (Stns S41 and S26) (chl α :phaeo = 0.09 to 0.18), and TN and Corg contents were also higher in the canyon, especially in the upper and middle parts (Stns S41, S26 and S34). The canyon detritus had a higher proportion of terrigenous organic matter (C:N = 9 to 12.5) than open-slope detritus.

On the open slope, CPE values were low, decreasing with increasing water depth. The quality of the phytodetritus was low and similar to the quality at the middle and deeper parts of the canyon. TN and Corg contents were lower than in the canyon, and the detritus had a higher proportion of organic material of pelagic origin (C:N = 7 to 8.9).

Meiofauna

We identified a total of 12 major taxa within the 2 study areas. Nematodes were the most abundant group within the canyon and the adjacent open slope, comprising between 40 and 90% of total metazoan abundance (Fig. 2).

Copepods were the second most abundant group in both study areas, comprising between 10 and 40% of total metazoan abundance, followed by polychaetes. Bivalves were more abundant in the canyon stations, but in low percentages, except at Stn S34. Amphipoda, Cumacea, Decapoda, Ostracoda, other Crustacea, Kinorincha and Halcaroidea occurred occasionally and in very low numbers, being insignificant in terms of abundance. On average, these taxa together represented about 1 to 2% of the total meiofauna. These taxa will not be analysed below in more detail.

Foraminiferal abundance is not expressed as a percentage of total meiofauna because foraminifers were only investigated in the >150 μm fraction, the >48 μm fraction being used to examine metazoans abundance.

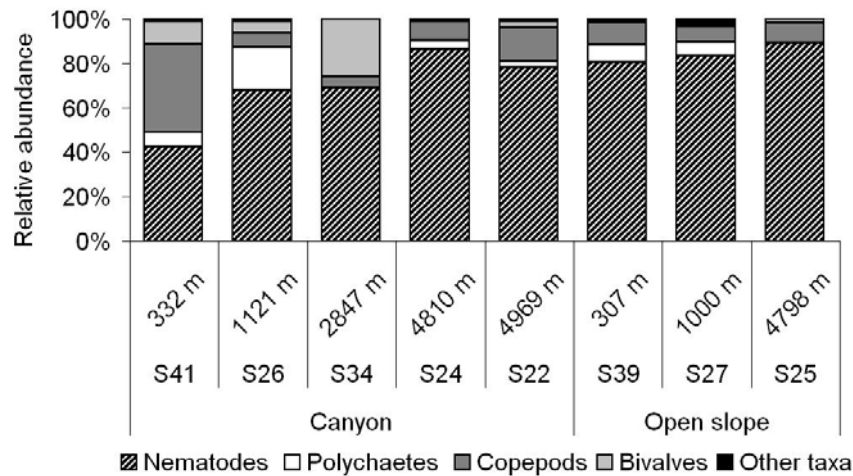


Fig. 2. Relative abundance of nematodes, polychaetes, copepods, bivalves and minor taxa along a depth gradient at Stns S41, S26, S34, S24, S22, S39, S27 and S25 in Nazaré canyon and on adjacent open slope

Foraminifera

Low to insignificant numbers of foraminifers were recorded in the upper and middle canyon (Fig. 3a). The highest total standing stocks were found in the deep canyon station, S24. Below this station the system widens into a fan, and foraminifer abundances here were similar to those on the nearby slope. In contrast, high total standing stocks of foraminifers were recorded along the open slope, displaying a clear decreasing trend with increasing water depth.

Elevated numbers of arborescent foraminifers (branching agglutinant) were observed in the open-slope sediments, most being recorded at Stn S27 (Fig. 3b). In the canyon arborescent foraminifers were almost completely absent, with the exception of Stn S22 at the lower end of the canyon.

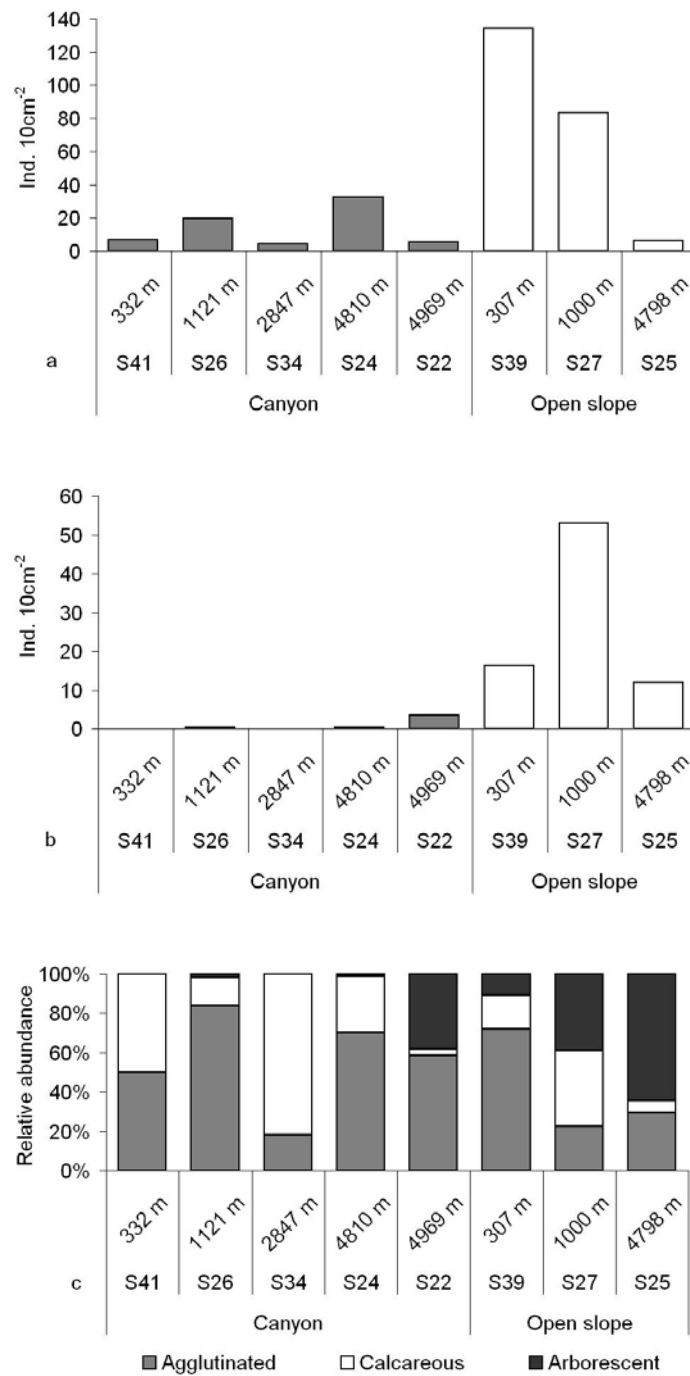


Fig. 3. (a)(b) Abundance of total standing stock of agglutinated and calcareous foraminifers, and arborescent foraminifers, and (c) relative abundance of agglutinated, calcareous and arborescent foraminifers, along bathymetric gradient and at Stns S41, S26, S34, S24, S22, S39, S27 and S25 in the Nazaré canyon and on adjacent open slope (n = 1, data from one replica)

In general, the canyon stations were dominated by agglutinated foraminifers (Fig. 3c), representing between the 60 and 80% of all individuals; the only exception being Stn S34, where >80% of the assemblage comprised calcareous foraminifera. At the head of the canyon (Stn S41), calcareous and agglutinated foraminifers were present in similar numbers. At the open-slope stations, arborescent, calcareous and agglutinated foraminifers were well represented. Agglutinated foraminifers dominated at the shallow open-slope station accounting for 70% of total foraminifers abundance. At 1000 m (Stn S27), calcareous and arborescent foraminifers were numerically dominant (80% of all individuals). The deepest site was numerically dominated by arborescent foraminifers (>60% of all individuals).

Metazoans

On the open slope, the abundance of most taxonomical groups and also nematode biomass decreased with increasing water depth (Fig. 4a,b,c,e,f). In contrast, in the canyon no clear decrease was observed. Stn S26 at 1121 m contained the highest abundance of most taxonomical groups and also the highest nematode biomass (Fig. 4a,b,d,e,f). The only depth-related pattern in the canyon was that the highest abundance of taxa and highest nematode biomass occurred in the upper part of the canyon (Stns S41 and S26).

Statistically, there were significant inter-station differences in the abundances of metazoans and nematode biomass as a function of depth at each location (canyon and open slope) (all $p \leq 0.001$, Table 2).

There were also significant differences in the mean abundance of nematodes and bivalves between the canyon and the slope ($p \leq 0.004$ and $p \leq 0.001$ respectively, Table 2). Mean abundance of nematodes was lower in the canyon than on the slope (53.5 ± 21.1 individuals 10 cm^{-2} and 73.1 ± 16.4 individuals 10 cm^{-2} respectively, mean \pm SE), and mean abundance of bivalves was higher in the canyon (4.6 ± 2.6 individuals 10 cm^{-2} and 0.2 ± 0.2 individuals 10 cm^{-2} respectively).

Chapter 2

Table 2. Results of univariate 2-way nested ANOVA; $df = 1$ and 5 for location and depth(location) respectively

Parameter	Location		Depth(Location)	
	F	$p \leq$	F	$p \leq$
Total meiofauna	3.249	0.081	14.410	0.001
Polychaeta	0.444	0.510	22.744	0.001
Nematoda	9.606	0.004	11.548	0.001
Copepoda	0.119	0.732	12.941	0.001
Bivalvia	24.514	0.001	8.775	0.001
Nem. Biomass	1.866	0.181	8.724	0.001
Diversity (H')	52.189	0.001	11.247	0.001
Evenness (J')	5.735	0.023	2.335	0.065

Distribution of meiobenthos

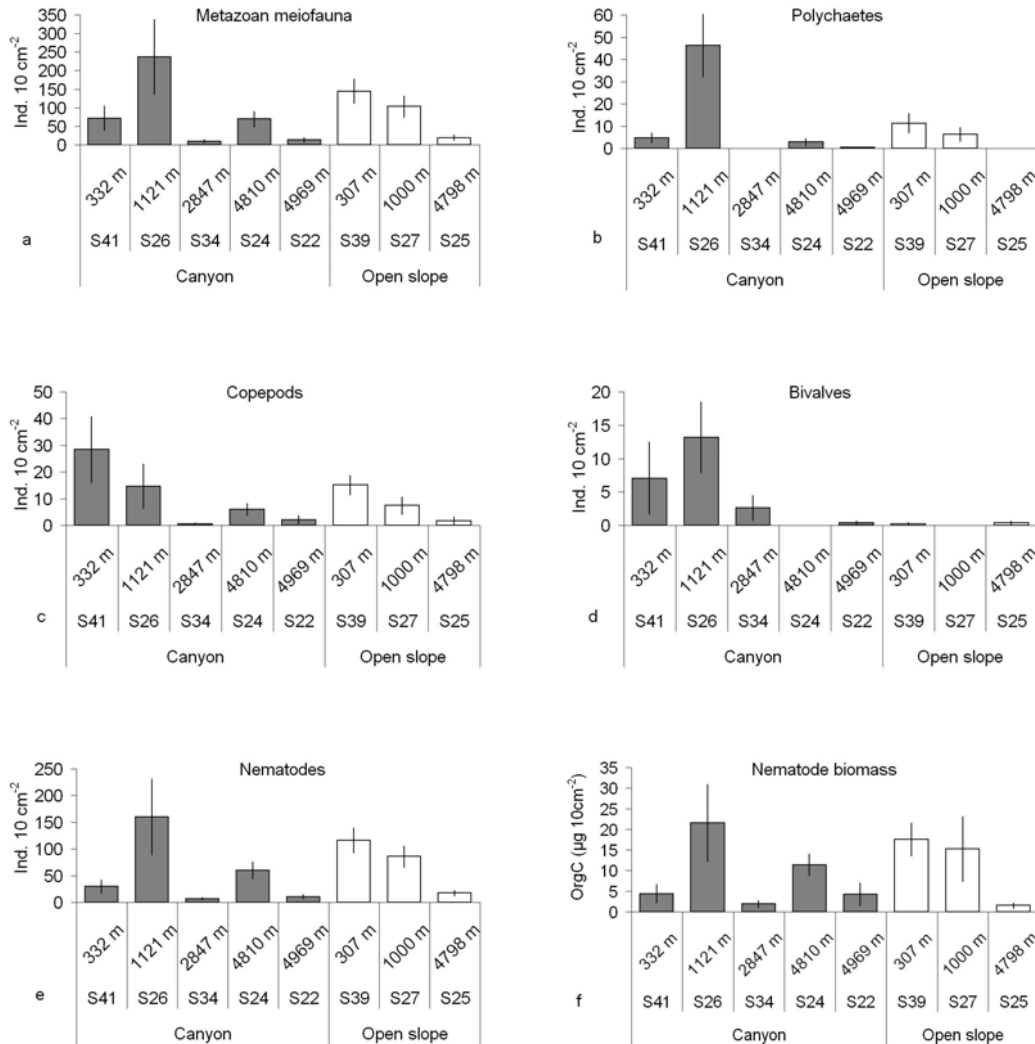


Fig. 4. (a) to (e) Mean \pm SE abundance of (a) metazoan meiofauna, (b) polychaetes, (c) copepods, (d) bivalves and (e) nematodes, and (f) nematode biomass along bathymetric gradient and at Stns S41, S26, S34, S24, S22, S39, S27 and S25 in Nazaré canyon and on adjacent open slope

Nematode assemblage

A total of 85 genera of nematodes was recorded (Table 3). For the canyon a total of 55 genera was recorded, of which only 3 (*Metalinhomoeus*, *Sabatieria* and *Sphaerolaimus*) were present at all canyon stations and 16 genera were exclusively present in the canyon. The open slope had a total of 68 genera, of which 11 (*Acantholaimus*, *Camacolaimus*, *Cervonema*, *Halaimus*, *Marylinia*, *Metalinhomoeus*, *Neochromadora*, *Paralongicyatholaimus*, *Sabatieria*, *Sphaerolaimus* and *Terschellingia*) were present at all open-slope stations and 31 genera were exclusively present in the open slope (Table 3). *Metalinhomoeus* and *Sabatieria* were the most abundant genera for both canyon and open slope, being highest in the canyon.

Table 3. List of nematode genera, showing feeding type, FT (Wieser 1953) and mean \pm SE abundance (individuals 10cm⁻²) for Nazaré canyon and adjacent open-slope stations (1A = selective deposit-feeder, 1B = non-selective deposit feeder, 2A = epigrowth feeder, and 2B = predator/omnivore)

Genera	FT	Canyon system					Open slope		
		S41	S26	S34	S24	S22	S39	S27	S25
<i>Acantholaimus</i>	2A		2.1 \pm 1.4	1.4 \pm 0.9	1.4 \pm 1.4		0.9 \pm 0.9	4.6 \pm 1.2	1.4 \pm 0.6
<i>Amphimonhystrella</i>	1B					0.2 \pm 0.2			0.4 \pm 0.4
<i>Araeolaimus</i>	1A				0.3 \pm 0.3		0.2 \pm 0.2		
<i>Ascolaimus</i>	1B						0.7 \pm 0.5		
<i>Axonolaimus</i>	1B	0.5 \pm 0.3	3.3 \pm 1.2				4.7 \pm 2.1		
<i>Bathyeuristomina</i>	2B							0.4 \pm 0.4	
<i>Camacolaimus</i>	2A				0.6 \pm 0.3		0.5 \pm 0.3	0.4 \pm 0.4	0.4 \pm 0.4
<i>Campylaimus</i>	1B		0.2 \pm 0.2				1.2 \pm 1.2		
<i>Cervonema</i>	1B		0.2 \pm 0.2		0.3 \pm 0.3	0.2 \pm 0.2	3.5 \pm 0.8	1.8 \pm 1.1	0.4 \pm 0.4
<i>Chaetonema</i>	1B					0.5 \pm 0.4	0.5 \pm 0.5		
<i>Chromadora</i>	2A	0.7 \pm 0.5	0.7 \pm 0.5		0.3 \pm 0.3		6.8 \pm 1.3	1.4 \pm 1.0	
<i>Chromadorita</i>	2A	0.2 \pm 0.2					0.5 \pm 0.3		
<i>Comesa</i>	1B							0.4 \pm 0.4	
<i>Comesoma</i>	1B					0.2 \pm 0.2			
<i>Crenopharynx</i>	1A						0.7 \pm 0.5	0.7 \pm 0.4	
<i>Cricolaimus</i>	2A						0.2 \pm 0.2		
<i>Cyatolaimus</i>	2A						0.5 \pm 0.5		
<i>Cylicolaimus</i>	2B						3.1 \pm 2.8		
<i>Daptonema</i>	1B		0.9 \pm 0.7				0.2 \pm 0.2	0.7 \pm 0.7	
<i>Desmocolex</i>	1A				0.3 \pm 0.3				
<i>Desmodora</i>	2A						5.2 \pm 4.1	3.5 \pm 1.2	
<i>Desmolaimus</i>	1B		0.2 \pm 0.2						
<i>Disconema</i>	1B				0.3 \pm 0.3			0.4 \pm 0.4	
<i>Diplopeltoides</i>	1A							0.7 \pm 0.4	0.4 \pm 0.4
<i>Diplopeltula</i>	1A					0.2 \pm 0.2	0.5 \pm 0.3		0.4 \pm 0.4
<i>Dolicholaimus</i>	2B						0.2 \pm 0.2		
<i>Dorylaimopsis</i>	2B						0.2 \pm 0.2	0.4 \pm 0.4	

Distribution of meiobenthos

Genera	FT	Canyon system					Open slope		
		S41	S26	S34	S24	S22	S39	S27	S25
<i>Elzalia</i>	1B					0.2±0.2		0.4±0.4	
<i>Endeolophos</i>	2A							0.7±0.4	0.4±0.4
<i>Enoplodes</i>	2B				0.6±0.3				
<i>Enoplolaimus</i>	2B	0.2±0.2	0.5±0.5				0.2±0.2		
<i>Filoncholaimus</i>	2B						0.2±0.2		
<i>Halalaimus</i>	1A	0.2±0.2			0.8±0.6		4.2±1.6	1.4±0.6	0.4±0.4
<i>Hopperia</i>	2B							0.7±0.7	
<i>Kraspedonema</i>	2A				0.3±0.3				
<i>Laimella</i>	2A						0.2±0.2		
<i>Leptolaimus</i>	1A				0.3±0.3				
<i>Limhomoeus</i>	2A						0.2±0.2		
<i>Longicyatholaimus</i>	2A				7.1±0.4		1.7±0.8	0.7±0.4	
<i>Marilynnia</i>	2A	1.7±0.6			0.8±0.6		6.4±0.9	0.4±0.4	1.4±0.8
<i>Metacyatholaimus</i>	2A					0.2±0.2			
<i>Metadesmolaimus</i>	1B				0.3±0.3				
<i>Metalinhomoeus</i>	1B	13.0±5.6	85.4±39.2	3.1±1.1	4.2±1.4	0.4±0.2	14.1±2.6	11.3±1.7	2.8±1.0
<i>Metoncholaimus</i>	2B	0.2±0.2			0.6±0.3				
<i>Microlaimus</i>	2A	1.2±0.4			0.3±0.3		0.5±0.3		0.4±0.4
<i>Molgolaimus</i>	1A							0.4±0.4	
<i>Nemanema</i>	1A				0.3±0.3			0.7±0.7	0.7±0.7
<i>Neochromadora</i>	2A	0.7±0.5	0.2±0.2	0.2±0.2			8.0±2.2	6.4±0.9	1.1±0.7
<i>Neotonchus</i>	2A				0.3±0.3				
<i>Onchium</i>	2A				0.3±0.3				
<i>Oncholaimus</i>	2B				0.3±0.3		0.2±0.2		0.4±0.4
<i>Oncholaimellus</i>	2B							0.7±0.7	
<i>Oxystomina</i>	1A	0.2±0.2	0.2±0.2			0.2±0.2	0.9±0.6	1.1±0.7	
<i>Paracanthochus</i>	2A				1.7±1.0				
<i>Paracomesoma</i>	1B				1.4±1.4	0.2±0.2		0.4±0.4	
<i>Paracyatholaimus</i>	2A	0.2±0.2			0.6±0.6		2.1±1.1	1.8±1.8	
<i>Paradontophora</i>	1B					0.2±0.2			
<i>Paralongicyatholaimus</i>	2A		0.7±0.7	0.5±0.3	0.6±0.6	0.7±0.5	1.9±1.1	0.4±0.4	1.4±0.6
<i>Paramesacanthion</i>	2B		0.2±0.2		1.7±1.0		0.5±0.3		
<i>Paralinhomoeus</i>	1B		1.7±1.7						
<i>Paranticoma</i>	2A								0.7±0.4
<i>Pareudesmocolex</i>	1A						0.2±0.2		
<i>Parasphaerolaimus</i>	2B		0.2±0.2						
<i>Pierrickia</i>	1B							3.5±1.7	
<i>Polysignia</i>	2A							0.4±0.4	
<i>Pomponema</i>	2B	0.5±0.3	0.2±0.2				2.1±1.1	0.4±0.4	
<i>Prooncholaimus</i>	2B	0.5±0.3							
<i>Pselionema</i>	1A					0.2±0.2	2.6±1.4	0.7±0.7	
<i>Pterygonema</i>	1A						0.2±0.2		
<i>Quadricoma</i>	1A						0.7±0.5		
<i>Sabatieria</i>	1B	2.6±0.7	53.1±21.3	0.5±0.3	7.6±2.8	1.1±0.5	11.1±1.9	14.1±4.0	0.4±0.4
<i>Setosabatieria</i>	1B		0.2±0.2				4.7±1.5	3.9±1.9	
<i>Sphaerolaimus</i>	2B	0.7±0.3	1.4±1.4	0.2±0.2	1.4±0.8	0.2±0.2	1.9±1.0	3.9±2.0	0.4±0.4
<i>Subsphaeroplumus</i>	2B						0.7±0.7	0.4±0.4	
<i>Steineria</i>	1B							0.4±0.4	
<i>Synodontium</i>	1B						0.2±0.2		
<i>Synonchiella</i>	2B						0.2±0.2	0.4±0.4	
<i>Syringolaimus</i>	2B					1.4±0.6		0.7±0.4	0.4±0.4
<i>Terschellingia</i>	1B	1.2±0.7	1.4±1.4			1.1±0.6	2.8±0.6	0.4±0.4	1.1±1.1
<i>Thalassoalaimus</i>	1A						0.2±0.2		
<i>Thalassomonhystera</i>	1B					0.2±0.2	0.2±0.2		
<i>Thoracostomopsis</i>	2B							0.4±0.4	
<i>Vasostoma</i>	2A		0.2±0.2		0.6±0.3	0.4±0.2			
<i>Viscosia</i>	2B	0.2±0.2			0.6±0.3	0.7±0.4	2.8±0.7	1.1±1.1	
<i>Wieseria</i>	1A						0.7±0.7		

The mean diversity (H') and evenness (J') indexes for the nematode assemblage were significantly higher on the open slope than in the canyon. Diversity on the slope was 2.3 ± 0.1 and 1.3 ± 0.2 in the canyon ($p \leq 0.001$, Table 2). Evenness was 0.9 ± 0.01 on the slope and 0.7 ± 0.1 in the canyon ($p \leq 0.023$, Table 2). Diversity decreased with increasing water depth on the open slope (Fig. 5a). In the canyon, it only did so in the upper and middle parts. Evenness did not change along the depth gradient on the slope (Fig. 5b), and in the canyon, Stns S26 and S34 had lower evenness values than the remaining canyon stations. Inter-station differences in diversity with depth at each location (canyon and open slope) were statistically significant ($p \leq 0.001$, Table 2).

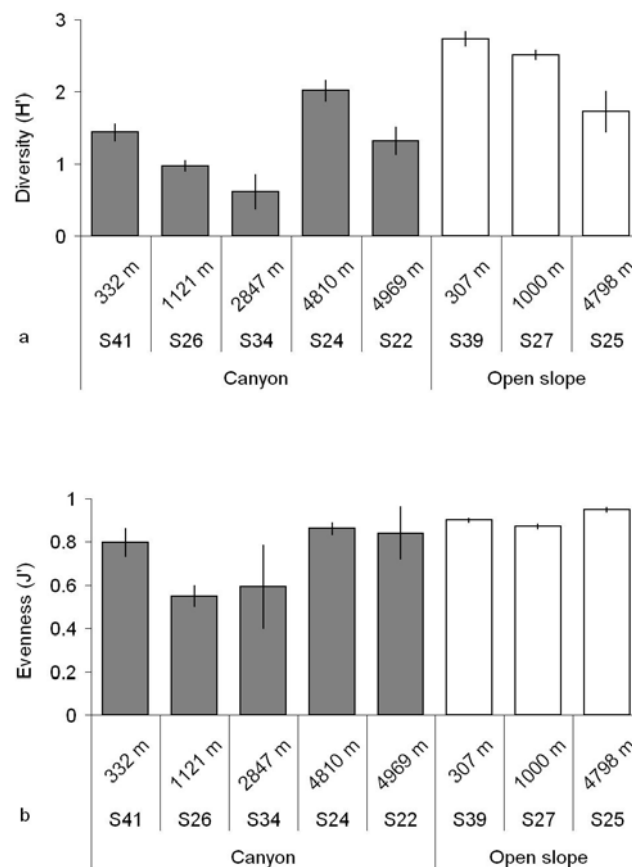


Fig. 5. Mean \pm SE diversity (Shannon-Wiener H'), and evenness (J') of nematode assemblage along bathymetric gradient and at Stns S41, S26, S34, S24, S22, S39, S27 and S25 in Nazaré canyon and on adjacent open slope

K-dominance curves of nematode abundance (Fig. 6) revealed 2 groups of curves in the canyon and 1 in the open slope. The curves for Stns S26, S34 and S41 indicated higher nematode dominance within these assemblages than at Stns S24 and S22 (Fig. 6a). In addition, the curves for Stns S24 and S22 were similar to those for the 3 open-slope stations (Fig. 6b), indicating that all these stations had similar nematode dominance.

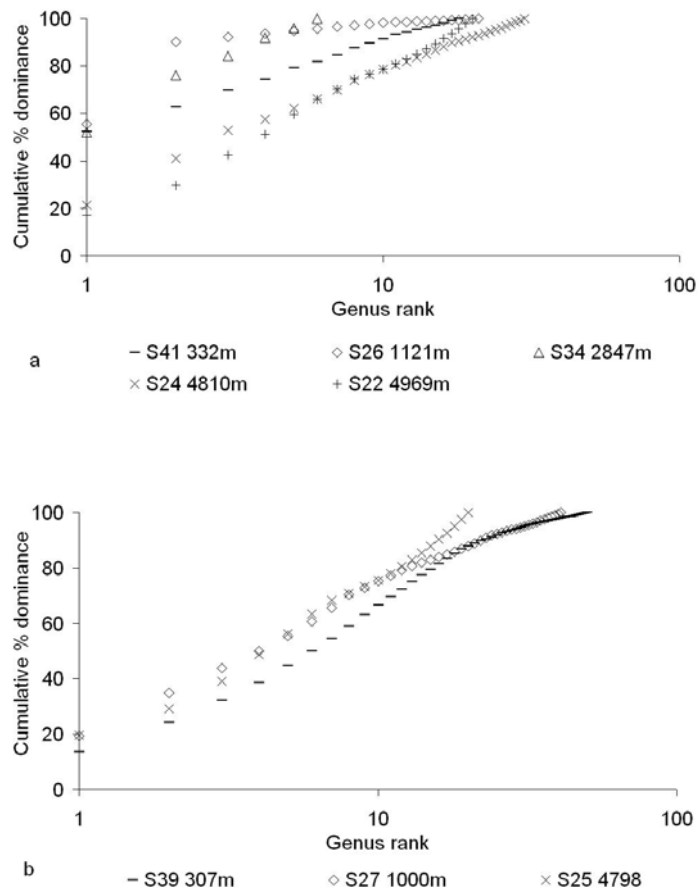


Fig. 6. Nematode K-dominance curves along depth gradient in (a) Nazaré canyon and (b) adjacent open-slope stations

The trophic structure of the nematode assemblages differed between canyon and open slope. On the open slope, the four different feeding types of Wieser (1953) were well represented in terms of abundance (Fig. 7a) and biomass (Fig. 7b), and no differences in the trophic structure were observed

along the depth gradient. In contrast, in the canyon, non-selective deposit-feeding nematodes (Feeding Type 1B) dominated in terms of abundance (Fig. 7a) and biomass (Fig. 7b). The assemblages of the upper and middle part of the canyon differed from that in the deeper part: Non-selective deposit feeders (Type 1B) were dominant in the upper and middle canyon areas, whereas selective deposit feeders (Type 1A) were unimportant; however, the latter feeding type was more important in the deeper part of the canyon, where it was present in proportions similar to those on the open slope.

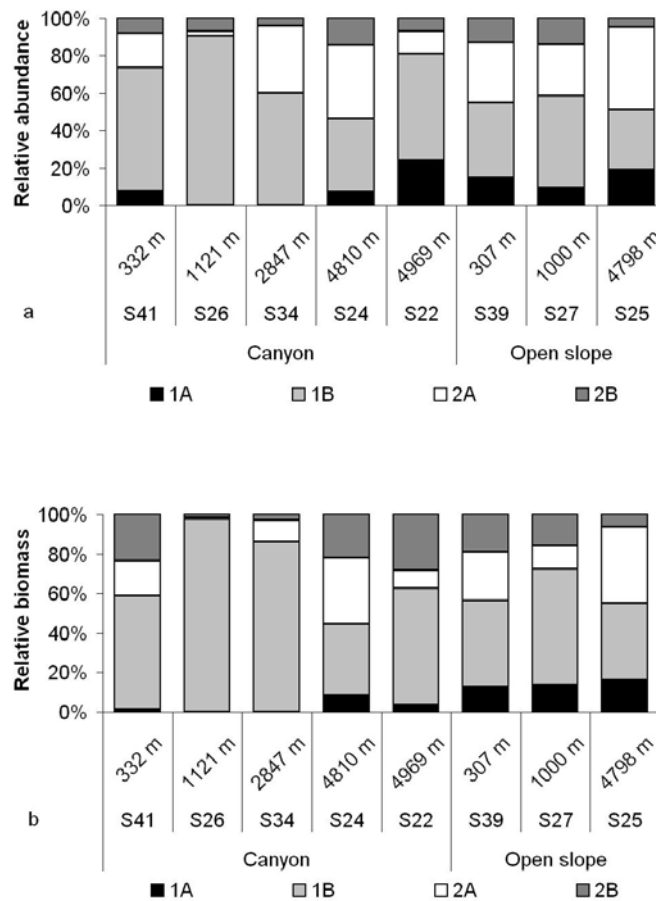


Fig. 7. (a) Relative abundance and (b) biomass of nematodes belonging to the 4 different feeding types described by Wieser (1953) along bathymetric gradient and at Stns S41, S26, S34, S24, S22, S39, S27 and S25 in Nazaré canyon and on adjacent open slope (1A = selective deposit-feeder, 1B = non-selective deposit-feeder, 2A = epigrowth feeder, 2B = predator/omnivore)

Relationships between benthic meiofauna and geochemical parameters

The correlation analysis revealed different levels of interactions for the canyon system and adjacent open slope (Table 4). In the canyon there were 21 correlations, with an average Kendall's tau correlation coefficient of 0.5. The abundance of total metazoans, copepods, polychaetes, bivalves, nematodes and also nematode biomass were positively correlated ($p \leq 0.01$) with the lability of the phytodetritus (chl a :phaeo). Diversity and evenness were negatively correlated with Corg ($p \leq 0.01$) and phytodetritus (CPE) content ($p \leq 0.05$ and 0.01 respectively). The nematode trophic group 1B was positively correlated with chl a :phaeo ($p \leq 0.01$) and CPE ($p \leq 0.01$). On the open slope, there were 13 correlations with an average Kendall's tau correlation coefficient of 0.6. The abundance of total metazoans, copepods, polychaetes, nematodes and the nematodes biomass was positively correlated with CPE ($p \leq 0.01$, nematode biomass $p \leq 0.05$). Diversity was also positively correlated with CPE ($p \leq 0.05$), as were the nematode trophic groups 1B, 2A ($p \leq 0.01$) and 2B ($p \leq 0.05$).

DISCUSSION

Meiofauna and organic matter levels

The meiofauna abundance recorded in the Nazaré canyon and adjacent open slope ranged between 9.9 and 236.5 ind.10 cm⁻². These values are low compared to those in temperate regions of the east Atlantic and off the Iberian Peninsula (see Soltwedel 2000), but within the range observed during springtime in the Western Iberian Margin. Most present-day studies on meiofauna use a mesh size $\leq 32 \mu\text{m}$. We used a $48 \mu\text{m}$ mesh size, which could

Table 3. Results of non-parametric Kendall's tau correlations analyses for metazoans, copepods, polychaetes, bivalves, nematodes, nematode biomass (Nem Biom), diversity (H'), evenness (J'), selective deposit feeder (1A), non-selective deposit feeder (1B), epigrowth feeder (2A), predator/omnivore (2B) for Nazaré canyon and adjacent open slope. Significant levels of $p \leq 0.05$ are in bold, for those of $p \leq 0.01$ are in bold and italics

Parameter	Metazoans	Copepods	Polychaetes	Bivalves	Nematodes	NemBiom	H'	J'	1A	1B	2A	2B
Canyon												
CPE	0.424	0.274	<i>0.457</i>	<i>0.549</i>	0.218	0.220	-0.338	-0.455	-0.126	<i>0.460</i>	-0.084	-0.311
chl a:phaeo	<i>0.734</i>	<i>0.629</i>	<i>0.753</i>	<i>0.465</i>	<i>0.565</i>	<i>0.485</i>	0.059	-0.323	-0.087	<i>0.693</i>	0.187	0.115
Corg	0.011	-0.174	0.012	0.247	-0.173	-0.118	-0.622	-0.426	-0.049	0.038	-0.354	-0.556
TN	0.100	0.204	0.062	0.230	-0.170	-0.118	-0.235	-0.250	-0.068	0.098	-0.052	-0.245
C:N	-0.277	-0.374	-0.259	-0.415	-0.070	-0.059	0.176	0.308	0.107	-0.279	0.020	0.221
Open slope												
CPE	<i>0.666</i>	<i>0.786</i>	<i>0.653</i>	0.051	<i>0.649</i>	0.550	0.603	-0.288	0.343	<i>0.678</i>	<i>0.800</i>	0.559
chl a:phaeo	-0.240	-0.360	-0.208	-0.153	-0.225	-0.131	-0.288	-0.131	-0.041	-0.244	-0.373	-0.123
Corg	-0.240	-0.360	-0.208	-0.153	-0.225	-0.131	-0.288	-0.131	-0.041	-0.244	-0.373	-0.123
TN	-0.240	-0.360	-0.208	-0.153	-0.225	-0.131	-0.288	-0.131	-0.041	-0.244	0.373	-0.123
C:N	0.400	0.280	0.458	-0.255	0.411	0.498	0.288	-0.655	0.398	0.407	0.267	0.532

have underestimated actual meiofauna densities. Using a comparable mesh size (50 μm), Rachor (1975) found meiofauna abundances at 38°N (~1° S from the Nazaré study area) ranging between 18 and 294 ind. 10 cm^{-2} during springtime at depths of 1469 to 5112 m. In wintertime, also at 38° N, and using a 40 μm mesh size, Thiel (1975) recorded meiofauna abundances ranging between 123 and 1387 ind. 10 cm^{-2} at depths of 250 to 5250 m, suggesting strong seasonality. On the NW Iberian margin (42 to 43° N) during summertime, Flach et al. (2002) observed meiofauna abundances ranging between 250 and 1800 ind. 10 cm^{-2} , at depths of 200 to 5000 m, but they used a smaller 32 μm mesh size. In terms of biomass, the values recorded for the Nazaré canyon and adjacent open slope are about 3 to 4 times lower than those reported for the NW Iberian margin during summer (Flach et al. 2002).

The average Corg content of the top 5 cm of sediment in the Nazaré canyon ranged between 1.52 and 1.86%, while on the adjacent open slope organic carbon contents ranged between 0.3 and 1.02%. These values are similar to those found in the past for the Nazaré canyon and slope in the NW Iberian margin (Epping et al. 2002). At other continental margins, similar Corg contents have also been observed (Duineveld et al 2001, Grémare et al. 2002).

The phytodetritus content (CPE) ranged between 5.7 and 92.4 μg 5 cm^{-3} in the Nazaré canyon sediments, and between 1.7 and 22.3 μg 5 cm^{-3} on the open slope. The open-slope values fall within the range given for other continental margins at similar depths (Soltwedel 1997, Soltwedel et al. 2000). In contrast, the values we found in the Nazaré canyon sediments are several orders of magnitudes higher than those found in other continental margins.

The lability of the phytodetritus in the canyon and adjacent slope sediments is refractory compared to that of other continental margins at similar depths. Soltwedel et al. (2000) found chl *a*: phaeo ratios of 0.4 to 0.7 at ~500 m, of 0.07 to 0.21 at ~1000 m, of 0.03 to 0.12 at ~3000 m and of 0.05 at ~4000 m depths on the Yermak Plateau. In the canyon and adjacent slope sediments chl *a*: phaeo ratios ranged between 0.02 and 0.18.

Distribution of meiofauna abundance and biomass

For continental margins, the abundance and biomass of benthic communities have been reported to decrease with increasing water depth (Tietjen 1992, Soltwedel 2000, Flach et al. 2002). This decrease has been related to decreased food availability (Gage & Tyler 1991). In the canyon and adjacent open-slope sediments, phytodetritus decreased with increasing water depth, and Corg content tended to be lower at greater depths (Table 1). However, a parallel decrease in meiofauna abundance and biomass only occurred on the open slope (Fig. 4). This is supported by the stronger positive correlation between the metazoan taxa and CPE contents on the open slope than in the canyon (Table 4).

For submarine canyons, higher abundances of fauna and higher biomasses have been reported and related to the higher organic content of these environments (Gage et al. 1995, Vetter & Dayton 1998, Duineveld et al. 2001). Moreover, the quality of organic matter also plays an important role in controlling benthic communities. In areas with high quantities of labile organic matter, faunal density and biomass have been found to be higher than in areas where similar quantities of refractory organic matter were observed (Dauwe & Middelburg 1998).

Higher organic contents (Corg, TN and CPE) were found throughout the canyon than on the adjacent slope, especially in the upper/middle parts (Table 1). Despite the fact that the bulk of the organic matter in the canyon was very refractory (C:N \approx 9 to 12), the amount and quality of organic matter available for direct consumption was higher in the upper part of the canyon (higher CPE contents and chl *a*:phaeo ratios) (Table 1). This suggests that the upper and middle canyon areas would constitute better feeding grounds for the benthos, and higher densities and biomass would be expected there. However, higher meiofaunal abundance and nematode biomass were not always observed in the canyon. Although meiofaunal densities in the deeper parts of the canyon seemed to parallel environmental organic levels, in the upper and middle areas this was not the case. Stns S41, S26 and S34 were always depleted in foraminifers compared to the open slope (Fig. 3).

Metazoans in general, and polychaetes and nematodes specifically (Fig. 4) were very abundant at St S26 (1121 m), but were depleted at St S41 and S34. This was also true for nematode biomass. In general, organisms on the adjacent open slope seemed to survive better with lower or similar background levels of Corg and CPE than those in the canyon.

The absence of a clear relationship between faunal abundance and biomass with organic content and metabolisable organic matter in the canyon suggests that some other environmental parameter(s) is/are responsible for faunal distributions. De Stigter et al. (2007) measured high near-bed tidal currents, average horizontal particle flux and deposition flux in the upper and middle parts of Nazaré canyon. The high currents may cause frequent resuspension and transport of surface sediments, leading to unstable sediment substrate, and high sedimentation rates may lead to fauna being buried by sediment. Such an environment is difficult to colonise because the meiofauna is either swept away by high currents or buried by unstable sediments and episodic depositional events, as confirmed by the lack of fragile arborescent foraminifers in the upper and middle canyon. Gage et al. (1995) also reported the absence of fragile surface-feeding macrofauna in the Setúbal canyon, where indications of vigorous bottom currents were found. In the Nazaré canyon, low numbers of calcareous and agglutinated foraminifers were found in the upper and middle parts. Previously, low abundances of foraminifers were recorded in the Wilmington canyon off the coast of New Jersey, and their absence was related to periodic mass wasting and high current activity in the study area (Jorissen et al. 1994). Further, the nematodes *Sabatieria* sp. and *Metalinhomoeus* sp., which have been shown to persist and thrive in very disturbed environments resulting from dredging and trawling activities (Schratzberger & Jennings 2002) were very dominant in the upper and middle parts of the Nazaré canyon. These observations seem to indicate that meiofauna abundance and biomass in the upper and middle canyon is strongly controlled by physical factors.

Nematode community structure

In the upper and middle parts of the Nazaré canyon, higher phytopigments and Corg concentrations were recorded, and the phytodetritus was less refractory. Here, low nematode diversity and evenness, and high *K*-dominance curves were found, and non-selective deposit-feeding nematodes were especially important. In agreement, the correlation analyses showed negative correlations of diversity and evenness with Corg and CPE, and a positive correlation of non-selective deposit-feeders with CPE and chl *a*:phaeo (Table 4). In the deeper canyon area and adjacent open slope, lower contents of phytopigments and Corg were recorded, and the phytodetritus was more refractory. Higher diversity and evenness, and lower *K*-dominance curves were found here. The trophic structure of the nematode assemblages was more diverse. The correlation analysis supported this, showing a positive correlation of diversity with CPE, and a higher number of trophic groups correlated to CPE (Table 4). Thus, diversity patterns of the nematode community and trophic structure both indicate that the differences in metabolisable organic matter between upper canyon regions and adjacent open slope, and deeper canyon regions play an important role in controlling the composition of the meiobenthos inhabiting these regions.

Two nematode genera, *Sabatieria* sp. and *Metalinhomoeus* sp., accounted for ~70% of the abundance in the upper canyon (Fig. 6a). Both these genera are non-selective deposit-feeders. *Sabatieria* sp. is well adapted to living in fine-sediment environments, with high Corg loads, low oxygen concentrations, and high sulphide concentrations (Jensen et al. 1992, Soetaert & Heip 1995). Suboxic sediments also characterise the upper part of the Nazaré canyon (Epping et al. 2002). *Metalinhomoeus* sp. has also been found to be very abundant in silty and very fine sand environments with high organic carbon content (Buchholz & Lampadariou 2002). Further, these genera are also found in highly physically-disturbed sedimentary conditions resulting from dredging and trawling. Thus, in the more disturbed and organically enriched conditions of the upper canyon, *Sabatieria* sp. and *Metalinhomoeus* sp. may constitute opportunistic colonisers. Flach (2003) also found that the

macrobenthic community in the Nazaré canyon was dominated by 2 small opportunistic polychaetes.

Conclusions

The Nazaré canyon contains higher amounts of organic matter than the adjacent open slope. In its upper and middle parts, the phytodetritus is fresher, and thus of higher nutritional value for the meiobenthos. However, contrary to expectations, the meiobenthos in this part of the canyon seem unable to fully exploit the high amounts of food resources the canyon provides. In comparison, the meiobenthos on the open slope is more abundant, although with less abundant food resources. The low abundance of fauna in the canyon may be due to the local high-velocity bottom currents and unstable sedimentary conditions hindering the settlement of meiobenthic communities. The upper canyon was dominated by 2 very opportunistic nematode genera (*Sabatieria* sp. and *Metalinhomoeus* sp.) that are able to withstand great sedimentary disturbance, high organic loads and suboxic conditions. The nematode community structure was related to organic concentrations. In the organically enriched upper canyon, lower diversities of the nematode assemblages and of the trophic structure were observed. Finally, the stations sampled in the canyon were situated in the thalweg, where physical disturbance by sediment transport and deposition is likely to be highest. A comparison with potentially less disturbed sites on terraces adjacent to the thalweg has yet to be made.

ACKNOWLEDGEMENTS

This research was supported by EUROSTRATAFORM project, EC contract EVK3-CT-2002-00079 funded by the European Commission, DG-XII, and the HERMES project, EC contract OCE-CT-2005-511234 funded by the European Commission's Sixth Framework Programme under the priority Sustainable Development, Global Change and Ecosystems. Shiptime on RV

'Pelagia' was provided by Royal NIOZ, Texel, The Netherlands. The authors thank all the crew of the research vessel 'Pelagia' for their work in getting the samples on deck, Dr. T. J. Kouwenhoven for helping out with sample processing on board and comments on the manuscript, and Dr. T. Soltwedel and Dr. C. Hasseman for providing the semiautomatic images system (analySIS®2.1) from the Alfred Wegener Institut. We also thank Dr. A. Lerchl from International University Bremen for providing microscopes, and the students A. Palacz, for his help with phytopigment analyses, and B. Alexander, for proof-reading the English of the manuscript.

LITERATURE CITED

- Andrassy I (1956) Die Rauminhalts und Gewichtsbestimmung der Fadenwuermer (Nematoden). *Acta Zool Acad Sci Hung* 1-3:1-15
- Buchholz TG, Lampadariou N (2002) Changes in composition and diversity of the Malia Bay nematode community (Crete, Greece) in relationship to sediment parameters. In: Bright M, Dworschak PC, Stachowitsch M (eds) *Vienna School of Marine Biology: a tribute to Jörg Ott*. *Facultas Universitätsverlag, Wien*, p 33-52
- Coelho H, Garcia AC, Neves R (2003) Aspects of circulation over submarine canyons: a numerical study. 4th Symposium on the Iberian Atlantic Margin. *Thalassas (Rev Cienc Mar Santiago de Compostela)* 19:141-143
- Curdia J, Carvalho S, Ravara A, Gage JD, Rodrigues AM, Quintino V (2004) Deep macrobenthic communities from Nazaré submarine canyon (NW Portugal). *Sci Mar* 68:171-180
- Dauwe B, Middelburg JJ (1998) Amino acids and hexosamines as indicators of organic matter degradation state in North Sea sediments. *Limnol Oceanogr* 43:782-798

- De Stigter HC, Boer W, De Jesus Mendes PA, Jesus CC, Thomsen L, Van den Bergh GD, Van Weering TCE (2007) Recent sediment transport and deposition in the Nazaré Canyon, Portuguese continental margin. *Mar Geol* (doi: 10.1016/j.margeo.2007.04.011)
- Duineveld G, Lavaleye M, Berghuis E, de Wilde P (2001) Activity and composition of the benthic fauna in the Whittard Canyon and the adjacent continental slope (NE Atlantic). *Oceanol Acta* 24:69-83
- Epping E, van der Zee C, Soetaert K, Helder W (2002) On the oxidation and burial of organic carbon in sediments of the Iberian margin and Nazaré Canyon (NE Atlantic). *Prog Oceanogr* 52:399-431
- Flach E (2003) Factors controlling soft bottom macrofauna along and across European continental margins. In: Wefer G, Billet D, Hebbeln D, Jørgensen B B, Schlüter M, van Weering T (eds) *Ocean margin systems*, Springer-Verlag, Berlin, p 351-363
- Flach E, Muthumbi A, Heip CHR (2002) Meiofauna and macrofauna community structure in relation to sediment composition at the Iberian margin compared to the Goban Spur (NE Atlantic). *Prog Oceanogr* 52:433-457
- Gage JD, Tyler PA (1991) *Deep-sea biology: a natural history of organisms at the deep-sea floor*. Cambridge University Press, Cambridge
- Gage JD, Lamont PA, Tyler PA (1995) Deep-sea macrobenthic communities at contrasting sites off Portugal, Preliminary Results. 1. Introduction and diversity comparisons. *Int Rev Ges Hydrobio* 80:235-250
- Garcia C, Coelho H, Neves R (2003) Some hydrological and nephelometric aspects over Nazaré and Setúbal (Portugal) submarine canyons. 4th Symposium on the IberianAtlantic Margin, Thalassas (Rev Cienc Mar Santiago de Compostela) 19:51-52
- Grémare A, Medernach L, de Bovee F, Amouroux JM, Vétion G, Albert P (2002) Relationships between sedimentary organics and benthic

- meiofauna on the continental shelf and the upper slope of the Gulf of Lion (NW Mediterranean). *Mar Ecol Prog Ser* 234:85-94
- Jensen P (1984) Measuring carbon content in nematodes. *Helgol Meeresunters* 38:83-86
- Jensen P, Rumohr J, Graf G (1992) Sedimentological and biological differences across a deep-sea ridge exposed to advection and accumulation of fine-grained particles. *Oceanol Acta* 15:287-296
- Jorissen FJ, Buzas MA, Culver SJ, Kuehl SA (1994) Vertical distribution of living benthic foraminifera in submarine canyons off New Jersey. *J Foraminifer Res* 24:28-36
- Krebs CJ (1989) *Ecological methodology*, Harper & Row, New York.
- Lambshead PJD, Platt HM, Shaw KM (1983) The detection of differences among assemblages of marine benthic species based on an assessment of dominance and diversity. *J Nat Hist* 17:859-874
- Leguerrier D, Niquil N, Boileau N, Rzeznik J, Sauriau PG, Le Moine O, Bacher C (2003) Numerical analysis of the food web of an intertidal mudflat ecosystem on the Atlantic coast of France. *Mar Ecol Prog Ser* 246:17-37
- Lohse L, Kloosterhuis RT, de Stigter HC, Helder W, van Raaphorst W, van Weering TCE (2000) Carbonate removal by acidification causes loss of nitrogenous compounds in continental margin sediments. *Mar Chem* 69:193-201
- Maurer D, Robertson G, Gerlinger T (1994) Comparison of community structure of soft-bottom macrobenthos of the Newport submarine canyon, California and the adjoining shelf. *Int Rev Ges Hydrobio* 79:591-603
- Ólafsson E, Elmgren R (1997) Seasonal dynamics of sublittoral meiobenthos in relation to phytoplankton sedimentation in the Baltic Sea. *Estuar Coast Shelf Sci* 45:149-164

- Pielou EC (1969) An introduction to mathematical ecology, Wiley-Interscience, New York
- Puig P, Ogston AS, Mullenbach BL, Nittrouer CA, Parson JD, Sternberg RW (2004) Storm-induced sediment gravity flows at the head of the Eel submarine canyon, northern California margin. *J Geophys Res*, 109, C03019, doi: 10.1029/2003JC001918
- Rachor E (1975) Quantitative Untersuchungen über das Meiobenthos der nord-atlantischen Tiefsee. *Meteor Forschergeb D* 21:1-10
- Schratzberger M, Jennings S (2002) Impacts of chronic trawling disturbance on meiofaunal communities. *Mar Biol* 141:991-1000
- Shuman FR, Lorenzen CF (1975). Quantitative degradation of chlorophyll by a marine herbivore. *Limnol Oceanogr* 20:580-586
- Soetaert K, Heip CHR (1995) Nematode assemblages of deep-sea and shelf break sites in the North Atlantic and Mediterranean Sea. *Mar Ecol Prog Ser* 125:171-138
- Soltwedel T (1997) Meiobenthos distribution pattern in the tropical East Atlantic: indication for fractionated sedimentation of organic matter to the sea floor? *Mar Biol* 129:747-756
- Soltwedel T (2000) Metazoan meiobenthos along continental margins: a review. *Prog Oceanogr* 46:59-84
- Soltwedel T, Mokievsky V, Schewe, I (2000) Benthic activity and biomass on the Yermak Plateau and in adjacent deep-sea regions northwest of Svalbard. *Deep-Sea Res Part I-Oceanogr Res Pap* 47:1761-1785
- Thiel H (1975) The size structure of the deep-sea benthos. *Int Rev Gesamten Hydrobiol* 60:575-606
- Thiel H (1978) Benthos in upwelling regions. In: Boje R, Tomczak M (eds) *Upwelling ecosystems*. Springer-Verlag, Berlin, p 124-138

Chapter 2

- Tietjen JH (1992) Abundance and biomass of metazoan meiobenthos in the deep sea. In: Rowe GT, Pariente V (eds) Deep-sea food chains and the global carbon cycle, Kluwer Academic, London, p 45-62
- Van Weering TCE, De Stigter HC, Boer W, De Haas H (2002) Recent sediment transport and accumulation on the NW Iberian margin. *Prog Oceanogr* 52:349-371
- Vanney JR, Mougnot D (1981) La plateforme continentale du Portugal et les provinces adjacentes: analyse géomorphologique. *Mem Serv Geol Portug*, 28:1-86
- Vetter EW, Dayton PK (1998) Macrofaunal communities within and adjacent to a detritus-rich submarine canyon system. *Deep-Sea Res Part II-Top Stud Oceanogr* 45:25-54
- Vitorino J, Oliveira A, Jouanneau JM, Drago T (2002) Winter dynamics on the northern Portuguese shelf. Part 1. Physical processes. *Prog Oceanogr* 52:129-153
- Wieser W (1953) Die Beziehung zwischen Mundhohlengestalt Ernährungsweise und Vorkommen bei freilebenden marinen Nematoden. *Ark Zool* 26:439-484
- Yentsch CS, Menzel DW (1963) A method for the determination of phytoplankton chlorophyll and phaeophytin by fluorescence. *Deep-Sea Res* 10:221-231

CHAPTER 3

Bioavailable organic matter in surface sediments of the Nazaré Canyon and adjacent slope (western Iberian Margin)

ABSTRACT

The distribution of bioavailable organic matter in surface sediments of the Nazaré submarine canyon and adjacent open slope was investigated. The concentration of chlorophyll a (chl a), phaeopigments (phaeo), chloroplast pigments equivalents (CPE) and total hydrolysable amino acids (THAA) decreased with increasing water depth, and were in general higher within the canyon (specially in the upper regions) than on the open slope. The concentrations were low on the canyon walls, increasing towards the canyon axis. The chl a:phaeo ratio, degradation index (DI), asp:β-ala and glu:γ-aba ratios were highest in the upper canyon, and similarly low in the deeper canyon and along the open slope. On the canyon axis and walls these lability indices were similar. THAA:OM and chl a:OM ratios indicated that the quality of the bulk organic matter in the canyon and slope was similar. Bioavailable organic matter accumulates in the upper canyon regions, and its quality is diluted with refractory material from deeper regions transported by the flood tides. Ebb tides transport the upper canyon organic matter down canyon, where it is dispersed across a bigger area under a

Submitted to Journal of Marine Systems as: R. García, L. Thomsen (*in rev*) Bioavailable organic matter in surface sediments of the Nazaré Canyon and adjacent slope (western Iberian Margin)., Manuscript N°: MARSYS-D-07-00046

more refractory state. Flume experiments demonstrate that arborescent foraminifera and polychaete pellet mounds, as found in the head of the canyon, enhance the deposition of phytodetritus under critical shear velocities ($4.8 \cdot 10^{-2} \pm 4.5 \cdot 10^{-3} \text{ g chl a m}^{-2} \text{ d}^{-1}$).

KEY WORDS: Nazaré canyon · Surface sediments · Phytodetritus · Amino acids · Lability · Biodeposition

INTRODUCTION

Over the past 10-20 years, understanding the exchange of energy and matter between the shelves and the open ocean has been the core subject of several multidisciplinary programmes (e.g. SEEP, OMEX, ECOMARGE). In several of these studies, submarine canyons have been identified as locally important conduits for particulate matter from the shelf to the deep ocean (Monaco et al. 1999, Durieu de Madron et al. 2000, Schmidt et al. 2001, Epping et al. 2002, Van Weering et al. 2002). In the Gulf of Lions, the cascading of dense shelf water induced the transport of sediments through the Cap de Creus canyon to the abyssal plain (Canals et al 2006), whereas for the Nazaré Canyon on the Western Iberian Margin, fine-grained suspended sediment from the adjacent shelf was trapped in the canyon and subsequently transported down the canyon by tidal currents and intermittent gravity flows (De Stigter et al. 2007).

The benthic fauna may play an important role in the transport and accumulation of the suspended matter. Especially suspension feeders can influence the particle transport by actively capturing particles from the water column and depositing them in or at the sediment surface (Graf & Rosenberg 1997), thus making organic matter available to benthic communities. In addition, feeding pits, faecal pellet mounds and tubes can locally change the flow, resulting in passive biodeposition of particles (Jumars & Nowell 1984, Graf & Rosenberg 1997). In the laboratory, with natural macrofaunal

communities from the Oslofjord, the concentration of phytodetritus and POC in the BBL decreased by 50% and 60% faster in the presence of benthic fauna (Thomsen & Flach 1997). In situ studies on the continental slope of the Barents Sea have shown that suspension-feeding communities increased the vertical carbon flux by a factor of 2 to 3.7 (Thomsen et al. 1995).

Most important for deep-sea benthic communities is the nutritional value of the organic matter reaching the sea floor (Gage & Tyler 1991). The quality of the organic matter in the Nazaré submarine canyon and its adjacent open slopes has not been addressed specifically. In terms of origin, the bulk organic matter throughout the Nazaré canyon is mainly derived from terrestrial sources, whereas that found on the adjacent slope and Iberian Margin is dominated by marine sources (Epping et al. 2002, De Stigter et al. 2007). The average sediment accumulation rates, derived from De Stigter et al. (2007), in the Nazaré canyon are ~18 times higher than on the adjacent open slope (22.5 and 1.26 g m⁻² d⁻¹ respectively). Assuming an average density of the mineral matrix of 2.4 g cm⁻³, the yearly sediment accumulation rate for both areas is 0.3 and 0.02 cm y⁻¹ respectively. Therefore, in the Nazaré canyon 1 cm of sediment is equivalent to 3.3 years of accumulation, whereas in the slope is equivalent to 50 years. Consequently, bulk organic matter in the surface sediment in the canyon has had less time to decay than at the open slope, and would be more concentrated and less refractory. Hence, the quality of the organic matter in this canyon could well be higher than on the adjacent slope.

As part of the EUROSTRATAFORM program and ongoing HERMES program, we studied the amount and quality of the organic matter in surface sediments of the Nazaré submarine canyon and adjacent open slope. The quality of the phytodetritus has been assessed using the chlorophyll *a* to phaeopigment ratio (Soltwedel et al. 2000, Levin et al. 2002), whereas the quality of the bioavailable organic matter has been assessed using an amino acid based degradation index (DI), and the ratios glutamic acid to β-alanine and aspartic acid to γ- amino butyric acid (Dauwe & Middelburg 1998, Dauwe et al. 1999). Using a mesocosm flume, we quantified the importance of

biogenic structures present on the canyon floor in passive biodeposition of suspended phytodetritus.

STUDY AREA

The hydrography of the Iberian Margin is dominated by a poleward current in winter favouring downwelling, and an equatorward current during summer favouring coastal upwelling, which triggers high primary production along the Iberian Margin (Vitorino et al. 2002, Coelho et al. 2003). The Iberian Margin is a productive area that exports high amounts of terrestrial and marine carbon to the open ocean (Thomsen et al. 2002). The Western Iberian Margin is characterised by a narrow shelf with a steep irregular slope and is dissected by several deep gullies and canyons. The Nazaré Canyon is the largest canyon on this margin and in Europe, and it is not directly fuelled by river discharge. The Nazaré canyon can be divided in three main sections (De Stigter et al. 2007): a) the upper part of the canyon characterized by a sharp V-shaped valley deeply incised into the shelf and steep upper slope, which begins at ~ 50 m depths and descends to ~ 2700 m depth over a length of 70 km measured along the thalweg, b) the middle part of the canyon is a broad meandering valley, with terraced slopes and V-shaped valley axial channel. It is incised into the middle slope and descends from ~ 2700 m to ~ 4000 m depth over 50 km, c) the lower canyon is a flat floored valley incised into the lower continental slope. It very gently descends from ~ 4000 m to ~ 5000 m depth over 100 km. While descending, the valley gradually increases in width from 3 km to 15 km at the mouth of the canyon. Much of the sediment being carried over the shelf and upper slope enters this canyon and is transported to the deep ocean by internal tide circulation and intermittent turbidity flows (Van Weering et al. 2002, De Stigter et al. 2007).

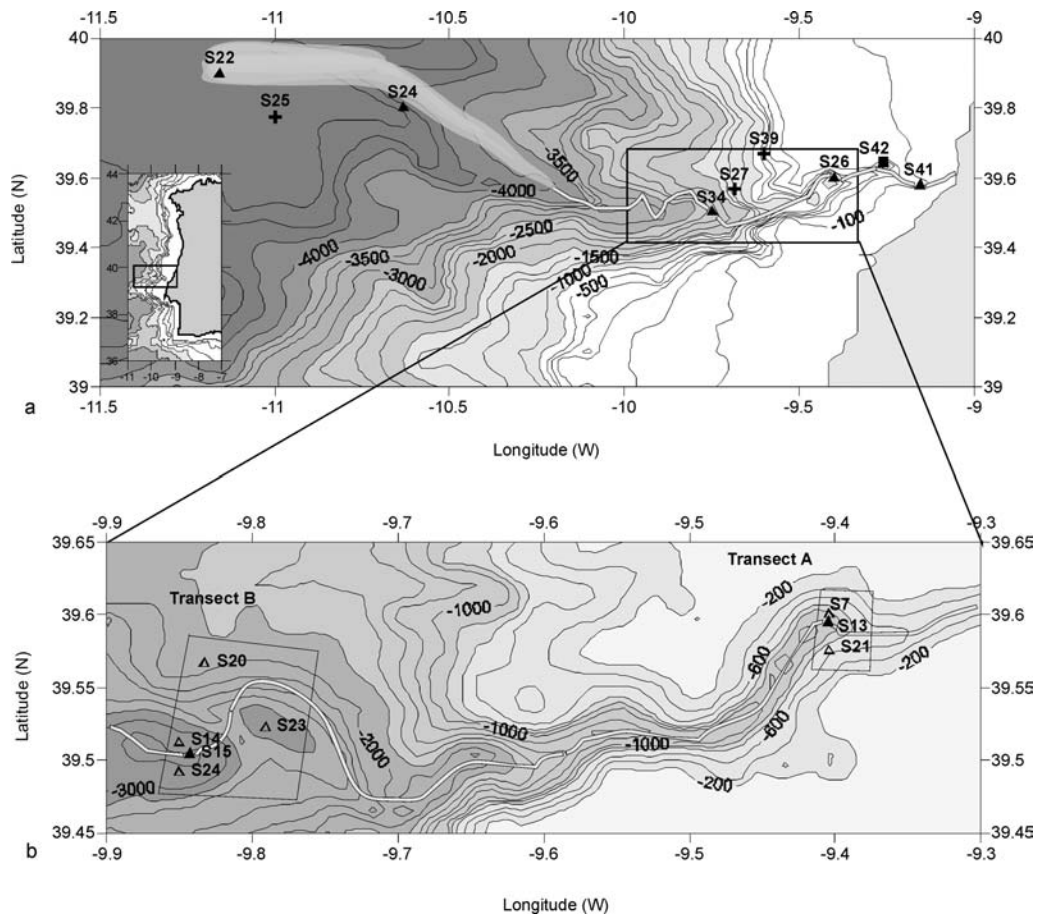


Fig. 1: Maps of the Nazaré canyon showing (a) the stations sampled during cruise 64PE225 in May 2004 and (b) during cruise 64PE236 in May 2005 with transect A in the upper canyon and transect B in the middle canyon. Stations labelled with + (S39, S27 and S25) were along the adjacent open slope; stations labelled with ▲ (S41, S26, S34, S24, S22, S13 and S15) were along the canyon axis; stations labelled with Δ were on the canyon walls (S21, S07 S20, S14, S24* and S23) Station S42 labelled with ■ corresponds to the box core taken for experimental work.

MATERIAL AND METHODS

Sampling

Surface sediment cores were collected during cruises 64PE225 and 64PE236 of RV Pelagia of Royal NIOZ in May 2004 and May 2005

respectively. In May 2004, 5 stations (S41, S26, S34, S24 and S22) along the Nazaré canyon and 3 stations (S39, S27 and S25) along the open slope were sampled (Fig. 1, Table 1). In May 2005, transect A with 3 stations (S21, S13 and S07) located in the upper canyon area at around 1000 m maximum depth, and transect B with 5 stations (S20, S14, S15, S24* and S23) located in the middle canyon area at around 3000 m maximum water depth were sampled.

At all stations, sediment samples were taken with a MUC 8+4 multiple corer developed by Oktopus GmbH, equipped with eight 6 cm diameter and four 10 cm diameter coring tubes of 61 cm length. For each station, three replicate cores ($\varnothing = 6$ cm) were used for geochemical analyses. We analysed the amino acid content of sedimentary aggregates, and the phytopigment content of surface sediments. Sedimentary aggregates for amino acid analysis were collected by siphoning the surface of each core and overlaying water with a 0.5 cm silicon tube. Aggregates were filtered over 0.2 μm filters and stored at -20°C until further analysis. The top 0.5 cm of the sediment was collected for phytopigment analysis and stored at -20°C . Cores were stored at in situ temperature in a temperature-controlled room and processed within 3 hours of collection.

Phytopigment analysis

Sediment bound chlorophyll *a* (chl *a*) and phaeopigments (phaeo) concentrations were determined following the fluorometric method of Yentsh & Menzel (1963). The sediment samples were freeze-dried and homogenised in a mortar. The pigments were extracted in 10 ml 90% acetone solution and fluorescence was measured directly in a Turner fluorometer following Shuman & Lorenzen (1975). Following Thiel (1978), the total of pigments measured is referred to as chloroplastic pigment equivalents (CPE). Chlorophyll *a* to phaeopigment (chl *a*:phaeo) concentration ratios were used to assess the freshness of phytocarbon reaching the sea floor.

Amino acid analysis

Amino acids are the most common forms of labile nitrogen found in sediments, most likely serving as principal food source for organism; and thus they are indicators of bioavailable organic matter (Cowie & Hedges 1992a). Bioavailable organic matter was assessed by HPLC measurements of the total hydrolysable amino acids (THAA) in sediment aggregates, using a slightly modified method of Cowie & Hedges (1992b) and Van Mooy et al. (2002). About 0.01 g homogenized, freeze dried material from the filters was weighed into ampoules and spiked with 0.1 ml of a charge-matched recovery standards solution: α - amino adipic acid 0.5 mM, for acidic amino acids; α -neopentyllysine 0.7 mM, for neutral amino acids; and δ -hydroxylysine 1.6 mM, for basic amino acids. After adding 1 ml 6N HCl (ultra pure) and purging with N₂ gas for 3 minutes, the sealed ampoules were hydrolysed for 24h at 110°C. After hydrolysis, samples were centrifuged at 8000 rpm for 15 minutes, and supernatants were dried on a rotor evaporator under vacuum at 55°C. The residues were resuspended in 0.5 ml ultra pure distilled water and taken into another drying cycle. This procedure was carried out twice. Finally, residues were resuspended in 1ml 0.2N H₃BO₃ buffer solution (pH = 9.5) to a final pH of 8.0 to 8.5, and transferred into clean Eppendorf vials through cellulose 0.8 μ m filters and stored at -20°C until analysis. An aliquot of the hydrolysate was made up to a volume of 450 μ l with ultra pure distilled water in HPLC vials resulting in a 10 to 40 times dilution depending on the expected amino acids concentration. Amino acids were quantified by reverse-phase HPLC (column Variant RPC18, 4.6x15cm, 5 μ m particle size, 100Å pore size) after pre-column (Phenomenex) derivatisation with ortho-phthaldialdehyde (OPA) solution (100 g OPA, 1 ml methanol, 8 ml KBO₂ pH 10.4, 103 μ l Brij-35 (Polyoxyethyleneglycol dodecyl ether) and 50 μ l Mercaptoethanol). In order to quantify between-run-variability, 25 μ l of O- methyl-threonine was added as an internal standard. Separation and quantification of fluorescent OPA derivatives were conducted on a Shimadzu HPLC. Gradient elution was carried out over 55 minutes using pure methanol and sodium acetate buffer solution (50 mM, pH = 6.4) as a solvent. The fluorescent detector was set at an

excitation wavelength of 340 nm and an emission wavelength of 455 nm. External standards of an amino acid mixture (Sigma N° 298468) were used for calibration and each sample was analysed in duplicate.

Statistical analysis

The one-sample Kolmogorov-Smirnov test was used for testing the normality of the data. Chl *a*, chl *a*:phaeo and glu:γ-aba were not normally distributed. Chl *a* was $\log_2(x + 1)$, and chl *a*:phaeo and glu:γ-aba were arcsine transformed. A nested ANOVA was constructed with water depth nested within transects to test for differences along the depth gradient in each transect. A paired sample T-test was used to test for similarity of sites between transects.

Flume experiments

During Cruise 64PE225, a boxcore was collected from Nazaré upper canyon (S42, 146 m), using a NIOZ boxcorer with 50-cm diameter cylindrical coring barrel. Before retrieval, the coring barrel was closed with a lid to prevent disturbance of the sediment-water interface. After recovery, subsamples of 30 cm diameter were taken and transported in the dark and at in situ temperature conditions to the laboratory, where they were transferred into an oval open-channel flume with channel width 76 cm, and plan area 17.68 m² ("racetrack flume"). The flow is controlled by a conveyor belt with paddles which enter the water vertically. Dimensions and propulsion system are identical to the seawater flume described by Nowell & Jumars (1987). Prior to the experiments, the benthic communities were left to adjust to the flume environment under low flow conditions (sheer velocity $u \approx 0.2 \text{ cm s}^{-1}$). The flume was calibrated at a water level of 21 cm with an average water temperature of 14°C and salinity of 34 ppt. The velocity profiles were measured with a Nortek ADV sensor at a sampling frequency of 25 Hz and each data point was measured for 30 minutes. The flume set up produced unidirectional and stable flow with a fully developed logarithmic layer over the 1 m² test section.

For each experiment simulating a "post-phytoplankton bloom", detrital aggregates from an algae culture of *Tetraselmis* and *Nannochloropsis* were added until an initial concentration of approximately 6 to 12 mg m⁻³ chlorophyll equivalents was obtained (final concentration of ~7500 aggregates dm⁻³). Chlorophyll concentrations in the flume were monitored with an in situ Turner fluorometer, calibrated with chlorophyll concentrations determined fluorometrically from water samples taken at different intervals during the length of each experiment. The critical shear velocity of the phytodetritus was determined using an erosion chamber (20 cm in diameter) according to the methods described by Thomsen & Gust (2000). Replicate flume experiments were carried out under bottom shear velocities of 0.6 cm s⁻¹ (corresponding to free stream velocities of 12 cm s⁻¹), sufficiently high to resuspend the phytodetritus. Bulk flow Reynolds number in the flume ($Re = uh/\nu$, where u = mean velocity, h = water depth, ν = kinematic viscosity) was 25 000, which according to Nowell & Jumars (1987) expresses turbulent conditions within the boundary layer.

All biodepositional fluxes presented are means calculated from the three parallel experiments. Biodepositional fluxes were obtained subtracting the depositional flux in control experiments with artificial sediments from the depositional fluxes in sediments with biogenic structures. This includes both, particle deposition to artificial sediments and deposition within the flume system (flow straighteners, corners, etc). The deposition in aggregate units was estimated from the chlorophyll concentrations in the flume over time, knowing that ~ 7500 aggregates dm⁻³ was approximately 6 to 12 mg m⁻³ chlorophyll equivalents (average ~ 8 mg m⁻³).

Table 1: Concentrations (cm^{-3} of bulk sediment) of chlorophyll a (chl a), phaeopigment (phaeo), chloroplastic pigment equivalent (CPE), the ratio of chlorophyll a to phaeopigments (chl a:phaeo) on the top 0.5 cm of sediment, and total hydrolyzable amino acids (THAA), degradation index (DI) and asp: β -ala and glu: γ -aba molar ratios on sediment aggregates in the Nazaré canyon transects and the open slope transect, \pm standard error; and nested ANOVA testing for differences with water depth within each transect.

Cruise	Site	Latitude (N)	Longitude (W)	Depth (m)	chl a ($\mu\text{g cm}^{-3}$)	phaeo ($\mu\text{g cm}^{-3}$)	CPE ($\mu\text{g cm}^{-3}$)	THAA (mg g^{-1})	chl a:phaeo	DI	asp: β -ala	glu: γ -aba	
<i>Transect along open slope May 2004</i>													
64PE225	S39	39° 39.9'	9° 35.9'	307	0.11 \pm 0.022	6.45 \pm 1.062	6.56 \pm 1.079	1.6 \pm 0.3	0.02 \pm 0.002	0.10	9.00 \pm 3.13	27.86 \pm 23.55	
64PE225	S27	39° 33.9'	9° 40.9'	1000	0.13 \pm 0.019	4.00 \pm 0.852	4.14 \pm 0.870	4.0 \pm 0.4	0.04 \pm 0.004	-0.30	5.87 \pm 1.10	4.71 \pm 0.73	
64PE225	S25	39° 46.5'	10° 59.9'	4798	0.02 \pm 0.002	1.07 \pm 0.103	1.09 \pm 0.101	3.5 \pm 0.5	0.02 \pm 0.003	-0.42	3.92 \pm 0.21	3.44 \pm 0.11	
<i>Transect along canyon May 2004</i>													
64PE225	S41	39° 34.8'	9° 09.2'	332	4.20 \pm 0.982	26.74 \pm 4.151	30.94 \pm 5.134	9.4 \pm 0.8	0.16 \pm 0.015	0.13	10.32 \pm 0.14	8.72 \pm 0.84	
64PE225	S26	39° 35.9'	9° 23.9'	1121	0.75 \pm 0.165	14.67 \pm 2.610	15.42 \pm 2.775	7.2 \pm 0.6	0.05 \pm 0.002	0.24	11.36 \pm 1.12	14.91 \pm 1.76	
64PE225	S34	39° 30.0'	9° 45.0'	2847	0.25 \pm 0.000	13.69 \pm 0.000	13.69 \pm 0.000	5.0 \pm 0.0	0.02 \pm 0.000	-0.24	7.12 \pm 0.00	5.47 \pm 0.00	
64PE225	S24	39° 48.0'	10° 37.9'	4810	0.05 \pm 0.000	2.85 \pm 0.000	2.85 \pm 0.000	4.8 \pm 0.4	0.02 \pm 0.000	-0.36	4.85 \pm 0.39	4.42 \pm 0.30	
64PE225	S22	39° 53.9'	11° 10.0'	4969	0.03 \pm 0.010	1.77 \pm 0.083	1.77 \pm 0.089	3.5 \pm 0.1	0.02 \pm 0.005	-0.66	4.19 \pm 0.51	3.94 \pm 0.28	
<i>Transect A (upper canyon) May 2005</i>													
64PE236	S21	39° 34.5'	9° 24.3'	532	0.30 \pm 0.153	7.97 \pm 3.947	8.27 \pm 4.097	2.7 \pm 0.1	0.04 \pm 0.003	-0.43	8.14 \pm 1.08	19.91 \pm 7.32	
64PE236	S13	39° 35.8'	9° 24.2'	927	0.64 \pm 0.186	17.07 \pm 4.293	17.71 \pm 4.478	6.0 \pm 0.5	0.04 \pm 0.003	-0.39	9.62 \pm 1.78	8.06 \pm 1.46	
64PE236	S07	39° 35.9'	9° 24.3'	1160	0.45 \pm 0.104	11.72 \pm 2.959	12.17 \pm 3.053	5.5 \pm 0.1	0.04 \pm 0.005	-0.50	7.07 \pm 0.81	7.63 \pm 1.23	
<i>Transect B (middle canyon) May 2005</i>													
64PE236	S20	39° 33.9'	9° 49.9'	1884	0.15 \pm 0.040	6.17 \pm 1.602	6.32 \pm 1.642	5.1 \pm 0.1	0.02 \pm 0.001	-0.52	5.70 \pm 0.54	7.41 \pm 2.87	
64PE236	S14	39° 30.7'	9° 51.0'	3091	0.14 \pm 0.036	5.09 \pm 1.755	5.22 \pm 1.791	4.1 \pm 0.1	0.03 \pm 0.006	-0.74	7.18 \pm 0.14	7.98 \pm 0.06	
64PE236	S15	39° 30.2'	9° 50.6'	3239	0.41 \pm 0.097	10.43 \pm 1.521	10.85 \pm 1.617	5.2 \pm 0.6	0.04 \pm 0.003	-0.40	9.00 \pm 1.43	8.65 \pm 0.69	
64PE236	S24*	39° 29.5'	9° 51.0'	3200	0.30 \pm 0.077	9.07 \pm 2.327	9.37 \pm 2.404	6.9 \pm 1.6	0.03 \pm 0.001	-0.38	7.46 \pm 1.25	8.50 \pm 0.84	
64PE236	S23	39° 31.3'	9° 47.5'	2844	0.13 \pm 0.051	4.24 \pm 1.774	4.37 \pm 1.825	4.0 \pm 1.3	0.03 \pm 0.004	-0.79	5.64 \pm 0.00	6.76 \pm 0.00	
Nested ANOVA					F	16.48	4.64	5.16	7.13	25.17	4.34	3.34	1.58
					p	≤ 0.001	≤ 0.001	≤ 0.001	≤ 0.001	≤ 0.001	≤ 0.01	≤ 0.05	> 0.05

RESULTS

Phytopigments in surface sediments and amino acids in sediment aggregates

For the open slope, the concentrations of chlorophyll *a* (chl *a*), phaeopigments (phaeo) and chloroplastic pigment equivalents (CPE) decreased with increasing water depth. In contrast, the concentration of total hydrolysable amino acids (THAA) increased (Fig. 2).

Along the canyon axis, these concentrations were significantly higher at corresponding water depths (Fig. 2, Table 1, 2). The highest concentrations (S41, 332 m and S26, 1121 m) were measured where the canyon was narrow (Fig. 1) and not yet open to the wider continental slope. All parameters showed a clear decrease with increasing water, approaching open slope values at the deepest station at 4969 m (S22). The differences in concentrations with depth within each transect were statistically significant (Table 1).

In cross-canyon transects, higher contents of CPE, chl *a*, phaeo were generally found on the canyon axis than on the walls (Fig. 3, Table 1). THAA concentrations increased towards the canyon axis in the upper canyon (transect A), but no significant trend was observed in the middle canyon (transect B).

Table 2: Paired samples two tailed T-Student test

Pair stations	chl <i>a</i>		phaeo		CPE		THAA		chl <i>a</i> :phaeo		DI		asp:β-ala		glu:γ-aba	
	T	p≤	T	p≤	T	p≤	T	p≤	T	p≤	T	p≤	T	p≤	T	p≤
S41-S39	9.6	0.01	4.7	0.05	4.9	0.05	14.8	0.05	17.8	0.01	18.2	0.05	0.4	ns	-0.5	ns
S26-S27	5.7	0.05	5.3	0.05	5.2	0.05	16.1	0.05	2.7	ns	4.4	ns	2.5	ns	4.3	ns
S24-S25	32.4	0.001	29.1	0.001	30	0.001	14.6	0.05	-0.5	ns	0.3	ns	8.2	ns	6.3	ns
S22-S25	1.2	ns	4.7	0.05	4.7	0.05	-0.1	ns	-0.3	ns	-1.1	ns	1.2	ns	1.3	ns

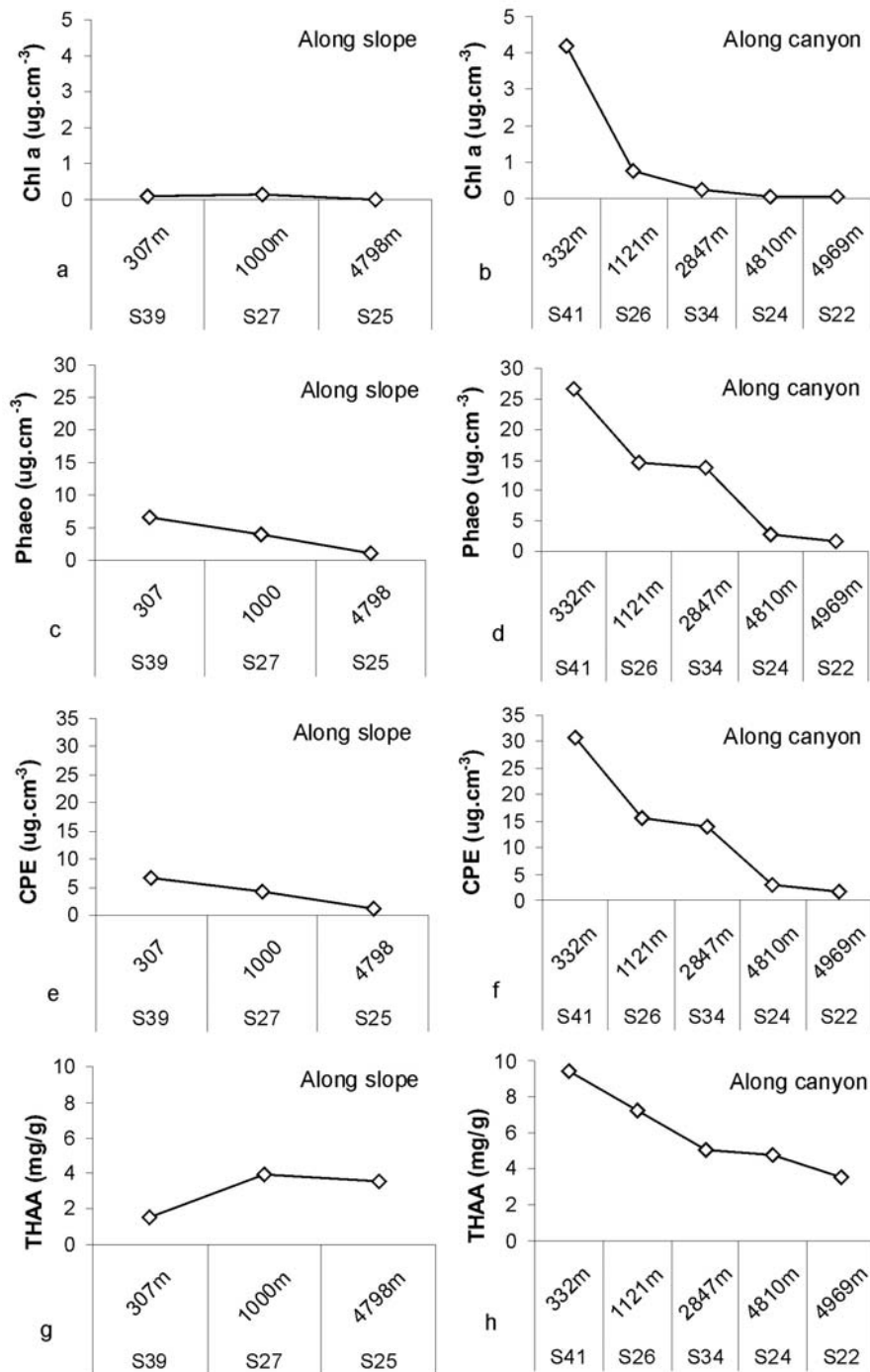


Fig. 2: Concentrations of (a,b) chlorophyll a (chl a), (c,d) phaeopigment (phaeo), (e,f) chloroplastical pigment equivalent (CPE) in surface sediments, and (g,h) total hydrolysable amino acid contents (THAA) in sediment aggregates along the open slope (left panel) and along the Nazaré canyon (right panel).

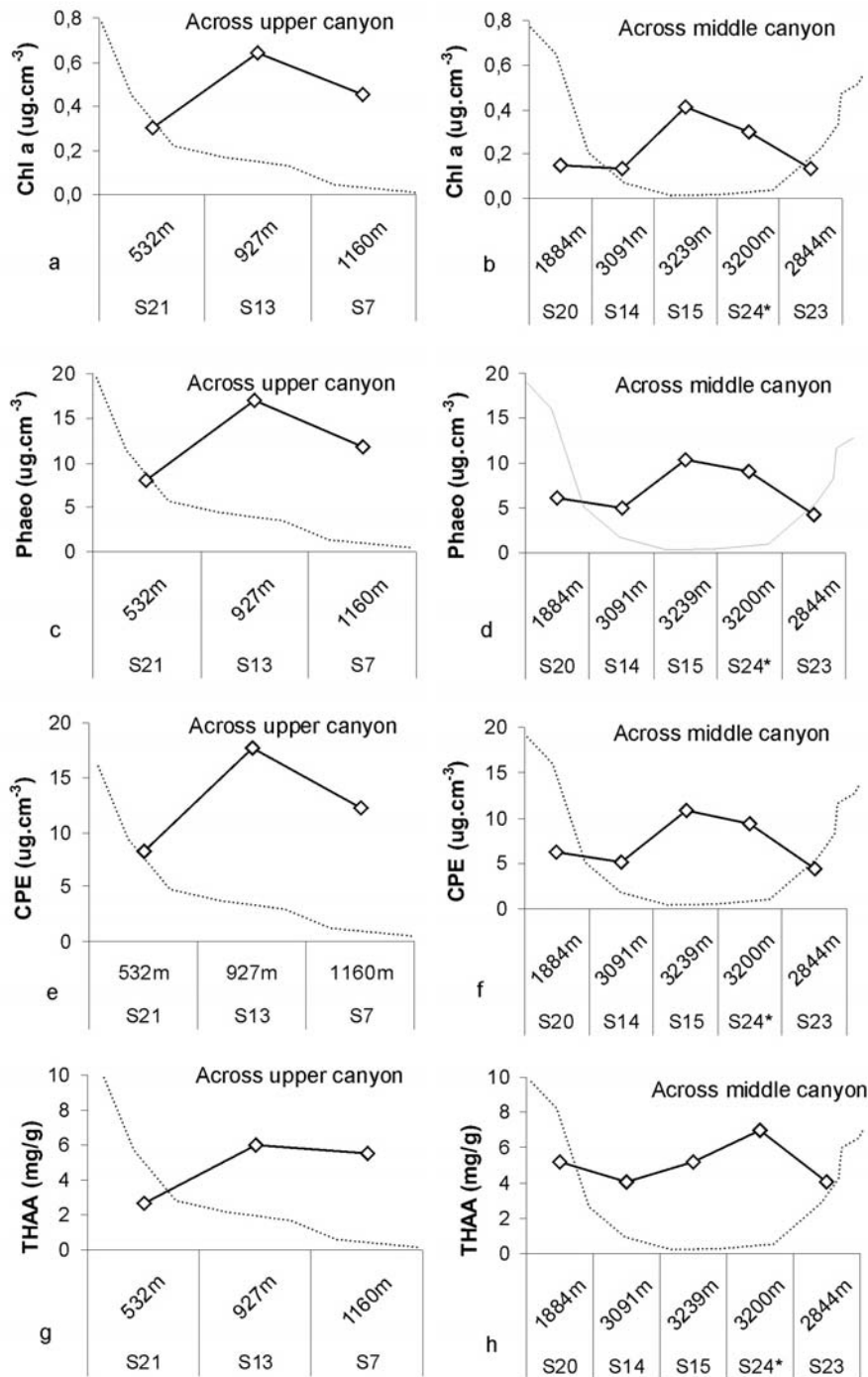


Fig. 3: Concentrations of (a,b) chlorophyll a (chl a), (c,d) phaeopigment (phaeo), (e,f) chloroplastical pigment equivalent (CPE) in surface sediments, and (g,h) total hydrolysable amino acid contents (THAA) in sediment aggregates across the upper Nazaré canyon (transect A, left panel) and across the middle Nazaré canyon (transect B, right panel). The dotted lines indicate schematically the canyon floor cross section.

Lability of organic matter in surface sediments and sediment aggregates

For the open slope, the chlorophyll *a* to phaeopigments ratio (chl *a*:phaeo) remained constant with increasing water depth, whereas the degradation index (DI) and the asp:β-ala and glu:γ-aba ratios showed a clear decrease (Fig 4a, c, e).

Along the canyon axis, the chl *a*:phaeo ratio, as well as the DI and the asp:β-ala and glu:γ-aba ratios showed a clear decrease with increasing water depth (Fig 4b, d, f). Generally, the differences with depth within each transect were statistically significant, except for glu:γ-aba (Table 1). The lability indices were highest at the upper canyon stations S41 and S26 (Fig. 4, Table 1). The chl *a*:phaeo ratio and DI were significantly higher at station S41 in the upper canyon than at station S39 at equivalent water depth on the slope (Table 2). No significant differences in chl *a*:phaeo ratio and DI were found between the remaining canyon and open slope deeper stations.

The results indicate that the organic matter becomes more refractory with depth along both the canyon axis and the open slope. The similarity in the ratios asp:β-ala and glu:γ-aba suggest that there is no significant difference in organic matter lability between the canyon and open slope for similar water depths.

Within cross canyon transects, no significant trend was found in chl *a*:phaeo ratio (Fig. 5a,b). The DI was low and constant across the upper canyon (transect A) (Fig. 5c). For the middle canyon (transect B), DI was equally low, with minimum values at the lower slope of the wall (Fig. 5d). In the upper canyon, the asp:β-ala ratio was highest at station S13 (Fig. 5e), whereas glu:γ-aba ratio decreased with increasing water depth. In the middle canyon (Fig. 5f), asp:β-ala ratio showed maximum values in the deepest part of the canyon, whereas the glu:γ-aba ratio remained similar across the canyon.

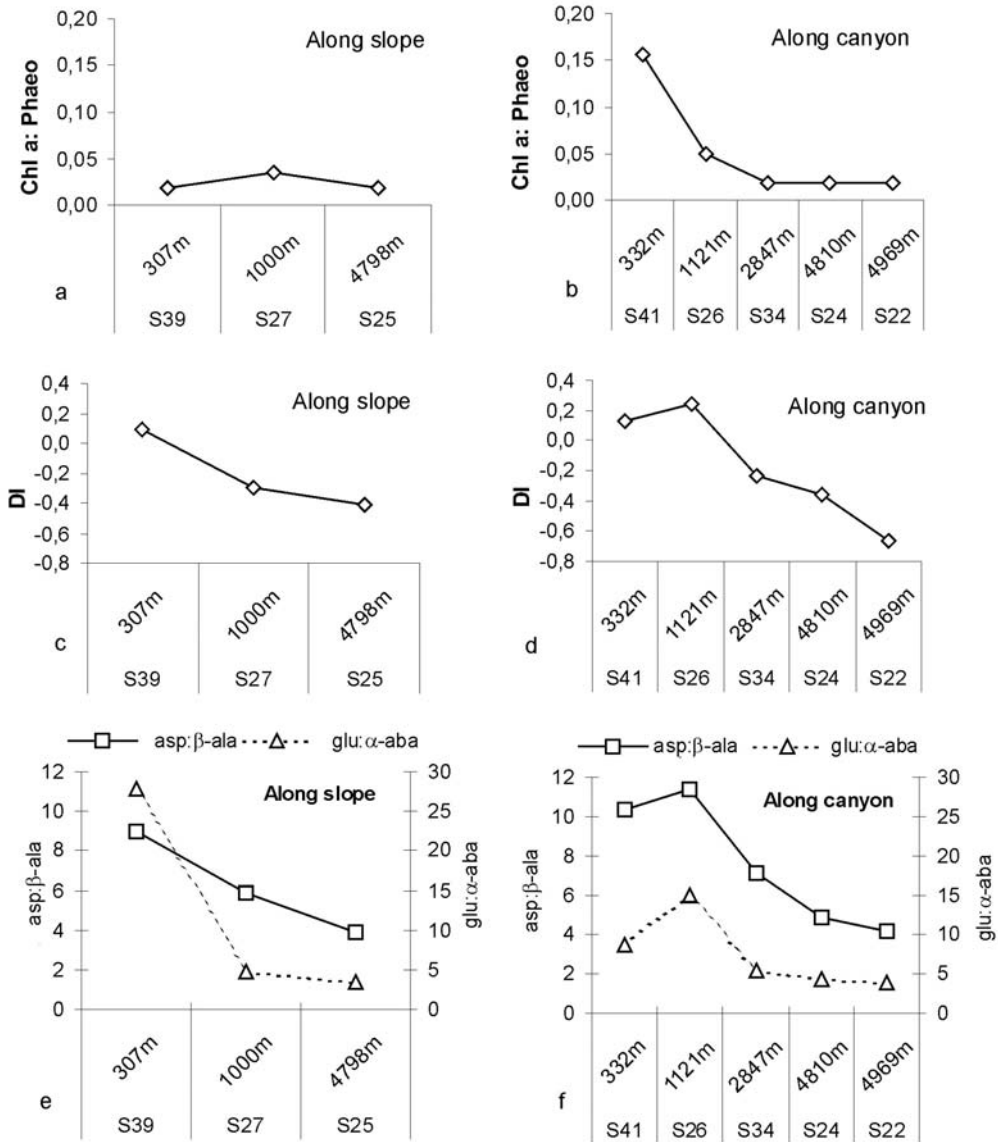


Fig. 4: (a,b) chl a:phaeo ratio in surface sediments, (c,d) degradation index (DI) and (e,f) asp:β-ala and glu: γ-aba ratios in sediment aggregates along the open slope (left panel) and along the Nazaré canyon (right panel).

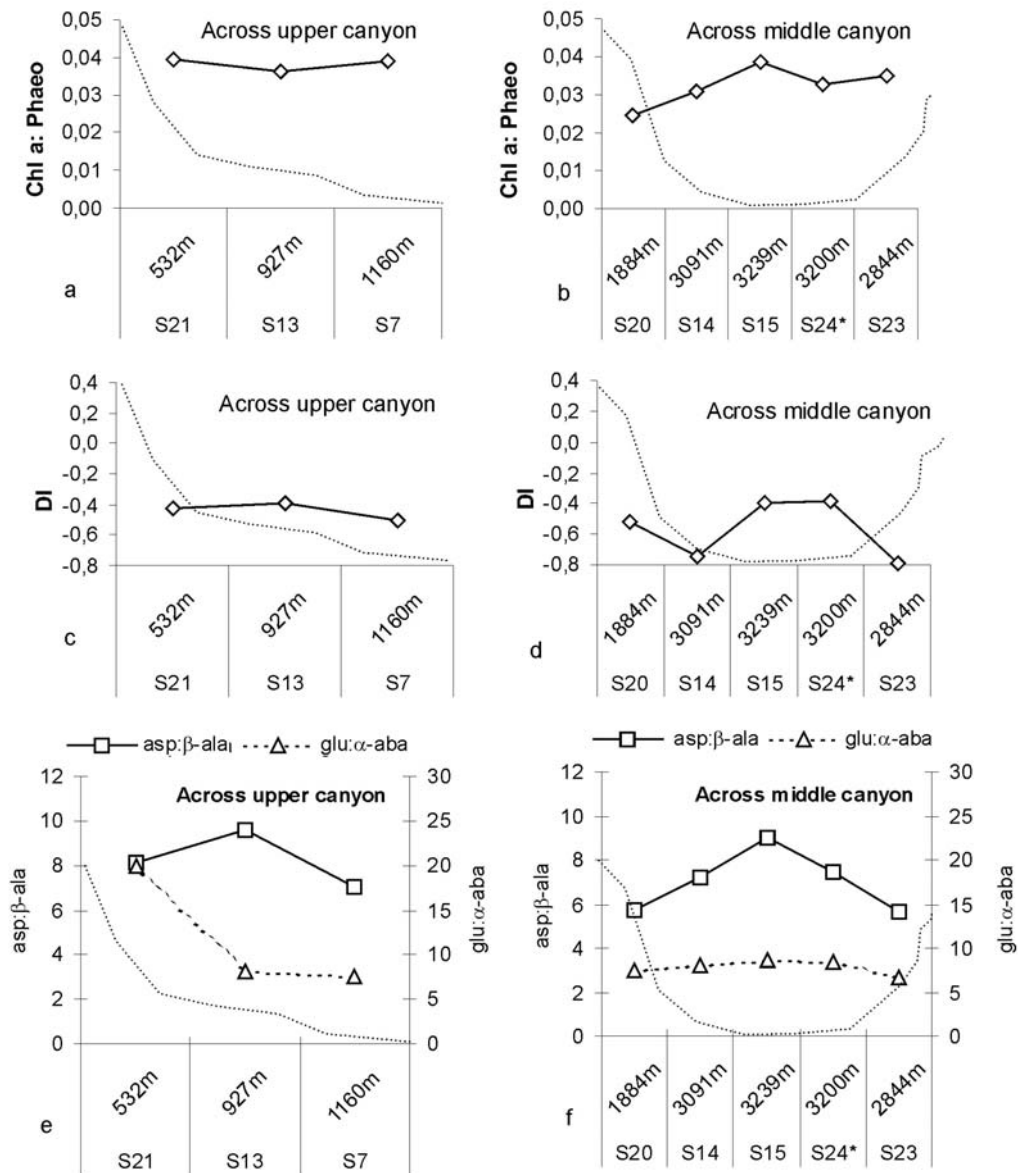


Fig. 5: (a,b) chl a:phaeo ratio in surface sediments, (c,d) degradation index (DI) and (e,f) asp:β-ala and glu: γ-aba ratios in sediment aggregates across the upper Nazaré canyon (transect A, left panel) and across the middle Nazaré canyon (transect B, right panel). The dotted lines indicate schematically the canyon floor cross section.

Biodeposition of algae aggregates

Small suspension feeding fauna forming biogenic structures on the surface of the sediment are found on the Nazaré canyon (Fig. 6). A total of 17 biogenic structures were identified from a 30 cm diameter mesocosm sample taken in the upper canyon. 13 structures corresponded to tube building fauna such as agglutinated foraminifera, 2 structures were polychaete pellet mounds and 2 were holes. This corresponds to a density of 200 biogenic structures m^{-2} . Under the experimental conditions and at critical shear velocity of $0.6 \text{ cm}\cdot\text{s}^{-1}$, a net deposition of phytodetritus aggregates was observed in the presence of biogenic structures as well as in the control experiment (Fig. 7, Table 3). The deposition rates in experiments with biogenic structures, calculated from the chlorophyll measurements over time, always exceeded the rates in control experiments (Table 3). The net biodeposition rate was estimated at $4.8 \cdot 10^{-2}$ (s.d. $4.5 \cdot 10^{-3}$) $\text{g chl } a \text{ m}^{-2} \text{ d}^{-1}$.

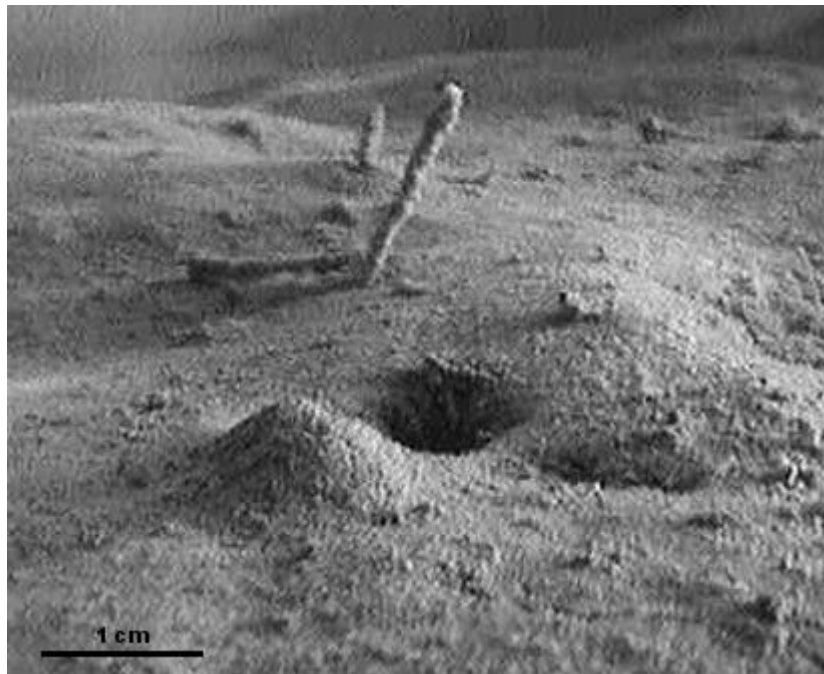


Fig. 6: Benthic biogenic structures present in the Nazaré canyon floor at station S42 (146 m) at the head of the canyon.

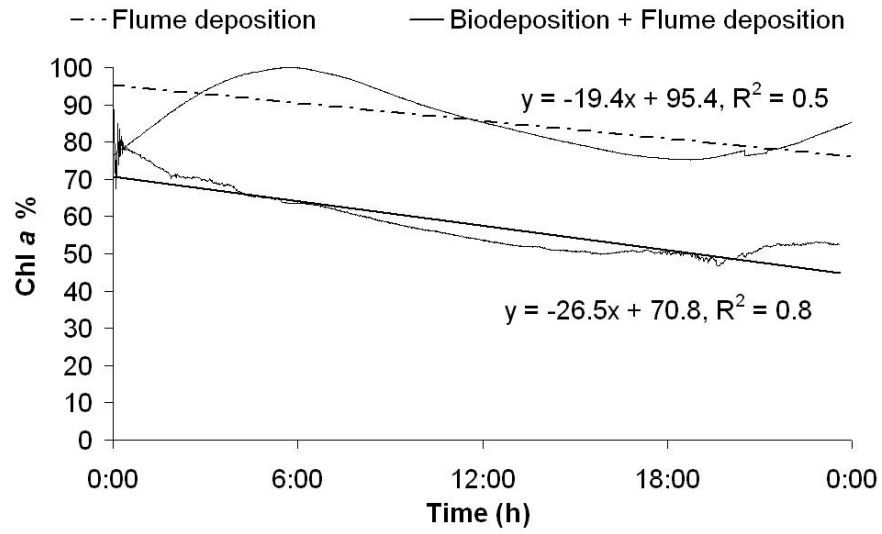


Fig. 7: Percentage decrease of chlorophyll a in the flume tank over time and under critical shear velocity of 0.6 cm.s^{-1} , with sediments containing biogenic structures (solid lines) and with control sediments (dashed line).

Table 3: Average deposition rates of algae aggregates ($\text{aggregates m}^{-2} \text{ d}^{-1}$) and chlorophyll a ($\text{g chl a m}^{-2} \text{ d}^{-1}$) on the Nazaré canyon mesocosm sample (30 cm^2 in diameter) during the experimental runs with fauna, during the control runs without fauna, and the resulting biodeposition. These deposition rates are calculated from the chlorophyll profiles obtained for each experimental run.

	Average deposition rates	
	$\text{aggregates.m}^{-2} \text{ d}^{-1} (\pm \text{SE})$	$\text{g chl a .m}^{-2} \text{ d}^{-1} (\pm \text{SE})$
Experiment with fauna	$17.6 \cdot 10^7 \pm 47.4 \cdot 10^6$	$1.6 \cdot 10^{-1} \pm 2.4 \cdot 10^{-2}$
Control without fauna	$12.3 \cdot 10^7 \pm 33.2 \cdot 10^6$	$1.1 \cdot 10^{-1} \pm 1.9 \cdot 10^{-2}$
Biodeposition	$52.9 \cdot 10^6 \pm 14.2 \cdot 10^5$	$4.8 \cdot 10^{-2} \pm 4.5 \cdot 10^{-3}$

DISCUSSION

Organic matter and lability patterns

The present study shows that the concentration of chl *a*, phaeo, CPE and THAA were significantly higher in the canyon stations than on the slope stations at equivalent water depths (Fig 2.), indicating that the Nazaré canyon accumulates higher amounts of phytodetritus and bioavailable organic matter than the open slope. This observation is in line with previous findings of higher sedimentary organic matter contents in the Nazaré canyon (Schmidt et al. 2001, Epping et al. 2002, Van Weering et al. 2002). Similar trends between canyons and adjacent slopes stations have been observed for other continental margin sediments (e.g. Duineveld et al. 2001, Riaux-Gobin et al. 2004, Fontanier et al. 2005). The differences in organic contents along the Nazaré canyon and adjacent slope could not be explained by the slightly different average particle size between canyon and slope sediments (~ 13 μm and ~ 8 μm respectively) (De Stigter et al. 2007). Within the canyon, the thalweg accumulates higher contents of organic matter, as shown by the higher chl *a*, phaeo, CPE and THAA concentrations along the axis relative to the walls. Moreover, the concentration of phytopigments and THAA decreased with increasing water depth, in parallel to the sedimentation rates measured in the Nazaré canyon (De Stigter et al. 2007). The relatively high organic content in the upper canyon indicates that a substantial part of the organic matter enters the canyon through the upper regions. The increasing content of phytopigments and THAA towards the axis suggests that the organic matter is transported laterally from the slope into the middle canyon via the walls.

The quality of phytodetritus and bioavailable organic matter (chl *a*:phaeo ratios, DI values, asp: β -ala and glu: γ -aba ratios) was higher in the upper canyon than in the deeper canyon and open slopes (Fig. 4), suggesting that the organic matter entering the canyon in the upper regions is relatively fresh. Across the canyon, this organic matter shared similar low labilities (constant chl *a*:phaeo ratio and DI) (Fig 5), and the DI was characteristic of

refractory POM from deep-sea sediments (Dauwe et al. 1999). The asp: β -ala and glu: γ -aba ratios however, were not consistent in their behaviours (Figure 5e,f). In the upper cross canyon section, the low glu: γ -aba ratio nearer the axis suggested more refractory conditions in the axis than in the walls, but the constant asp: β -ala ratios suggested similar lability across the canyon. In the middle cross canyon section, the constant glu: γ -aba ratios suggested similar low labilities across the canyon; but the higher asp: β -ala ratio near the axis suggested less refractory conditions in the axis. These trends are believed to be the result of different degradation pathways of asp and glu into their respective β -ala and γ -aba degradation products, or to different degradation rates, or both (Lee et al. 2000). The inconsistency in these ratios yields doubts about their validity as a good measure of organic matter lability.

The phytodetritus in the Nazaré canyon and adjacent slope surface sediments is very refractory when compared to the Yermak Plateau and western European continental margins (Soltwedel 1997, Soltwedel et al. 2000), and falls within the range recorded for Mediterranean canyons (Riaux-Gobin et al. 2004). The DI, asp: β -ala and glu: γ -aba ratios values are within the range recorded for the Skaggerrak, a deposition area of refractory organic matter in the North Sea (Dauwe & Middelburg 1998). As observed for the Mid Atlantic Bight (Biscaye et al. 1994), labile organic matter from primary production on the western Iberian Margin may be partly mineralised on the shelf areas, leaving the refractory fraction to be transported down canyon and slope.

The Nazaré canyon receives high amounts of organic matter from terrestrial origin (Epping et al. 2002, De Stigter et al. 2007), diluting the fresh phytodetritus and bioavailable organic matter. Based on the ratio THAA:TOC (Cowie & Hedges 1994, Dauwe & Middelburg 1998), the chl *a*:OM and THAA:OM ratios can be used as indicators of bulk organic matter quality. Using organic matter contents reported by De Stigter et al. (2007) chl *a*:OM and THAA:OM reveal similar carbon qualities for both canyon and slope surface sediments (Fig. 8a, b). This suggests that the quality of the bulk organic matter in the benthic boundary layer is similar for both areas, and thus

the quality of the material deposited on the sediment independent of the higher sedimentation rates reported for the canyon (De Stigter et al. 2007) (see Introduction). Fine sediments are resuspended and transported up and down the Nazaré canyon by strong bottom currents during each flooding and ebbing tide, deposition occurring during the slack tide (De Stigter et al. 2007). This means that refractory organic matter from deeper canyon regions is transported up canyon and mixed with fresher shelf material entering the canyon as indicated by the 10 times higher chl α :OM ratio and higher quality indices (chl α :phaeo, DI, etc.), phenomenon that may be diluting the quality of the organic matter to slope levels.

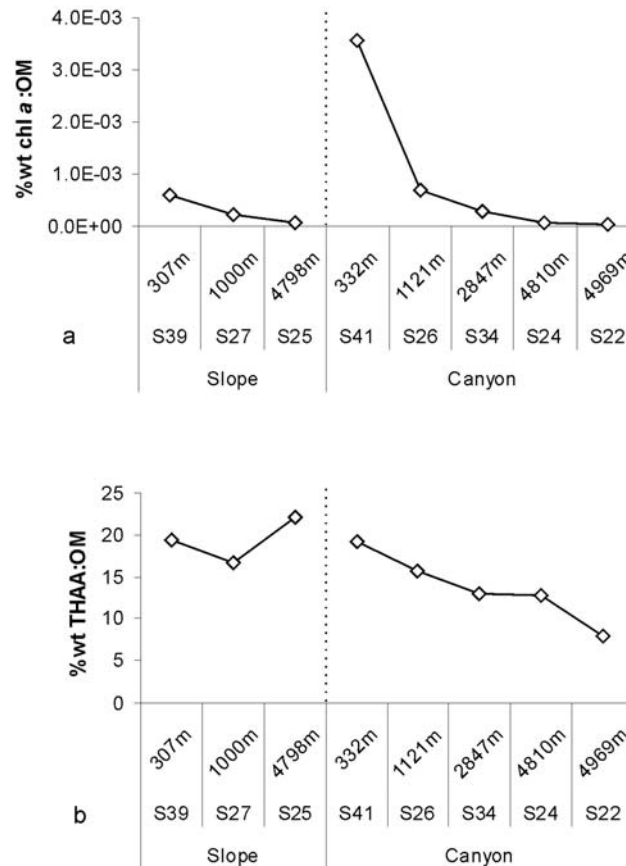


Fig. 8: a) Bioavailable phytodetritus (chl α :OM, weight %) and b) bioavailable organic matter (THAA:OM, weight %) in surface sediments along Nazaré canyon and the open slope.

Summarizing, the canyon in general, and especially the upper region, shows considerably higher contents of phytodetritus and bioavailable organic matter than the adjacent open slope. The bulk organic matter quality is similar for the canyon and open slope, but the quality of phytodetritus and bioavailable organic matter is higher in the upper canyon, indicating that fresh material enters the canyon predominantly from the shelf. Therefore, organic matter would be more available to consumers in the upper canyon, where a higher abundance of meiofauna has been observed (García et al. 2007).

Biodeposition in the Nazaré canyon

In line with observations of arborescent agglutinated foraminifera on the terraces of the upper Nazaré canyon (Koho et al. *in rev*), a density of 200 biogenic structures m^{-2} , mostly dominated by arborescent foraminifera, has been observed for the present study. This density accounted for an average deposition rate of $4.8 \cdot 10^{-2} \pm 4.5 \cdot 10^{-3} \text{ g chl } a \text{ m}^{-2} \text{ d}^{-1}$ when incubated in a flume. The physical characteristics of the artificial aggregates used in the experiment were similar to those of natural aggregates in the upper Nazaré canyon. The median size of natural aggregates in the upper part of the canyon ranged between 140 and 220 μm , with a settling velocity ranging between 0.02 and 0.04 cm s^{-1} and a critical shear velocity between 0.57 and 0.88 cm s^{-1} (Mendes *pers comm*). The median size of the artificial aggregates was 234 μm , their average settling velocity was 0.05 cm s^{-1} , and critical shear velocity was 0.6 cm s^{-1} . Therefore, the biodeposition rates estimated from the flume experiment and the real biodeposition rates under natural condition may compare well.

At the critical shear velocity (0.6 cm s^{-1}) no deposition of algae aggregates is to be expected, as it corresponds to the velocity at which artificial aggregates were always in suspension in the water column. Benthic flumes, however, cannot fully mimic field conditions and aggregates get temporarily caught in the flow straighteners and corners. Consequently, cycles of deposition and resuspension of material are observed in control experiments (Fig. 7). The net deposition during control experiments is subtracted from the net deposition in experimental runs, to yield the deposition due to biogenic

structures in natural sediments (Table 3). This deposition ($4.8 \cdot 10^{-2} \pm 4.5 \cdot 10^{-3}$ g chl *a* m⁻² d⁻¹) corresponds to an annual chl *a* deposition of 17.52 ± 1.65 g chl *a* m⁻² y⁻¹. The average chlorophyll *a* concentration during the flume experiments was 8 mg m⁻³, whereas average in situ concentrations of chlorophyll in the benthic boundary layer (BBL) at continental margins are as low as 0.1 mg m⁻³ (Thomsen & Ritzrau 1996, Lavaleye et al 2002). Assuming a linear relationship between deposition and aggregate concentration a corrected annual biodeposition rate of 0.2 g chl *a* m⁻² y⁻¹ is predicted. Considering a C:Chl conversion factor of 40 (Pusceddu et al. 1999) the annual carbon flux in the head of canyon due to biodeposition would be 8 g C m⁻² y⁻¹ which is 50% of the flux estimated by Epping et al (2002). A 50% higher particle deposition rate due to animal activities has been reported for typical continental margin settings (Graf & Rosenberg 1997, Thomsen et al. 2002). The sediments chl *a* concentration in the upper canyon were higher than on the open slope. Thus, the chl *a* concentration in the BBL in the canyon may be higher than the one reported for continental margins, and the chl *a* biodeposition rate in the canyon could be underestimated.

Conclusions

High amounts of organic matter accumulate in the Nazaré submarine canyon, especially in the narrow upper/middle regions. The flume experiments demonstrate that benthic biogenic structures contribute substantially to the deposition of phytodetritus at critical shear velocities. In the upper canyon the quality of bulk organic matter is lowered by dilution with more refractory material transported upwards the canyon from deeper regions by tidal circulation. Organic matter from the upper/middle regions is also flushed down canyon by the tides. At 2000 to 3000 m the canyon widens, and the organic matter is dispersed over a larger area, explaining the lower concentrations of phytodetritus and amino acids recorded in the middle/deeper canyon regions. Organic matter undergoes diagenetic alteration during accumulation and transport; hence the bulk and bioavailable organic matter in the middle and lower canyon was more refractory than on

the upper canyon. The increasing content of phytodetritus and bioavailable organic matter towards the canyon axis suggests that the organic matter is transported laterally from the slope into the canyon via the walls.

ACKNOWLEDGEMENTS

This study was supported by EUROSTRATAFORM project, EC contract EVK3-CT-2002-00079 funded by the European Commission, DG-XII; and the HERMES project, EC contract OCE-CT-2005-511234 funded by the European Commission's Sixth Framework Program under the priority Sustainable Development, Global Change and Ecosystems. Ship time on RV 'Pelagia' was provided by Royal NIOZ, Texel, The Netherlands. The authors thank all of the crew from the RV 'Pelagia' for their work, and several researchers participating in both cruises for the valuable help provided during core deployment, retrieval and sample processing. We thank A. Palacz for helping with chloropigment measurements, A. Moje for her work with HPLC analysis, and A. Purser for proofreading the English of the manuscript. We are very thankful to both reviewers and to Dr. Eric Epping for the constructive critics made on the manuscript.

LITERATURE CITED

- Biscaye PE, Flagg CN, Falkowski PG (1994) The shelf edge exchange processes experiment, SEEP-II: an introduction to hypotheses, results and conclusions. *Deep-Sea Res Part II-Top Stud Oceanogr* 41 (2-3):231-252
- Canals M, Puig P, Durrieu de Madron X, Heussner S, Palanques A, Fabres J (2006) Flushing submarine canyons. *Nature* 444:354-357

- Coelho H, Garcia AC, Neves R (2003) Aspects of circulation over submarine canyons: A numerical study 4th Symposium on the Iberian Atlantic Margin. *Thalassas (Rev Cienc Mar Santiago de Compostela)* 19:141-143
- Cowie GL, Hedges JI (1992a) Sources and reactivities of amino acids in a coastal marine environment. *Limnol Oceanogr* 37:703-724
- Cowie GL, Hedges JI. (1992b) Improved amino acid quantification in environmental samples: charge-matched recovery standards and reduced analysis time. *Mar Chem* 37:223–238.
- Cowie GL, Hedges JI (1994) Biochemical indicators of diagenetic alteration in natural organic mixtures. *Nature* 369:304-307
- Dauwe B, Middelburg JJ (1998) Amino acids and hexosamines as indicators of organic matter degradation state in North Sea sediments. *Limnol Oceanogr* 43:782-798
- Dauwe B, Middelburg JJ, Herman PMJ, Heip CHR (1999) Linking diagenetic alteration of amino acids and bulk organic matter reactivity. *Limnol Oceanogr* 44:1809-1814
- De Stigter HC, Boer W, Dias de Jesus CC, Thomsen L, Van den Bergh G, Van Weering TCE (2007) Sediment transport and deposition in Nazaré Canyon, Portuguese continental margin. *Mar Geol* (doi: 10.1016/j.margeo.2007.04.011).
- Duineveld G, Lavaleye M, Berghuis E, de Wilde P (2001) Activity and composition of the benthic fauna in the Whittard Canyon and the adjacent continental slope (NE Atlantic). *Oceanol Acta* 24:69-83
- Durieux de Madron X, Abassi A, Heussner S, Monaco A, Aloisi JC, Radakovitch O, Giresse P, Buscail R, Kerherve P (2000) Particulate matter and organic carbon budgets for the Gulf of Lions (NW Mediterranean). *Oceanol Acta* 23 (6):717-730
- Epping E, van der Zee C, Soetaert K, Helder W (2002) On the oxidation and burial of organic carbon in sediments of the Iberian margin and Nazaré Canyon (NE Atlantic). *Prog Oceanogr* 52:399-431

- Fontanier C, Jorissen FJ, Chaillou G, Anschutz P, Grémare A, Griveaud C (2005) Live foraminiferal faunas from a 2800 m deep lower canyon station from the Bay of Biscay: Faunal response to focusing of refractory organic matter. *Deep-Sea Res Part I-Oceanogr Res Pap* 52:1189-1227
- Gage JD, Tyler PA (1991) *Deep-sea biology: A natural history of organisms at the deep-sea floor*, Vol. Cambridge University Press, Cambridge
- García R, Koho KA, De Stigter HC, Epping E, Koning E, Thomsen L (2007) Distribution of meiobenthos in the Nazaré Canyon and adjacent slope (western Iberian Margin) in relation to sedimentary composition. *Mar Ecol Prog Ser* 240: 207-220
- Graf G, Rosenberg R (1997) Bioresuspension and biodeposition: A review. *J Mar Sys* 11:269-278
- Koho K.A., Kouwenhoven T.J, de Stigter H.C., van der Zwaan G.J. (*in revision*) Benthic foraminifera in the Nazaré canyon, Portuguese continental margin: influence of sedimentary disturbance on fauna. *Mar Micropaleontol*
- Jumars PA, Nowell ARM (1984) Effects of benthos on sediment transport: difficulties with functional grouping. *Cont Shelf Res* 3:115-130
- Lavaleye MSS, Duineveld GCA, Berghuis EM, Kok A, Witbaard RI (2002) A comparison between the megafauna communities on the N.W. Iberian and Celtic continental margins—effects of coastal upwelling? *Progr Oceanogr* 52:459–476
- Lee C, Wakeham SG, Hedges JI (2000) Composition and flux of particulate amino acids and chloropigments in equatorial Pacific seawater and sediments. *Deep-Sea Res Part I-Oceanogr Res Pap* 47:1535-1568
- Levin L, Gutierrez D, Rathburn A, Neira C, Sellanes J, Munoz P, Gallardo V, Salamanca M (2002) Benthic processes on the Peru margin: a transect across the oxygen minimum zone during the 1997-98 El Niño. *Progr Oceanogr* 53:1-27

- Monaco A, Durieux de Madron X, Radakovitch O, Heussner S, Carbonne J (1999) Origin and variability of downward biogeochemical fluxes on the Rhône continental margin (NW Mediterranean). *Deep-Sea Res Part I-Oceanogr Res Pap* 46:1483-1511
- Nowell ARM, Jumars PA (1987) Flumes: theoretical and experimental considerations for simulation of benthic environments. *Oceanographical Mar Biol Ann Rev* 25:91-112
- Pusceddu A, Sara G, Armeni M, Fabiano M, Mazzola A (1999) Seasonal and spatial changes in the sediment organic matter of a semi-enclosed marine system (W-Mediterranean Sea). *Hydrobiol* 397:59-70
- Riaux-Gobin C, Dinet A, Dugue G, Vétion G, Maria E, Grémare A (2004) Phytodetritus at the sediment-water interface, NW Mediterranean Basin: spatial repartition, living cells signatures, meiofaunal relationships. *Sci Mar* 68:7-21
- Schmidt S, de Stigter HC, Van Weering TCE (2001) Enhanced short-term sediment deposition within the Nazaré Canyon, North-East Atlantic. *Mar Geol* 173:55-67
- Shuman FR, Lorenzen CF (1975) Quantitative degradation of chlorophyll by a marine herbivore. *Limnol Oceanogr* 20:580-586
- Soltwedel T (1997) Temporal variabilities in benthic activity and biomass on the western European continental margin, *Oceanol Acta* 20: 871-879
- Soltwedel T, Mokievsky V, Schewe I (2000) Benthic activity and biomass on the Yermak Plateau and in adjacent deep-sea regions northwest of Svalbard. *Deep-Sea Res Part I-Oceanogr Res Pap* 47:1761-1785
- Thiel JH (1978) Abundance and biomass of metazoan meiobenthos in the deep sea. In: Rowe GT, Pariente V (eds) *Deep-sea Food Chains and the Global Carbon Cycle*. Kluwer Academic Publisher, London, pp 124-138
- Thomsen, L., G. Graf, K. v. Juterzenka and U. Witte (1995) An in situ experiment to investigate the depletion of seston above an interface

Chapter 3

feeder field on the continental slope of the western Barents Sea. *Mar Ecol Prog Ser* 123:295-300

Thomsen, L. and W. Ritzrau (1996) Aggregate studies in the benthic boundary layer at a continental margin. *J Sea Res* 36:143-146

Thomsen L, Flach E (1997) Mesocosm observations of fluxes of particulate matter within the benthic boundary layer. *J Sea Res* 37:67-79

Thomsen L, Gust G (2000) Sediment erosion thresholds and characteristics of resuspended aggregates on the western European continental margin. *Deep-Sea Res Part I-Oceanogr Res Pap* 47:1881-1897

Thomsen L, van Weering T, Gust G (2002) Processes in the benthic boundary layer at the Iberian continental margin and their implication for carbon mineralization. *Progr Oceanogr* 52:315-329

Van Mooy BAS, Keil RG, Devol AH (2002) Impact of suboxia on sinking particulate organic carbon: Enhanced carbon flux and preferential degradation of amino acids via denitrification. *Geochim Cosmochim Acta* 66:457-465

Van Weering TCE, De Stigter HC, Boer W, De Haas H (2002) Recent sediment transport and accumulation on the NW Iberian margin. *Progr Oceanogr* 52:349-371

Vitorino J, Oliveira A, Jouanneau JM, Drago T (2002) Winter dynamics on the northern Portuguese shelf. Part 1: physical processes. *Progr Oceanogr* 52:29-153

Yentsch CS, Menzel DW (1963) A Method for the Determination of Phytoplankton Chlorophyll and Phaeophytin by Fluorescence. *Deep-Sea Res* 10:221-231

CHAPTER 4

Organic content, bioturbation and deposition rates in two contrasting submarine canyons.

ABSTRACT

The oceanographically different conditions characterizing the Western Iberian Margin (NE Atlantic) and the Gulf of Lions (Mediterranean) may play an important role in determining the biogeochemical characteristics of the sediments. To investigate this, we compared the Nazaré and Cap de Creus canyons, and their respective adjacent open slopes in terms of organic carbon (C_{org}) contents, chlorophyll a (chl a) concentrations, C:N and chl a:phaeopigment ratios, bioturbation rates, chl a and ²¹⁰Pb deposition and background concentrations in sediments. To estimate bioturbation rates, deposition and background concentrations we fitted sediment chl a and ²¹⁰Pb profiles simultaneously in a diagenetic model. To account for the possibility that the decay of chl a may be lower in the deep sea than in shallow areas, we estimated the diagenetic parameters with two models; an F-ratio test was used to select the model best explaining the data. In one approach (model 1), the decay rate of chl a as given by Sun et al. (1993) for estuaries was used, whilst in the other approach (model 2), chlorophyll decay rate was an extra parameter to be estimated. In most of the cases, the diagenetic parameters were best explained with model 1, thus indicating that the chl a decay rate as

Submitted to Progress in Oceanography as: R. García, D. van Oevelen, K. Soetaert, L. Thomsen, H. C. De Stigter, E. Epping (*submitted*) Organic content, bioturbation and deposition rates in two contrasting submarine canyons. Manuscript Ref. No.: PROOCE-D-07-00007

estimated from the relationship in Sun et al. (1993) remains valid to estimate bioturbation rates and deposition in deep sea sediments. A Bayesian analysis on the modelled parameters indicated we obtained robust results. Corg contents, chl a concentrations, chl a:phaeo ratios, bioturbation rates, deposition and background concentrations of chl a and ²¹⁰Pb indicated that the Cap de Creus canyon and adjacent slope were less active in terms of organic matter accumulation and burial than the Nazaré canyon and respective open slope.

KEY WORDS: Organic contents, Bioturbation, Deposition, Diagenetic model, Contrasting submarine canyons

INTRODUCTION

Submarine canyons are major transport systems of sedimentary organic matter from the shelf to the deep ocean (Durrieu de Madron 1994, Mullenbach & Nittrouer 2000, Canals et al. 2006, Palanques et al. 2006a), and accumulate high amounts of sediments and organic matter (Carson et al. 1986, Monaco et al. 1990, Epping et al. 2002, Van Weering et al. 2002). Downward transport and the redistribution of sediments in the canyon are controlled by hydrodynamic processes, such as down-slope and along-slope bottom currents, internal waves and gravity flows, interacting with bottom topography. The amount and diagenetic characteristics of the particulate organic matter deposited on the sea floor depend on its origin and the degree of diagenetic transformation while residing in the benthic boundary layer (Cowie et al. 1992, Thomsen et al. 2002).

Once deposited, the particulate organic matter sustains a wide variety of benthic organisms (Gage & Tyler 1991). Their life habits may enhance further transport of the organic particles from the sediment water interface into the sedimentary column, a process called bioturbation (Aller 2001). Bioturbation or particle reworking is important because it affects the physical

structure of the sediment (Aller 1982, 1994, Wheatcroft et al. 1990) and exerts a direct control on carbon mineralization and burial efficiency (Sun et al. 1993, Green et al. 2002). Organic matter deposition and bioturbation rates have been determined from the sediment distribution of single tracers, such as ^{210}Pb , ^{234}Th and chl *a*, which are strongly associated with organic particles (i.e. Soetaert et al. 1996a, Boon & Duineveld 1998, Turnewitsch et al. 2000, Schmidt et al. 2001, Green et al. 2002).

Oceanographically different conditions in contrasting continental margins will affect the transport, deposition and accumulation of organic matter in the respective submarine canyons and surrounding slopes. These processes may also affect the movement and feeding activity of benthic organisms, which in turn may affect the concentration and lability of the organic matter in the sediment. To investigate the influence of oceanographically different conditions on the sediment's biogeochemical characteristics, concentrations of chl *a*, chl *a*:phaeo ratios, organic carbon contents, and C:N ratios were determined in the Nazaré and Cap de Creus canyons, and respective adjacent continental slopes. Part of the chl *a* data and chl *a*:phaeo ratios of the Nazaré canyon and adjacent open slope were discussed in García & Thomsen (*in rev*), where the spatial distribution of bioavailable organic matter in surface sediments (0-0.5 cm) was investigated. Here, we present and compare vertical profiles for two submarine canyons and their respective adjacent slopes from two oceanographically distinct areas. A diagenetic model has been used to derive bioturbation rates and deposition rates of organic matter. We used a novel approach, modelling chl *a* and ^{210}Pb sediment-depth profiles simultaneously, rather than separately, allowing to better constrain the model parameters.

Marine environments are heterogeneous in terms of organic matter composition, reactivity, oxic/anoxic conditions, benthic fauna composition and activity. In general, at larger water depths organic matter has had more time to decay before deposition compared to shallower stations. Thus, we hypothesised a priori that the decay rate of chl *a* should decrease with water depth and should demonstrate site-specific (canyon-slope and interregional)

differences. To account for this anticipated variation in decay rate, we fitted two models to the data. In one model the chlorophyll decay rate was *a priori* derived from the empirical relationship from Sun et al. (1991, 1993). The chl *a* decay rate in the other model however, was fitted against the data as an additional free model parameter. An F-test, taking into account the different number of model parameters in the models, was used to single out the model that significantly fitted the data best. Finally, different from other studies estimating bioturbation rates and deposition of chl *a* and ²¹⁰Pb, we estimate the uncertainty of the derived model parameters, using a Markov chain Monte Carlo approach.

STUDY AREAS

The Gulf of Lions is a micro-tidal and river dominated continental margin characterized by a broad shelf and incised by several submarine canyons (Palanques et al. 2006b). The Cap de Creus canyon is located in the most western part of the Gulf of Lions, where the shelf narrows and where the wind driven coastal circulation and the Liguro-Provençal or Northern current converge (Millot 1990) (Fig. 1). The water column within the canyon is not stratified and had mean temperatures of ~ 13 °C. The canyon represents an important area of sediment transport for the entire Gulf of Lions because it funnels a larger amount of suspended sediments towards deeper water than other canyons in the area (Palanques et al. 2006b). Primary production in the Gulf of Lions range between 78 and 142 g C m⁻² y⁻¹ (Lefevre et al. 1997).

In contrast, the Western Iberian Margin is a tidal margin characterized by a narrow shelf and a steep irregular slope incised by deep gullies and canyons. The Nazaré canyon is located in the middle part of this margin (Fig. 1), is the largest canyon in the area, and intersects the entire continental shelf (Vanney & Mougenot 1981). The water column along the Western Iberian Margin is stratified, grading from relatively warm (14 to 18 °C) and saline (35.4 to 35.8) water at the surface to cold (2 °C) and less saline

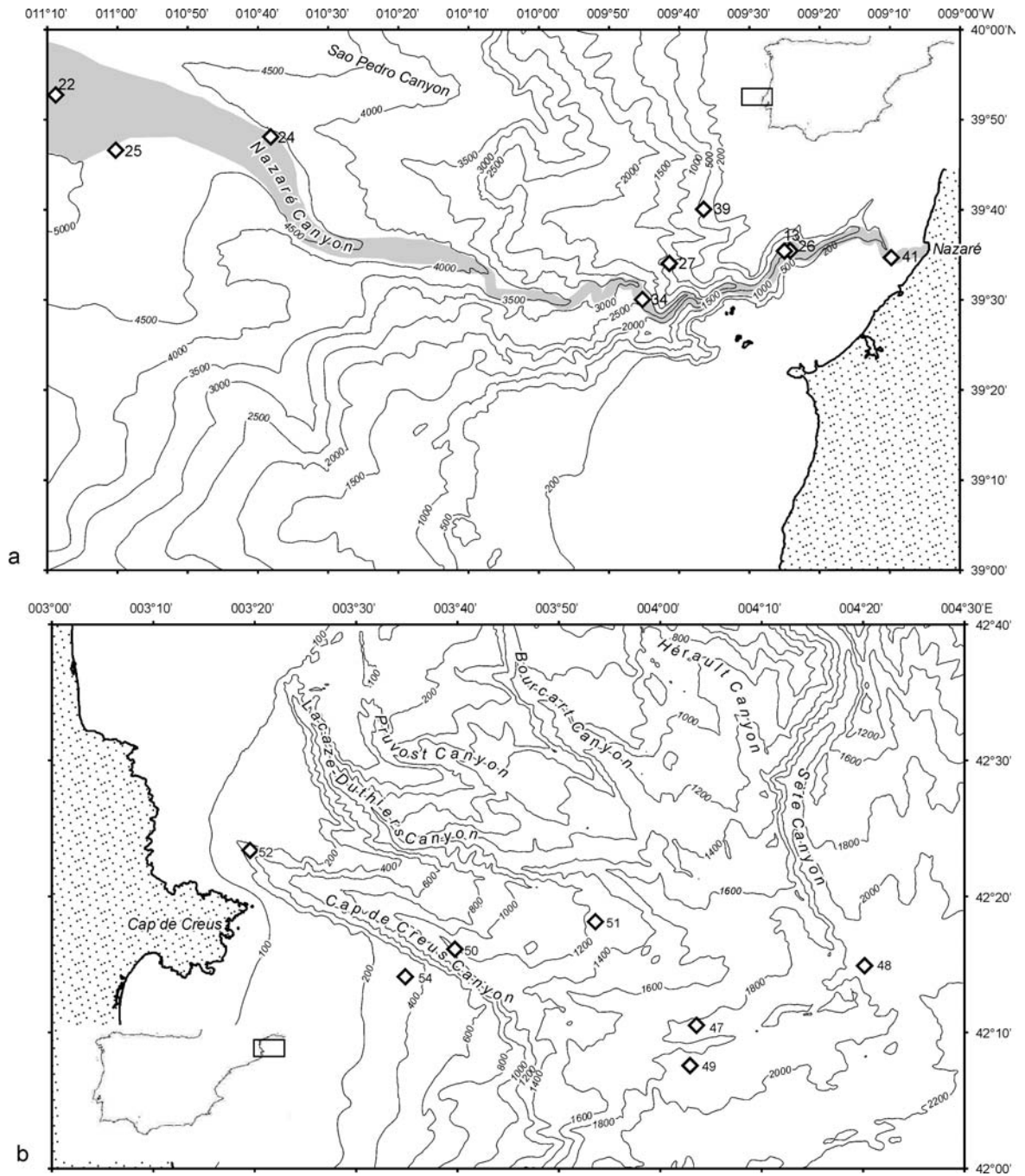


Fig. 1: Maps of the Western Iberian Margin and Gulf of Lions showing the stations sampled in a) the Nazaré canyon (St41, St26, St13, St34, St24 and St 22) and adjacent open slope (St39, St27 and St25), and in b) the Cap de Creus canyon (St52, St50, St47 and St48) and adjacent open slope (St 54, St51 and St49).

(34.8) water at 5000 m depth. A distinct salinity maximum of up to 36.2 found between 600 and 1500 m is associated with a vein of Mediterranean water flowing along the margin (Mazé et al. 1997, Fiúza et al. 1998). The upper and middle canyon captures suspended particulate matter from the adjacent shelf and is affected by internal tide circulation of water with strong bottom current speeds (De Stigter et al. 2007). Intermittent sediment gravity flows have been registered in the canyon, which, coupled to the internal tide circulation produce a net downward canyon transport of particulate material (De Stigter et al. 2007). Surface water productivities at the Western Iberian Margin vary between 154 and 556 g C m⁻² y⁻¹ (Álvarez-Salgado et al. 2003).

MATERIAL AND METHODS

Sampling

Sediment cores were collected along a depth gradient inside the canyons and their adjacent slopes during cruises RV Pelagia 64PE225 and 64PE236 of Royal NIOZ in May 2004 and May 2005 respectively. The Nazaré canyon was sampled at 6 stations inside the canyon (St 41, St 26, St 34, St 24, St 22 and St 13) and at 3 stations on the adjacent open slope (St 39, St 27 and St 25). The Cap de Creus canyon was sampled at 4 stations (St 52, St 50, St 47 and St 48) and the adjacent open slope at 3 stations (St 54, St 51 and St 49) (Table 1, Fig. 1).

Sediment samples were taken with the MUC 8+4 multiple-corer developed by Oktopus GmbH. The MUC is equipped with eight 6-cm diameter and four 10-cm diameter coring tubes of 61 cm length. From each station, three 6-cm tubes were used for chlorophyll *a* and phaeopigment analysis, four 6 cm tubes were used for organic carbon and nitrogen analysis, and one 10-cm multicore tube was used for ²¹⁰Pb analysis. Cores were stored at in-situ temperature in a temperature-controlled room and processed within 3 hours. The cores for chlorophyll *a* and phaeopigment analysis were sub-sectioned at

0.5 cm intervals down to 1 cm, at 1 cm intervals from 1 down to 5 cm, at 2 cm intervals from 5 down to 9 cm, and at 3 cm intervals from 9 down to 15 cm. The cores for organic carbon and nitrogen were sub-sectioned at 0.25 cm intervals down to 1 cm, 0.5 cm intervals down to 3 cm, 1 cm intervals down to 7 cm and at 2 cm intervals until the bottom of the core. These samples were stored in plastic bags at -20°C until analysis. The cores for ^{210}Pb analysis were stored at 5°C until analysis in upright position, and sub-sectioned in the laboratory at 0.5 cm interval down to 5 cm, and at 1 cm interval below 5 cm.

Table 1: Accessory parameters used in the model to estimate bioturbation rates and fluxes through the sediment water interface, where ϕ_0 = porosity at the sediment-water interface; ϕ_∞ = porosity at infinite depth; x^ϕ = attenuation porosity coefficient; ω = sediment accumulation; * = ω from station 64PE218-57 at 151m, a shallower station sampled previous year; and ** = ω from station 64PE218-08 at 4806m, same station sampled the previous year.

Stations	Latitude (N)	Longitude (W)	Temperature (°C)	ϕ_0 (V/V)	ϕ_∞ (V/V)	x^ϕ (cm)	ω (cm d ⁻¹)
<i>Cruise 64PE225 May 2004</i>							
Gulf of Lions							
Open Slope							
St 54	42°13.9'	3°35.5'	13.2	0.76	0.62	3.56	2.50E-04
St 51	42°18.0'	3°54.0'	13.2	0.88	0.64	2.28	4.90E-05
St 49	42°07.5'	4°03.5'	13.1	0.74	0.56	2.89	3.50E-05
Cap de Creus canyon							
St 52	42°23.3'	3°19.8'	13.2	-	-	-	-
St 50	42°15.9'	3°40.0'	13.2	0.84	0.62	2.16	1.70E-04
St 47	42°10.4'	4°04.2'	13.1	0.74	0.63	1.23	1.50E-04
St 48	42°14.9'	4°20.7'	13.2	0.79	0.58	1.3	8.40E-05
Western Iberian Margin							
Open Slope							
St 39	39°39.9'	9°35.9'	11.9	0.58	0.46	0.06	1.2E-04*
St 27	39°33.9'	9°40.9'	9	0.82	0.66	6.75	7.90E-05
St 25	39°46.5'	10°59.9'	2	0.95	0.73	0.59	4.1E-06**
Nazaré canyon							
St 41	39°34.8'	9°09.9'	11.8	0.86	0.76	5.07	1.30E-03
St 26	39°35.9'	9°23.9'	8.6	0.83	0.36	5.07	2.30E-03
St 34	39°30.0'	9°45.9'	4.3	0.79	0.41	1.7	-
St 24	39°48.0'	10°37.9'	2	0.9	0.78	1.61	-
St 22	39°53.9'	11°10.0'	1.8	0.83	0.68	6.18	5.20E-06
<i>Cruise 64PE236 May 2005</i>							
Nazaré canyon							
St 13	39°35.8'	9°24.3'	9.3	0.71	0.78	1.01	6.20E-04

Chlorophyll α and phaeopigment analysis

Pigments from the sediment samples were extracted following the method of Yentsch & Menzel (1963). Sediment samples were freeze-dried and homogenised in a mortar and pigment extracts therefore represent the total extractable pigment pool of free and bound fractions (Sun et al. 1991). Pigments were extracted (~1 g dried sediment) in 10 ml 90% acetone solution and stored in the dark and at ~6 °C for ~24 h (shaken twice) and centrifuged at 4500 rpm for 20 minutes. The supernatant was measured in a TD-700 Turner fluorometer following Shuman & Lorenzen (1975).

Organic carbon and nitrogen analysis

Sediment organic carbon and nitrogen were measured using a ThermoFinnigan flash element analyser following the procedures described by Lohse et al. (2000). Sediment was dried at 60°C for 24h and homogenized in a mortar mill. Subsequently, 10 to 25 mg of sediment was weighed into tin-cups (Microanalysis, Ø = 8mm, L = 5mm), and 10 µl of 6% sulphurous acid added into the sample cups. The samples were dried at 60°C for 20 to 60 min and the acid addition was repeated until termination of effervescence. Tin cups were transferred into a second tin cup, in which they were pinched, closed and compacted to spherical balls. These samples were analyzed for organic carbon and nitrogen. A second set of samples was treated equally but was not acidified. When analyzed, these unacidified samples estimate total carbon (organic and inorganic fraction) and nitrogen.

^{210}Pb analysis

The activity of ^{210}Pb was measured indirectly from its granddaughter ^{210}Po with half-life 138.4 days, as described in Boer et al. (2006). 100 to 500 mg of freeze-dried and ground sediment samples were spiked with ^{209}Po and hydrolysed with acid (5 ml concentrated HNO_3 and concentrated HF) in a microwave oven for 3h. Then, 2 ml 3.5% HClO_4 was added and the acids were removed by evaporation. The resulting precipitate was resuspended in 5 ml

concentrated HCl for 30 min, and buffered with 40 ml 0.5 M HCl (with 12 g/l boric acid), 4 ml NH₄OH and 5 ml of 40 g/l ascorbic acid (in 0.5 M HCl). Po-isotopes were deposited by suspending a silver disk in the solution, which was heated at 80°C for 4h. Silver plates were left in solution overnight at room temperature, and the activity of ²¹⁰Pb was measured via α-spectrometry with Canberra Passivated Implanted Planar Silicon (PIPS) detectors.

Sediment porosity

Sediment porosity was determined from the loss of weight of known volumes of sediment after freeze-drying and assuming a density of the mineral matrix of 2.4 g cm⁻³. Depth profiles of porosity for the different stations were fitted to the equation:

$$\phi_x = [\phi_\infty + (\phi_0 - \phi_\infty)] \cdot e^{\left(\frac{-x}{x^\phi}\right)} \quad \text{Eq. 1}$$

in which ϕ_∞ is the porosity at infinite depth (v/v), ϕ_0 is the porosity at the sediment-water interface (v/v), x is depth in sediment (cm) and x^ϕ is the depth attenuation coefficient for porosity (cm). The estimated values for ϕ_∞ , ϕ_0 and x^ϕ are used in the diagenetic model (Table 1).

Diagenetic model

Assuming steady state conditions and first-order degradation, bioturbation can be obtained from the general diagenetic equation (Berner 1980, Boudreau 1997), which describes the concentration changes of a particulate tracer C_i as a function of time (t) and depth (x) due to advection, mixing and the biogeochemical reactions in sediments:

$$\frac{\partial(1-\phi)C_i}{\partial t} = 0 = \frac{\partial}{\partial x} \left((1-\phi_x)Db_x \left(\frac{\partial C_i}{\partial x} \right) - \omega(1-\phi_\infty) \left(\frac{\partial C_i}{\partial x} \right) - \lambda_i(1-\phi_x)C_i \right) \quad \text{Eq. 2}$$

where C_i is the excess of the tracer i per cm³ of solid sediment, t is time (d), x is depth in the sediment (cm), ϕ is the porosity (v/v), Db_x is bioturbation coefficient or bioturbation rate (cm² d⁻¹), ω is the advection or sedimentation

rate (cm d^{-1}), and λ is the first order decay constant of the tracer (d^{-1}); $(1-\phi) C_i$ is the excess of the tracer per cm^3 of bulk sediment. For comparison with data, a background (refractory) concentration should be added to the excess concentration. Bioturbation was assumed to be constant in an upper well-mixed layer of 10 centimetre thickness, below which it declines exponentially.

At the sediment-water interface ($x=0$), an advective input flux J_i is imposed:

$$J_i = -(1-\phi_0)Db_0 \left. \frac{\partial C_i}{\partial x} \right|_{x=0} + \omega(1-\phi_\infty)C_{i,x=0} \quad \text{Eq. 3}$$

Whilst at infinite depth, it is assumed that the excess tracer concentration is 0:

$$C_\infty = 0$$

To obtain mixed-layer bioturbation (Db_0) and deposition rates across the sediment water interface we simultaneously fitted chl a ($\mu\text{g cm}^{-3}$) and ^{210}Pb (dpm cm^{-3}) concentrations over sediment depth. This means we ran the model in parallel for chl a and ^{210}Pb , where both shared all parameters (Db_0 , ω , ϕ_x ...) except for the decay rate λ_i . The decay rate was fixed for ^{210}Pb and either imposed (model 1) or estimated (model 2) for chlorophyll a .

The values for porosity (ϕ_x) and sediment accumulation rate (ω) are given in Table 1. The decay rate (λ) for ^{210}Pb was 0.031 yr^{-1} as obtained from the radioactive decay of its parent radionuclide ^{226}Ra , and, for model 1, λ for chl a was estimated with the equation derived by Sun et al. (1993) from core incubations:

$$\ln \lambda = \Lambda - 6160 \cdot T^{-1} \quad \text{Eq. 4}$$

in which T is temperature (degrees Kelvin) and Λ = is a parameter that gives an indication about the degradation history of the chl a arriving to a given location. Model 1 has the empirically derived value of 18.3 for Λ (see Sun et al. 1993). Model 2 has Λ as a free parameter to account for the fact that other factors may play an important role in determining chl a decay. These two approaches will be referred to as model 1 and model 2, respectively.

Overall, the following parameters were estimated by fitting the model(s) to data: the two deposition rates $J_{chl a}$, J_{Pb210} , and background concentrations of chl a and ^{210}Pb and the mixed-layer bioturbation rate (Db_o). Model 2 has the decay rate of chlorophyll ($\lambda_{chl a}$) as additional fitting parameter. The modelling strategy for model 1 and model 2 is schematically shown in Fig. 2.

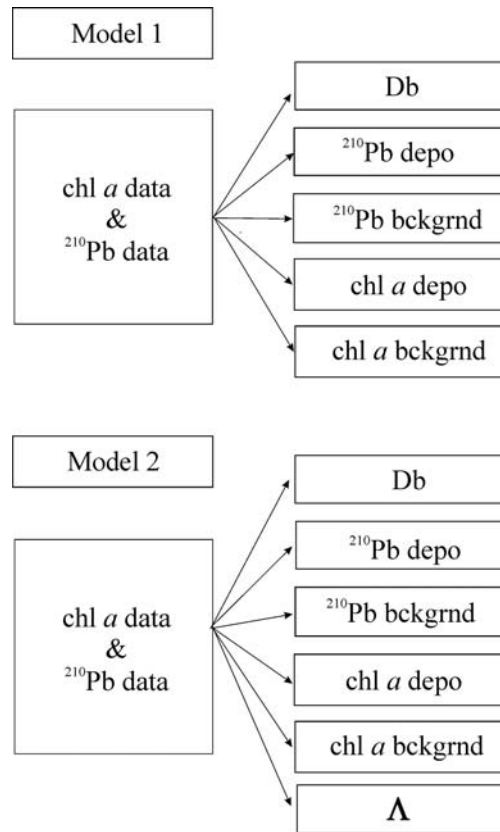


Fig. 2: Schematic representation of the model approaches (model 1 and model 2) and the derived diagenetic parameters; where Db = bioturbation rate, ^{210}Pb depo = ^{210}Pb deposition, ^{210}Pb bckgrnd = ^{210}Pb background concentration, chl a depo = chl a deposition, chl a bckgrnd = chl a background concentration, and Λ = the factor in Sun et al. (1993) set as 18.3 in the chl a decay relationship (Eq 4.)

Two bioturbation modes can be distinguished: a) diffusive mixing, when particles are mixed in a way resulting in diffusive-looking tracers profiles (Boudreau 1986a), b) non-local mixing, when particles are exchanged between

non-adjacent sediment layers resulting in tracer profiles with sub-surface peaks (Boudreau 1986b). The diagenetic model used here can simulate both diffusive mixing and non-local mixing conditions (Soetaert et al. 1996a). However, fits with non-local mixing expressions were not successful (see Results), therefore we only report on model fits for those stations that could be fitted with diffusive mixing conditions.

Model comparison and uncertainty analysis

The two models described in the previous section differ in only in one respect: model 1 has a fixed Λ , whereas Λ is a fitting parameter in model 2. The addition of one fit parameter to a model (model 2) implies that the fit of model output to the data will always be better than the fit obtained with the simpler model (model 1). The question is whether the improvement of the fit outweighs the cost of adding an additional parameter. In order to test for this we used a one tailed F-test (Sokal & Rohlf 1995), similarly as in Soetaert et al. (1996a). The null hypothesis is that there is no difference between the residual variance between the modelled and observed data in the more elaborated approach (model 2) compared to the simpler one (model 1). The alternative hypothesis is that the complex approach significantly reduces the residual variance. The null hypothesis is rejected when the calculated F value $> F$ -distribution with (df_1-df_2/df_2) degrees of freedoms. The F value is calculated as:

$$F = \frac{\left(\frac{SSR_1 - SSR_2}{df_1 - df_2} \right)}{\left(\frac{SSR_2}{df_2} \right)} \quad \text{Eq. 5}$$

where SSR_1 and SSR_2 are the sum of the squared residuals of observed and modelled values of the simple and elaborated model respectively, and df_1 and df_2 are the respective degrees of freedom (number of observations – number of parameters-1).

Parameter estimates derived by model fitting always have an associated error, because parameters are fitted to uncertain data. Bayesian analysis provides a means to quantify this parameter uncertainty (Gelman et al. 2003). Here, a prior parameter uncertainty (e.g. minimum and maximum values from the literature) is updated with the likelihood of finding model output given the observations. The prior distribution times the likelihood gives the posterior probability distribution, which defines the uncertainty of the model parameters and the relation between parameters. Bayesian inference was run with a Markov Chain Monte Carlo (MCMC) simulation using the simple yet effective Metropolis algorithm. The MCMC was initiated with the parameter combination that gave the optimal fit (see below) to avoid a burn-in period, and with a non-informative prior parameter distribution. We choose a uniform distribution within a minimum value of $1E-10$ and a maximum value of $1E+6$. By choosing such large prior parameter ranges, the posterior distribution effectively is determined only by the information given by the data.

Starting from a parameter combination, a new combination is selected by a random step (jump) in parameter space by the MCMC. If this parameter combination gives a better fit to the data than the previous one, the new parameter set is accepted and used as new starting point for a next random step. If the new parameter combination fits worse, it is accepted with a probability equal to the ratio of probabilities of the tested versus the existing parameter combination. The jump length for each parameter in the MCMC was (manually) optimised such that around 20% of the runs were accepted. The model was run 100,000 times, which gave 10,000 to 20,000 accepted runs. Convergence of the MCMC was checked by visual inspection. The distribution of parameter values in the set of accepted runs represents the posterior probability distribution of each parameter, from which the mean and standard deviation of each parameter can be calculated. Note that this technique has only rarely been used in the field of biogeochemistry and ecology (i.e. Andersson et al. 2006, van Oevelen et al. 2006).

Model solving and fitting

As neither the porosity nor the bioturbation rate was constant with sediment depth, the diagenetic equations were approximated by numerical differencing, using the scheme as given in Soetaert et al. (1996b). The model was implemented on a personal computer, in the simulation environment FEMME (Soetaert et al. 2002). This environment takes care of solving the model and performs the calibration and Bayesian analysis. The steady-state profiles were estimated by solving the system of equations using the Newton-Raphson method (Soetaert et al. 2002). As the resulting equations are linear, convergence is achieved in one Newton-Raphson step. Model calibration was performed using the Levenberg-Marquardt algorithm. During calibration, a model cost function, which quantifies the difference between data and model output, is minimised.

The cost function was defined as:

$$Min = \left(\sum_i \sum_j^{var\ obs} \frac{(x_{i,j}^{mod} - x_{i,j}^{obs})^2}{\sigma_{i,j}^2} \right) \quad \text{Eq. 6}$$

where $x_{i,j}^{mod}$ is the modelled value, $x_{i,j}^{obs}$ is the corresponding mean observed value and $\sigma_{i,j}$ is the observed standard deviation. This weighting of the residuals by the standard deviation serves two purposes. First of all, it ensures that the model cost function is a-dimensionalised, (and therefore residuals consisting of chl *a* and ^{210}Pb can be meaningfully merged), and secondly, it gives less weight to less certain data. However, this procedure requires robust estimates of standard deviations. To this end, standardized relative and absolute errors for chl *a* observations were obtained by plotting the standard deviation of the chl *a* data against the respective mean values. The relative error and absolute error were taken as the slope and the intersection of the linear fit of the data. When no significant linear fit was obtained the relative error was set to zero and the absolute error was calculated as the mean of the standard deviations. This is a more robust fitting procedure than using standard deviations based directly from the data, as the latter may skew the

model fit considerably to fitting those values where standard deviations were (perhaps erroneously) estimated to be very small.

For ^{210}Pb there were no replicated observations and thus the relative and absolute errors could not be obtained. However, we reasoned that the variability of ^{210}Pb data should be smaller than for the chl *a* data because ^{210}Pb is more stable over time. The coefficient of variation (the standard deviation divided by the mean) obtained for the chl *a* data was ~20%, thus we set smaller errors for ^{210}Pb at a coefficient of variation of 10%.

Graphs representing model fits and Bayesian results were created with the R-software (R Development Core Team, 2005).

RESULTS

Sediment composition

The open slope of the Gulf of Lions and Western Iberian Margin had similar concentrations of chl *a*, contents of Corg, chl *a*:phaeo and C:N ratios at equivalent water depths (Table 2). Concentrations of chl *a* tended to decrease with increasing water depth, while Corg contents did not show a clear pattern with depth. The Cap de Creus canyon stations had lower chl *a* concentrations and Corg contents than the Nazaré canyons stations at equivalent water depth (Table 2). The upper/middle parts of the Nazaré canyon had highest chl *a* concentrations, and stations St 41 and St 26 showed the highest chl *a*:phaeo ratios (Table 2). The remaining stations from both canyon ecosystems had similar chl *a*:phaeo ratios. C:N ratios in both canyons at equivalent water depths were similar, but in the Nazaré canyon there was a clear increase in C:N ratios with increasing water depth (Table 2).

When comparing canyons against open slopes, canyon stations generally recorded higher concentrations of chl *a* and of Corg than adjacent open slope stations (Table 2). This was particularly true for the Western Iberian Margin, where the Nazaré canyon stations had markedly higher chl *a*

concentrations and Corg contents than open slope stations at equivalent depth. In the Gulf of Lions, the Cap de Creus canyon had only slightly higher chl *a* concentrations than open slope stations, and Corg contents were similar in both systems. The chl *a*:phaeo ratios in the upper regions of the Nazaré canyon were higher than on the adjacent slope at equivalent depths (Table 2). The deeper canyon and slope stations had similar ratios. In the Cap de Creus canyon and adjacent slope chl *a*:phaeo ratios were always similar. C:N ratios were always higher in both canyon systems compared to the slopes (Table 2).

Model output

Stations St 52, St 25, St 34 and St 24 were missing ^{210}Pb data, and model fits based on chlorophyll data alone did not result in well-constrained parameter estimates (results not shown). At stations St 26, St 24 and St 34, the chl *a* profiles showed subsurface peaks that could be indicative of non-local mixing processes (Fig. 3). Station St 26 also had a subsurface peak in the ^{210}Pb profile, but fitting both profiles simultaneously with the same non-local exchange model did not produce satisfactory results (St 34 and St 24 were missing ^{210}Pb data). The chl *a* concentration of station St 22 was low at the surface and then increased abruptly at 5 cm depth. This profile could also not be fitted with the simple non-local mixing expression. The inadequacy of the model to reproduce these features may indicate that these sub-surface peaks may not be of biotic origin or reflect transient perturbations, e.g. due to turbidity flows. Therefore, modelling results for these stations are not presented.

Table 2: Characteristics of the sampling stations, listing station numbers, water depths, the chlorophyll *a* concentrations, the chlorophyll *a* to phaeopigments ratios, the organic carbon contents, and the atomic C:N ratios of the organic matter in the upper 0.5 cm of the sediment and in the upper 15 cm (chlorophyll) or upper 20 cm (organic matter).

Stations	Depth (m)	chl <i>a</i> (0-0.5 cm) ($\mu\text{g cm}^{-2}$)	chl <i>a</i> (0-15 cm) ($\mu\text{g cm}^{-2}$)	Corg (0-0.5 cm) (%)	Corg (0-20 cm) (%)	chl <i>a</i> :phaeo (0-0.5 cm)	chl <i>a</i> :phaeo (0-15 cm)	C:N (0-0.5 cm)	C:N (0-20 cm)
Gulf of Lions									
Open Slope									
St 54	343	0.12	0.61	0.55	0.55	0.05	0.03	8.72	8.33
St 51	1209	0.09	0.06	-	-	0.03	0.01	-	-
St 49	1874	0.07	0.06	0.44	0.39	0.03	0.03	6.18	6.99
Cap de Creus canyon									
St 52	344	0.72	1.62	0.55	0.41	0.05	0.04	11.08	8.29
St 50	1215	0.1	0.39	0.86	0.67	0.03	0.03	8.21	9.2
St 47	1801	0.08	0.12	0.68	0.44	0.02	0.02	11.5	9.34
St 48	2112	0.08	0.09	-	-	0.04	0.03	-	-
Western Iberian									
Open Slope									
St 39	307	0.11	0.61	0.34	0.3	0.02	0.02	8.43	8.57
St 27	1000	0.13	0.5	0.98	1.02	0.03	0.03	8.48	8.8
St 25	4798	0.02	0.05	0.69	0.49	0.02	0.02	7.36	7.05
Nazaré canyon									
St 41	332	4.2	9.18	1.85	1.66	0.16	0.08	8.58	9.56
St 13	927	0.64	2.21	-	-	0.04	0.04	-	-
St 26	1121	0.75	14.71	1.73	0.96	0.05	0.16	9.44	10.94
St 34	2847	0.25	1.68	1.63	1	0.02	0.03	10.65	9.22
St 24	4810	0.05	0.62	1.55	1.03	0.02	0.03	11.09	11.7
St 22	4969	0.03	0.82	1.36	1.42	0.02	0.04	10.59	17.73

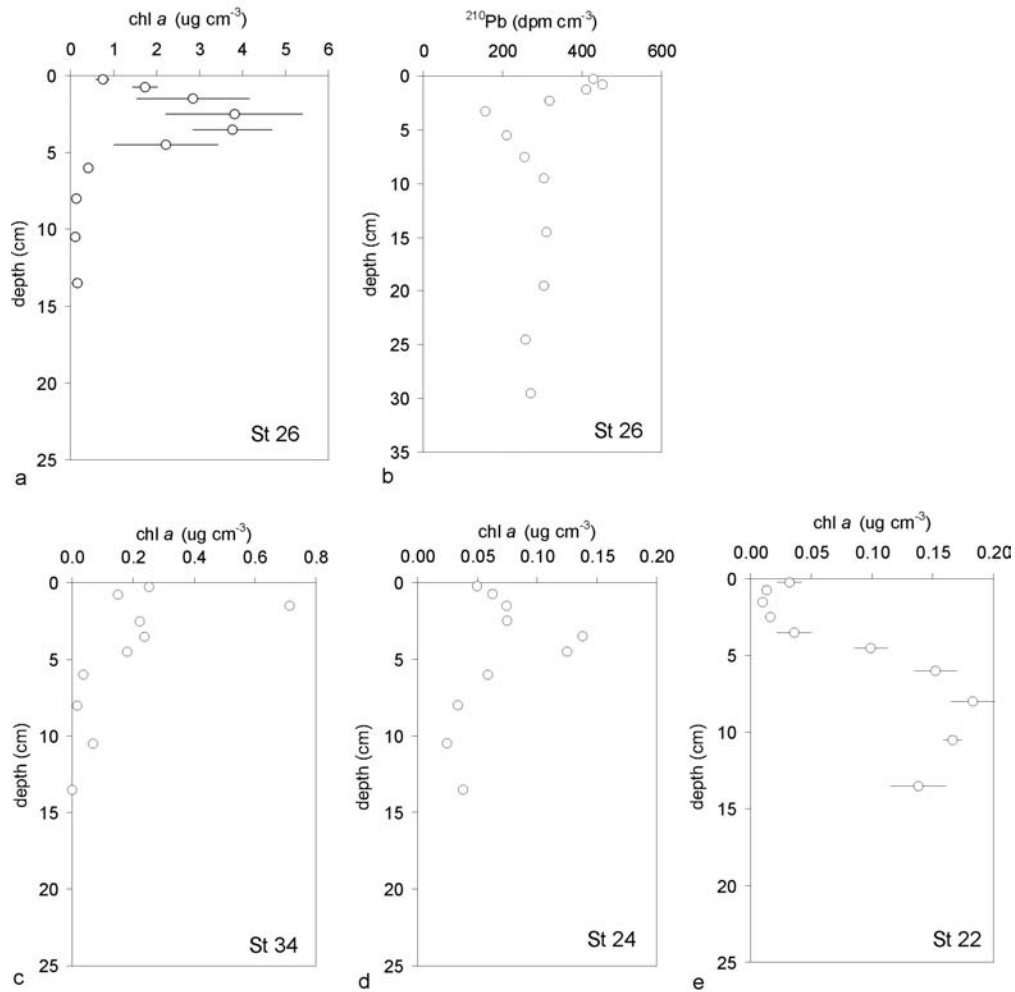


Fig. 3: Stations in the Nazaré canyon showing chl *a* and ^{210}Pb profiles with subsurface maxima that could not be fitted by the model.

The profiles of the stations that could be fitted with the diagenetic model all show a good data versus model correspondence (Fig. 4). For stations St 41 and St 48 the more parameter-rich model (model 2) resulted in a significantly better fit of the chl *a* and ^{210}Pb data. The F-test of station St 49 showed that model 2 is close to being significantly better than model 1 ($\alpha = 0.06$, Table 3). The observations clearly show a penetration of degradable chl *a* down to 1.6 cm in model 2. Degradable chl *a* concentrations in model 1 vanish in the top 0.5 cm of the sediment (data not shown), whereas model 2 explains chl *a* penetration almost perfectly (Fig. 4). The fits of the other chl *a* data points, deeper than 2 cm, is indistinguishable between both models, because of

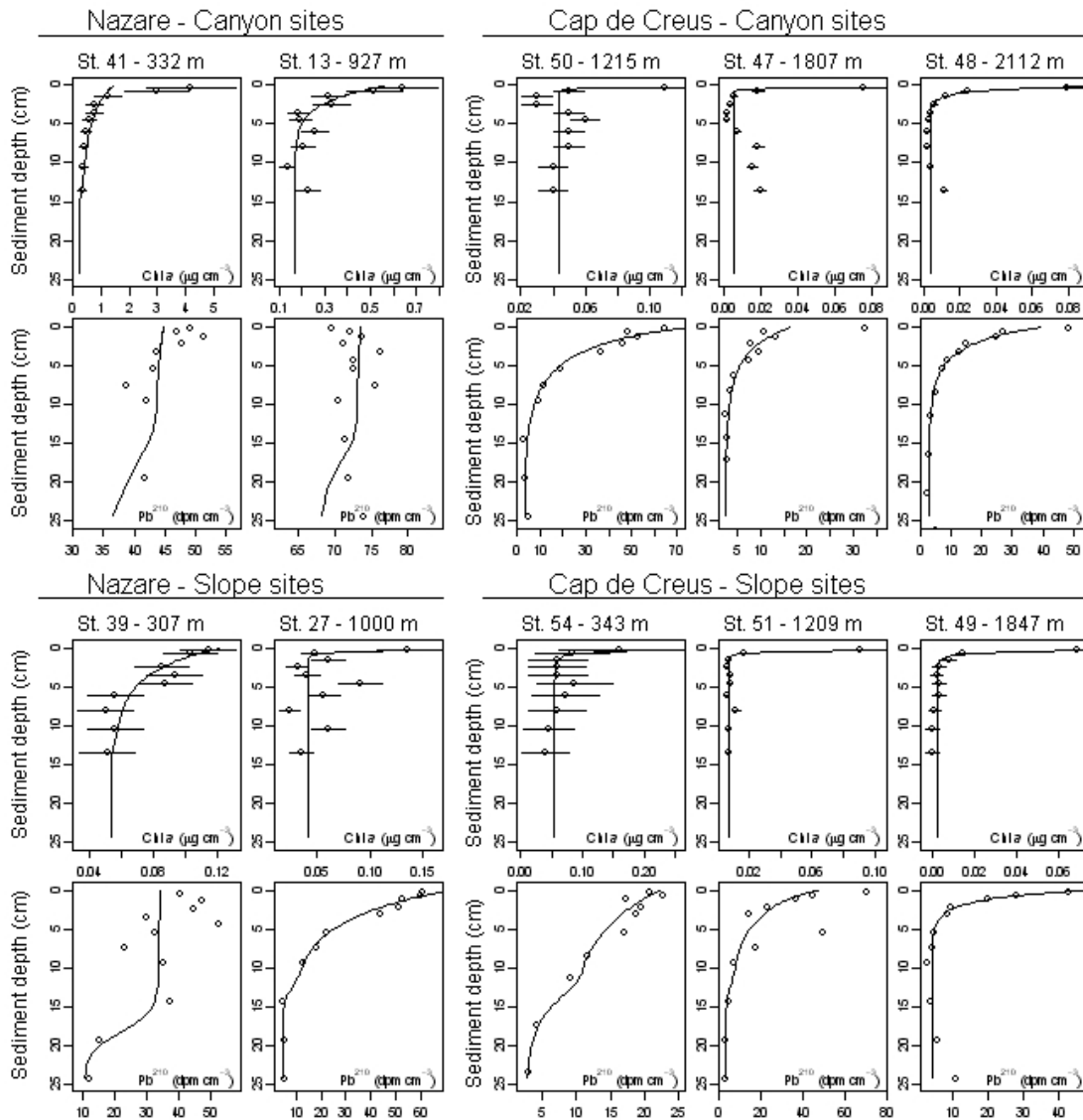


Fig. 4: Modelled (solid line) versus observed mean (dots) +/- standard deviation (horizontal dash) chl a and ^{210}Pb profiles. Model profiles of stations St 41, St 48 and St 49 were obtained with model 2, the remaining profiles were obtained with model 1.

the straight vertical profile. Hence model 2 can only improve the fit of 3 out of 10 data points and therefore cannot strongly improve the total explained variance. Fitted chl a deposition by model 1 is considerably higher than for the two stations hundreds of meters higher up the slope, which is not very realistic. For these reasons we have chosen the results from model 2 as being most representative for this station. The chl a deposition rates based on model

2 are depressed with about a factor 20 to 40 in stations St 48 and St 49 compared to the other stations hundreds of meters shallower. The profiles of the other stations were not significantly better fitted with model 2 and therefore the results from model 1 are presented (Table 3, Fig. 4).

The Bayesian analysis for stations fitted with model 1 or model 2 generally shows a similar pattern, but differences in the Bayesian analysis between the model 1 and model 2 are apparent (Fig. 5 and 6). The posterior probability distribution of the parameters in model 1 (station St 51 is taken as representative example) shows that model parameters are normally distributed and are generally not correlated, except for ^{210}Pb deposition and the biodiffusion coefficient (Db), which are positively correlated (Fig. 5). This means that a combination of high Db and high ^{210}Pb deposition may produce a similarly good fit as a combination of low Db and low ^{210}Pb deposition.

The posterior distributions for the model parameters in model 2 are more complex (station St 48 taken as representative example), but most striking is the strong positive correlation (0.94) between chl a deposition and degradation (Fig. 6). Other weaker correlations exist between the parameters ^{210}Pb background, ^{210}Pb deposition and biodiffusion coefficient (Db) and between the parameters chl a background and degradation (Fig. 6).

Most model parameters were well constrained by the fitting as shown by low coefficients of variation ($\text{CoV}=\text{standard deviation}/\text{mean}$) that range from $1.3\text{E-}07$ to 1.52 for all stations, with an average value of 0.22 (Table 3). Also, the parameter ranges are significantly constrained with respect to the initial uncertainty range that was set for each parameter (see Material and Methods for initial ranges).

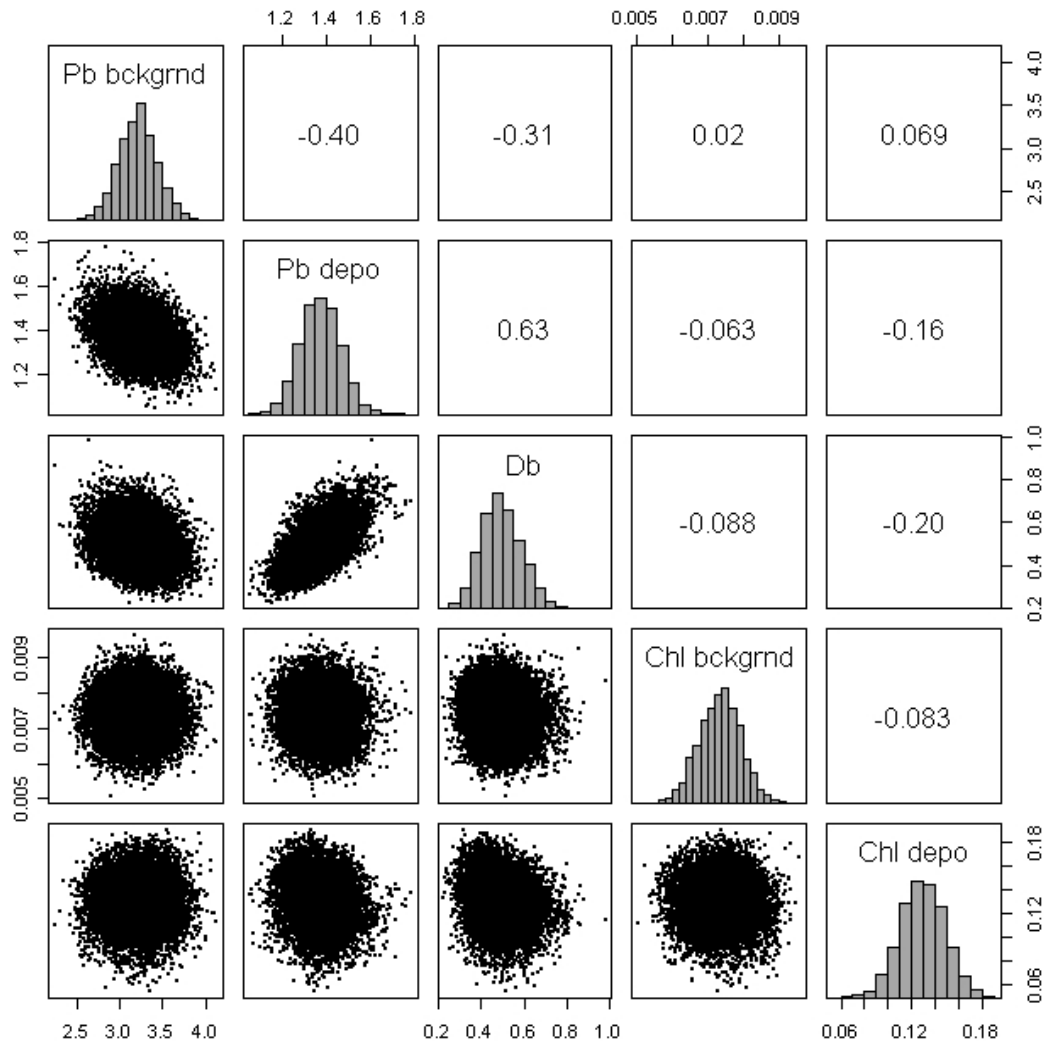


Fig. 5: Posterior parameter probability distribution (resulting from the Bayesian analysis) for station St 51, as generated with model 1, where Pb bckgrnd = ^{210}Pb background concentration (dpm cm^{-3}), Pb depo = ^{210}Pb deposition ($\text{dpm cm}^{-2} \text{y}^{-1}$), Db = bioturbation rate ($\text{cm}^{-2} \text{y}^{-1}$), Chl bckgrnd = chl a background ($\mu\text{g cm}^{-3}$), and Chl depo = chl a deposition ($\mu\text{g cm}^{-2} \text{y}^{-1}$). Each dot in a plot represents an accepted parameter combination; the histograms on the diagonal represent the posterior probability distribution for each single parameter; the values in the upper panel reflect the correlation coefficient (r).

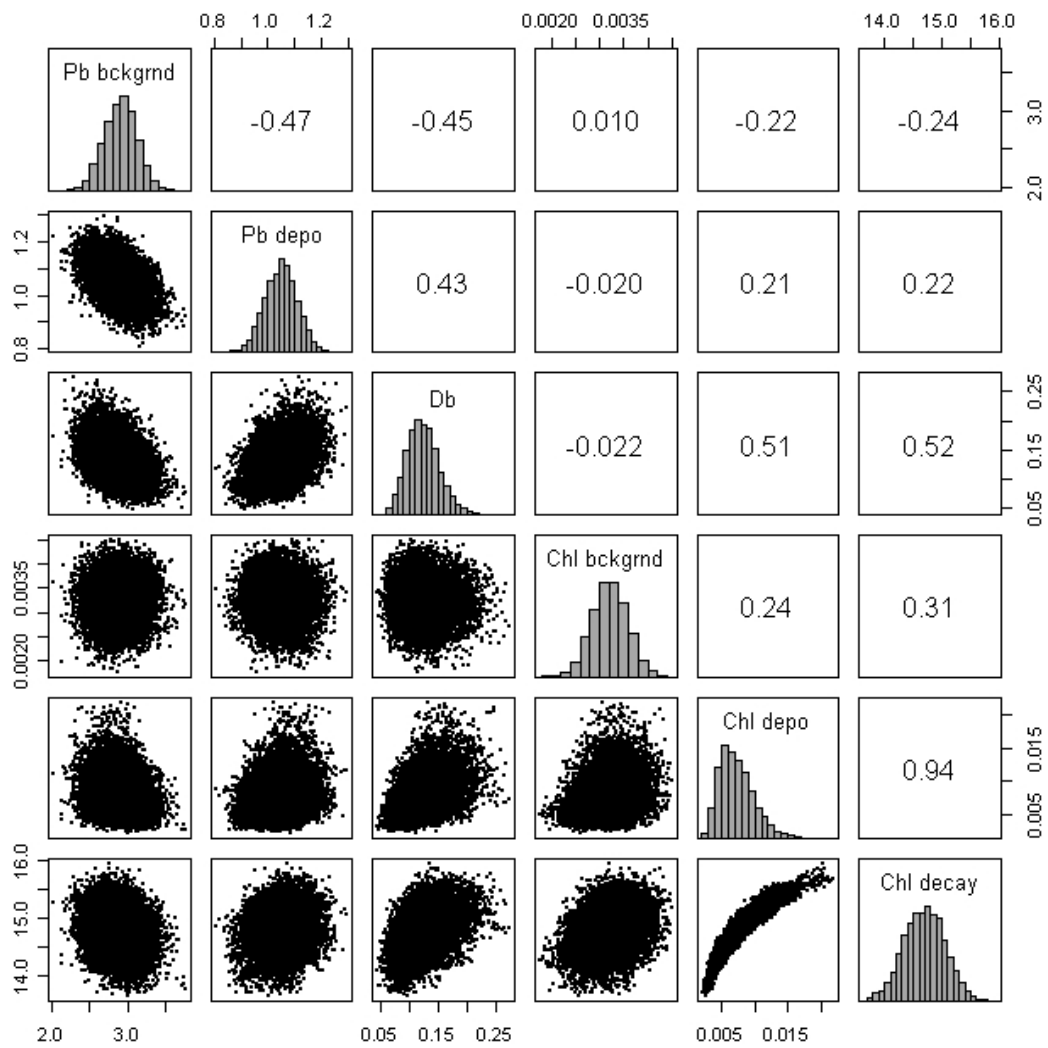


Fig. 6: Results of the Bayesian analysis for station St 48 fitted with model 2, where $Pb\ bckgrnd = {}^{210}Pb$ background concentration ($dpm\ cm^{-3}$), $Pb\ depo = {}^{210}Pb$ deposition ($dpm\ cm^{-2}\ y^{-1}$), $Db =$ bioturbation rate ($cm^{-2}\ y^{-1}$), $Chl\ bckgrnd = chl\ a$ background ($\mu g\ cm^{-3}$), and $Chl\ depo = chl\ a$ deposition ($\mu g\ cm^{-2}\ y^{-1}$), $Chl\ decay = \Lambda$ factor in (Eq 4.). See also Fig. 5.

Table 3: F- test comparing the residual variance between the simpler model 1 and the more complex model 2, and the mean \pm standard deviation of the posterior parameter probability distribution, as obtained with the Bayesian analysis. Db = bioturbation rates, chl a Depo and Pb²¹⁰ Depo = depositions of chl a and Pb²¹⁰, chl a_{background} = background concentration of chl a, Pb²¹⁰_{background} = background concentration of Pb²¹⁰, λ = degradation parameter in Eq. 4 and λ = decay rate of chl a. When F- test is not significant the reported parameters are from model 1, and when is significant (*) the reported parameters are from model 2. (†) refers to model 2 parameters whose accuracy is considered dubious (see Discussion).

Stations	Depth (m)	F- test (1 vs 2)	Best model	Pb ²¹⁰ Depo (dpm cm ⁻² y ⁻¹)	Pb ²¹⁰ _{background} (dpm cm ⁻³)	Db (cm ² y ⁻¹)	chl a Depo ($\mu\text{g cm}^{-2}\text{y}^{-1}$)	chl a _{background} ($\mu\text{g cm}^{-3}$)	λ (d ⁻¹)
Gulf of Lions									
Open Slope									
St 54	343	0.91	1	1.80 \pm 0.11	2.65 \pm 0.21	1.83 \pm 0.43	0.36 \pm 0.20	0.06 \pm 0.02	18.3
St 51	1209	0.57	1	1.37 \pm 0.09	3.21 \pm 0.22	0.50 \pm 0.09	0.13 \pm 0.02	0.01 \pm 0.001	18.3
St 49	1874	0.06	2	0.52 \pm 0.04	4.11 \pm 0.20	0.03 \pm 0.01	0.004 \pm 0.0003 [†]	0.002 \pm 0.001 [†]	14.53 \pm 0.03 [†]
Cap de Creus canyon									
St 50	1215	0.78	1	3.12 \pm 0.16	3.38 \pm 0.27	0.09 \pm 0.02	0.30 \pm 0.07	0.04 \pm 0.003	18.3
St 47	1801	0.15	1	0.50 \pm 0.05	2.55 \pm 0.22	0.12 \pm 0.06	0.40 \pm 0.22	0.01 \pm 0.001	18.3
St 48	2112	0.001*	2	1.05 \pm 0.06	2.90 \pm 0.21	0.12 \pm 0.03	0.007 \pm 0.0003 [†]	0.003 \pm 0.0004 [†]	14.70 \pm 0.36 [†]
Western Iberian									
Open Slope									
St 39	307	0.6	1	7.25 \pm 0.48	9.98 \pm 0.81	160.92 \pm 71.92	1.58 \pm 0.60	0.05 \pm 0.01	18.3
St 27	1000	0.9	1	1.99 \pm 0.19	4.29 \pm 0.29	0.50 \pm 0.06	0.12 \pm 0.04	0.04 \pm 0.004	18.3
Nazarié canyon									
St 41	332	0.05*	2	3.03 \pm 1.16	29.45 \pm 4.88	35.21 \pm 53.47	1.71 \pm 0.66	0.25 \pm 0.12	16.13 \pm 0.22
St 13	927	0.97	1	0.73 \pm 0.52	67.19 \pm 4.29	44.87 \pm 18.74	1.53 \pm 0.39	0.17 \pm 0.02	18.3

Bioturbation, chl *a* and ²¹⁰Pb deposition rates, background concentrations and decay rates

Estimated bioturbation rates, deposition rates of chl *a* and of ²¹⁰Pb, and background concentrations of chl *a* and of ²¹⁰Pb were generally higher in the Western Iberian Margin than in the Gulf of Lions (Table 3). Bioturbation rates in the Western Iberian Margin ranged between 0.50 ± 0.06 and 160.92 ± 71.92 cm² y⁻¹ and, in the Gulf of Lions between 0.03 ± 0.01 and 1.83 ± 0.43 cm² y⁻¹. Chl *a* deposition ranged between 0.12 ± 0.04 and 1.71 ± 0.66 µg cm⁻² y⁻¹ in the Western Iberian Margin and between 0.004 ± 0.0003 and 0.40 ± 0.22 µg cm⁻² y⁻¹ in the Gulf of Lions. Depositions of ²¹⁰Pb ranged between 0.73 ± 0.52 and 7.25 ± 0.48 dpm cm⁻² y⁻¹ in the Western Iberian Margin, and in the Gulf of Lions they ranged between 0.50 ± 0.05 and 3.12 ± 0.16 dpm cm⁻² y⁻¹. Background concentrations of chl *a* varied between 0.04 ± 0.004 and 0.25 ± 0.12 µg cm⁻³ in the Western Iberian Margin and between 0.002 ± 0.001 and 0.06 ± 0.02 µg cm⁻³ in the Gulf of Lions. Background concentrations of ²¹⁰Pb ranged between 4.29 ± 0.29 and 67.19 ± 4.29 dpm cm⁻³, and between 2.55 ± 0.22 and 4.11 ± 0.20 dpm cm⁻³ in the Western Iberian Margin and in the Gulf of Lions, respectively.

Bioturbation rates in the Nazaré canyon and adjacent slope did not show a clear pattern with depth. Differently, in the Cap de Creus canyon stations bioturbation rates were similar ~ 0.10 cm² y⁻¹, while at the adjacent slope bioturbation rates appeared higher and decreased from 1.83 ± 0.43 cm² y⁻¹ at the shallower station to 0.03 ± 0.01 cm² y⁻¹ at the deepest station (Table 3).

Deposition rates of chl *a* in the Nazaré canyon and adjacent slope are similar with values of ~ 1 µg cm⁻² y⁻¹. In the Cap de Creus canyon chl *a* deposition was slightly higher than on the adjacent slope at equivalent water depths, and decreased with increasing water depths from values of ~ 0.3 µg cm⁻² y⁻¹ to values of ~ 0.005 µg cm⁻² y⁻¹ in both areas (Table 3).

^{210}Pb deposition (0.73 ± 0.52 and 3.03 ± 1.16 dpm cm⁻² y⁻¹) was lower in the Nazaré canyon than at the adjacent slope at equivalent water depths (1.99 ± 0.19 and 7.25 ± 0.48 dpm cm⁻² y⁻¹) (Table 3). In the Cap de Creus canyon ^{210}Pb depositions tended to be higher than on the adjacent slope. ^{210}Pb depositions ranged between 0.50 ± 0.05 and 3.12 ± 0.16 dpm cm⁻² y⁻¹ in the canyon, and between 0.52 ± 0.04 and 1.80 ± 0.11 dpm cm⁻² y⁻¹ on the open slope.

The Nazaré canyon had higher background concentrations of chl *a* and of ^{210}Pb than the adjacent slope (Table 3). Background concentrations of chl *a* in the canyon were 0.17 ± 0.02 and 0.25 ± 0.12 µg cm⁻³, and on the open slope they were 0.04 ± 0.004 and 0.05 ± 0.01 µg cm⁻³. Background concentrations of ^{210}Pb were 29.45 ± 4.88 and 67.19 ± 4.29 dpm cm⁻³ in the canyon, and 4.29 ± 0.29 and 9.98 ± 0.81 dpm cm⁻³ on the open slope. In the Cap de Creus canyon and adjacent slope background concentrations of chl *a* and of ^{210}Pb were similar, ranging between 0.002 and 0.06 µg cm⁻³, and between 2.55 and 4.11 dpm cm⁻³ respectively.

The decay rates of chl *a* in model 1, derived from the temperature-dependence degradation relationship from Sun et al. (1993), ranged between 0.029 and 0.04 d⁻¹. The decay rates of chl *a* estimated with the more elaborate model 2 were an order of magnitude lower, ranging between 0.001 and 0.004 d⁻¹ (Table 3).

DISCUSSION

Model results

Using a combined observation and diagenetic modelling approach, two submarine canyon ecosystems with oceanographically different regimes, and their respective adjacent slopes, have been found to differ in terms of several biogeochemical sedimentary characteristics. The simple steady-state

diagenetic model that fitted simultaneously chl *a* and ^{210}Pb sediment profiles allowed (1) to single out those sediments that behave in a way that cannot be explained by steady-state diagenesis which includes only diffusive mixing, (2) to test in how far decay rates linked to organic matter mineralisation are only temperature-dependent, i.e. the algal material did not undergo significant diagenetic alteration before deposition, and (3) to characterise the sediments in terms of deposition rates, decay rates, and bioturbation rates.

Most of the stations in the Nazaré canyon had pronounced subsurface peaks in chl *a* and/or ^{210}Pb (Fig. 3) that could not be explained with the biodiffusion process adopted in the diagenetic model (Eq. 2). Subsurface peaks were also discernable in some of the Cap de Creus Canyon sites, but not to the extent that they could not be represented with a simple biodiffusional model approach. Such subsurface peaks can be caused either by non-local mixing effectuated by large benthic fauna (Meysman et al. 2003) or by physical processes such as turbidite flows that may deposit low chl *a* sediment on top of sediments with high chl *a* concentrations (Fig. 3). From the available data we cannot identify the process that has caused these non-diffusive chl *a* profiles and we have therefore not attempted to model these profiles. It is however noteworthy that most of these deviations were associated to canyon sites.

The stations exhibiting diffusive mixing conditions in the sediments were fitted with two models. In one model chl *a* decay rate was fixed based on *in situ* temperature and using the empirical degradation relationship derived by Sun et al. (1993), whilst in the other model chl *a* decay rate was an extra parameter to be fitted. This permitted to test if the chl *a* degradation rate is only temperature dependent, or also strongly depend on other site/depth specific factors. We used an F-test to establish whether the additional free model parameter significantly improved the fits of the data. Surprisingly, in most of the cases (7 out of 10), the extra fitting parameter did not significantly improve the fitting. This falsified our initial assumption that the chlorophyll-derived matter was strongly altered (aged) before settling. Apparently, using the chl *a* decay rate as derived by Sun et al. (1993) from incubations of shallow estuarine sediments, and which is widely used for different environments (e.g.

Boon & Duineveld 1998, Gerino et al. 1998, Green et al. 2002), is a good-enough estimate for most continental slopes and submarine canyons investigated in this study.

In three stations (St 41, St 48 and St 49) however, the data were (quasi-) significantly better fitted (see Results) when assuming a decay rate deviating from the Sun et al. (1993) relationship. The penetration of chlorophyll in these sediments was significantly underestimated when adhering to the imposed chl *a* decay rates. There are two possible reasons for such discrepancy: either the decay rates were overestimated (and thus chl *a* disappears too fast), or the bioturbation rates were underestimated (and thus chl *a* was not diluted fast enough in the sediment). If we varied the decay rates, the derived decay rates of chl *a* were up to an order of magnitude lower than the ones estimated in model 1 (Table 3). The decay rate of chl *a* is an important parameter to estimate the chlorophyll deposition rates, which increase linearly with decay rates. Although the estimated deposition rates of ²¹⁰Pb are not noteworthy lower at station St 48 and St 49, the chlorophyll deposition rates based on model 2, are depressed with about a factor 20 to 40 compared to the other stations from the same area. This casts doubts on the lowered decay rates and on the accuracy of the derived chlorophyll deposition rates.

Another possible explanation for the discrepancy could be that the bioturbation was underestimated. As organisms tend to favourably handle fresh over more refractory material, the bioturbation rates estimated by modelling short-lived tracers (such as chlorophyll) may yield higher values than those obtained by long-lived tracers (²¹⁰Pb), a process called age-dependent mixing (Smith, 1993), although this concept was recently challenged (Reed et al. 2006). The coefficient that governs exponential decay of a tracer with sediment depth is $-\sqrt{\lambda/Db}$, hence the fit of a given profile can be improved by decreasing λ with a certain factor or increasing Db with the same amount. Based on the data, we cannot distinguish between these two alternative scenarios, and a combination of an overestimation of λ and an underestimation of Db could also be possible; thus we will not discuss the chlorophyll modelling results from stations St 49, St 48 and St 41 any further.

The robustness of the diagenetic model parameters was assessed with a Bayesian analysis (Andersson et al. 2006). This technique provides a means to determine the probability distribution of the model parameters and their correlations after fitting to observational data (Fig. 5 and 6). Most parameters were well constrained by the data as indicated by the small coefficients of variation (CV) (Table 4) and the reduced posterior parameter ranges obtained with the Bayesian analysis (not shown). Two noteworthy exceptions are the bioturbation and ^{210}Pb deposition rates of stations St 13 and St 41, which were badly constrained (CV 0.71, 1.52). This is due to the fact that the ^{210}Pb profile does not show the normal decrease with sediment depth (Fig. 4). Most model parameters are normally distributed and uncorrelated, especially when obtained with model 1 (Fig. 5). However, chl *a* deposition and decay are strongly positively correlated in model 2 (Fig. 6). This correlation is easily explained, because a vertical profile of chl *a* will not change drastically when a higher deposition of chl *a* is accompanied by a higher degradation rate of chl *a*. The negative correlation between fitted ^{210}Pb background concentration and deposition rates (Fig. 6) can be explained by the following reasoning. A lower ^{210}Pb deposition should be accompanied with a higher ^{210}Pb background value in order to keep the ^{210}Pb concentration in the mixed layer near the observed concentration.

Patterns in the biogeochemical parameters

The Cap de Creus canyon and open slope sediments seemed to be less active than the Nazaré canyon and respective open slope in terms of bioturbation rates and chl *a* and ^{210}Pb depositions (Table 3). This was confirmed by the chl *a* and Corg contents (Table 2), that were respectively 3 to 30 times lower and 1.5 to 4 times lower in the Cap de Creus canyon than in the Nazaré canyon. The respective open slopes shared similar chl *a* and Corg contents, but the markedly lower chl *a* and ^{210}Pb background concentrations in the Cap de Creus canyon and open slope sediments confirmed they were less active in terms of organic matter deposition and burial (Table 3). These differences may be partly explained by the generally higher primary

productivity in the Western Iberian Margin (Álvarez-Salgado et al. 2003) than in the Gulf of Lions (Lefevre et al. 1997).

The Cap de Creus and Nazaré canyons also showed different organic matter accumulation patterns. When compared to the respective open slopes, the Nazaré canyon had 5 to 30 times higher chl *a* contents, 2 to 5 times higher Corg contents (Table 2) and higher chl *a* and ²¹⁰Pb background concentrations (Table 3). Differently, the Cap de Creus canyon and respective adjacent open slope were similar with respect to their chl *a* and Corg contents (Table 2), their chl *a* and ²¹⁰Pb background concentrations and the chl *a* deposition rates (Table 3). In contrast, bioturbation rates were lower in the canyon, and ²¹⁰Pb depositions were slightly higher. More than half of the chl *a* and ²¹⁰Pb profiles in the Nazaré canyon had clear subsurface peaks indicating a high sediment disturbance (Fig. 3). Overall, the Nazaré canyon ecosystem is more active in terms of organic matter accumulation and burial than the Cap de Creus canyon. While the Cap de Creus canyon may trap some bulk organic matter, only little labile phytodetritus accumulates within the canyon. Only the upper part traps some phytodetritus, as chl *a* concentrations were slightly higher (2 to 6 times) than on the adjacent slope, but still considerably lower than in the Nazaré canyon. The higher primary productivities in the Western Iberian Margin alone may not fully explain these different organic matter accumulations in the Nazaré and Cap de Creus canyons. The transport mechanisms of suspended particles triggered by different current regimes are more likely to be responsible for the observed differences in the sediments.

The Western Iberian Margin is characterised by tide driven currents, internal waves and upwelling regime (McCave & Hall 2002, Vitorino et al. 2002) that favours the formation of nepheloid layer transporting suspended material offshore (Oliveira et al. 2002, Van Weering et al. 2002). The presence of dense nepheloid layers in the upper Nazaré canyon indicates transport of shelf material into the canyon (De Stigter et al. 2007). Tide driven currents within the canyon resuspend and deposit sedimentary material in cycles; this material is transported up and down canyon with the ebb and flood tides, producing a net down canyon transport that can be coupled with sporadic

turbidity flows (De Stigter et al. 2007). This oceanographic regime favours the sedimentation of suspended material and burial, which would explain the high organic contents, depositions and background concentrations in the Nazaré canyon. Faster sediment and carbon accumulations have previously been reported for the Nazaré canyon than for the Iberian continental slope (Schmidt et al. 2001, Van Weering et al. 2002, Epping et al. 2002, De Stigter et al. 2007). In contrast with the previous studies, ^{210}Pb deposition was lower in the Nazaré canyon than at the adjacent slope and chl *a* deposition was similar (Table 3). In combination with the higher background values of ^{210}Pb and chl *a* found in the canyon, this may suggest that continuous deposition may not be the case. The profiles of ^{210}Pb in the Nazaré canyon (Fig. 4) do not show the traditional decrease with sediment depth, which suggests mixed conditions. Intense animal reworking or sediment slides falling on top of each other may produce this type of profile. The latter seems more probable in view of the other canyon stations showing subsurface peaks could not be explain with the bioturbative process adopted in the diagenetic model. In the canyon, the observed ^{210}Pb concentrations are close to background values; thus the model estimates that a small deposition is necessary to maintain the observed ^{210}Pb concentrations because assumes constant deposition (Eq. 2).

An oceanographically different regime characterises the Gulf of Lions. The convergence of the shelf cyclonic circulation of water and the Liguro-Provençal current nearby the Cap de Creus canyon causes downwelling of shelf water on the slope along with down-canyon sediment transport (Palanques et al. 2006b). Nepheloid layers produced by along-slope contour currents disperse suspended material offshore (Durrieu de Madron et al. 1990, Durrieu de Madron 1994). Most of the time, fine-grained sediment and organic matter may be spread out evenly over the canyon and adjacent slope by settling without much focusing of deposition in the canyon. All chl *a* and ^{210}Pb profiles give evidence of low deposition and low bioturbation rate, well in accordance with the relatively low primary productivity and lack of tidal transport mechanism. Seasonally, dense shelf water cascading events occur in the Gulf of Lions (Durrieu de Madron et al. 2005), and can intensify the downwelling of

shelf water along the slope and canyons. Sporadically, the downslope currents are large enough to resuspend sand, which subsequently erodes fine-grained cohesive sediments and form giant furrows field and transport large amounts of organic material to the deep ocean (Canals et al. 2006). Under these conditions the canyon floor is eroded away. Altogether, this oceanographic regime would explain the low and homogenous organic contents and phytodetritus labilities, low depositions, bioturbation rates, and background concentrations in the Cap de Creus canyon.

Conclusions

The Nazaré canyon and adjacent slope are more active in terms of organic matter deposition and burial, and generally show higher organic contents and background concentrations than the Cap de Creus canyon and respective slope. Most of the vertical tracer profiles in the Nazaré canyon sediment show evidence of strong perturbations or predominance of transient effects, which cannot be explained by steady-state bioturbative transport and decay.

These differences in organic matter accumulation and burial can be attributed to the oceanographically different conditions prevailing in the Western Iberian Margin and Gulf of Lions.

ACKNOWLEDGEMENTS

This study was supported by EUROSTRATAFORM project, EC contract EVK3-CT-2002-00079 funded by the European Commission, DG-XII, and the HERMES project, EC contract OCE-CT-2005-511234 funded by the European Commission's Sixth Framework Programme under the priority Sustainable Development, Global Change and Ecosystems. Shiptime on RV 'Pelagia' was provided by Royal NIOZ, Texel, The Netherlands. The authors thank all of the crew from the R V 'Pelagia' for their work, and Dr. Erica

Koning, Dr. Tanja Kouwenhoven and Karoliina Koho for valuable help provided during core deployment, retrieval and sample processing. We thank A. Palacz for assisting with chloropigment measurements, Wim Boer and Sharyn Crayford from NIOZ for ²¹⁰Pb and C-N analysis respectively. This is publication number *** from the NIOO-KNAW.

LITERATURE CITED

- Aller, R. C. (1982) The effect of macrobenthos on chemical properties of marine sediments and overlying water. In: McCall, P. L., Tevesz, M. S. S. (Eds.), *Animal-Sediment-Relations*. Plenum Publishing Co., New York, pp. 53-102.
- Aller RC (1994) Bioturbation and Remineralization of Sedimentary Organic-Matter - Effects of Redox Oscillation. *Chem Geol* 114:331-345
- Aller RC (2001) Transport and reactions in the bioirrigated zone. In: Boudreau BP, Jorgensen BB (eds) *The Benthic Boundary Layer Transport Processes and Biogeochemistry*. Oxford University Press, Oxford, p 269-301
- Álvarez-Salgado XA, Figueiras FG, Pérez FF, Groom S, Nogueira E, Borges AV, Chou L, Moncoiffé G, Ríos AF, Miller AEJ, Frankignoulle M, Savidge G, Wollast R (2003) The Portugal coastal counter current off NW Spain: new insights on its biogeochemical variability. *Prog Ocean* 56:281-321
- Andersson JH, Middelburg JJ, Soetaert K (2006) Identifiability and uncertain analysis of bio-irrigation rates. *J Mar Res* 64:407-429
- Berner, R. A. (1980) *Early Diagenesis: A Theoretical Approach*. Princeton University Press, Princeton, N. J., 241pp.
- Boer W, van den Bergh GD, de Haas H, de Stigter HC, Gieles R, van Weering TCE (2006) Validation of accumulation rates in Teluk Banten

- (Indonesia) from commonly applied ^{210}Pb models, using the 1883 Krakatau tephra as time marker. *Mar Geol* 227:263-277
- Boon AR, Duineveld GCA (1998) Chlorophyll a as a marker for bioturbation and carbon flux in southern and central North Sea sediments. *Mar Ecol Prog Ser* 162:33-43
- Boudreau, B. P. (1986a) Mathematics of tracer mixing in sediments: I Spatially-dependent, diffusive mixing. *Am J Sci* 286:161-198.
- Boudreau, B. P. (1986b) Mathematics of tracer mixing in sediments: II Non-local mixing and biological conveyor-belt phenomena. *Am J Sci* 286: 199-238.
- Boudreau, B.P. (1997) *Diagenetic Models and Their Implementation: Modelling transport and Reactions in Aquatic Sediments*. Heidelberg, Springer-Verlag, 414pp.
- Canals M, Puig P, Durrieu de Madron X, Heussner S, Palanques A, Fabres J (2006) Flushing submarine canyons. *Nature* 444:354-357
- Carson B, Baker ET, Hickey BM, Nittrouer CA, Demaster DJ, Thorbjarnarson KW, Snyder GW (1986) Modern Sediment Dispersal and Accumulation in Quinault Submarine-Canyon - a Summary. *Mar Geol* 71:1-13
- Cowie GL, Hedges JI, Calvert S (1992) Sources and relative reactivities of amino acids, neutral sugars, and lignin in an intermittently anoxic marine environment. *Geochim Cosmochim Ac* 56:1963-1978
- De Stigter HC, Boer W, Dias de Jesus CC, Thomsen L, Van den Bergh G, Van Weering TCE (2007) Sediment transport and deposition in Nazaré Canyon, Portuguese continental margin. *Mar Geol* (doi: 10.1016/j.margeo.2007.04.011).
- Durrieu de Madron X, Nyffeler F, Godet CH (1990) Hydrographic structure and nepheloid spatial distribution in the Gulf of Lions continental margin. *Cont Shelf Res* 10:915-929

- Durrieu de Madron X (1994) Hydrography and Nepheloid Structures in the Grand-Rhone Canyon. *Cont Shelf Res* 14:457-477
- Durrieu de Madron X, Radakovitch O, Heussner S, Loye-Pilot MD, Monaco A (1999) Role of the climatological and current variability on shelf-slope exchanges of particulate matter: Evidence from the Rhône continental margin (NW Mediterranean). *Deep-Sea Res Part I-Oceanogr Res Pap* 46:1513-1538
- Durrieu de Madron X, Zervakis V, Theocharis A, Georgopoulos D (2005) Comments on "Cascades of dense water around the world ocean". *Prog Oceanogr* 64:83-90
- Epping E, van der Zee C, Soetaert K, Helder W (2002) On the oxidation and burial of organic carbon in sediments of the Iberian margin and Nazaré Canyon (NE Atlantic). *Prog Oceanogr* 52:399-431
- Fiúza AFG, Hamann M, Ambar I, Diaz del Rio G, Gonzalez N, Cabanas JM (1998) Water masses and their circulation off western Iberia during May 1993. *Deep-Sea Res Part II-Top Stud Oceanogr* 45:1127-1160
- Gage JD, Tyler PA (1991) *Deep-sea biology: A natural history of organisms at the deep-sea floor*, Vol. Cambridge University Press, Cambridge
- García R, Thomsen L (submitted) Spatial distribution of bioavailable organic matter in surface sediments of the Nazaré canyon, Western Iberian Margin. *J Mar Sys*, Manuscript Ref. No.: MARSYS-D-07-00046
- Gerino M, Aller RC, Lee C, Cochran JK, Aller JY, Green MA, Hirschberg D (1998) Comparison of different tracers and methods used to quantify bioturbation during a spring bloom: ²³⁴thorium, luminophores and chlorophyll a. *Estuar Coast Shelf S* 46:531-547
- Green MA, Aller RC, Cochran JK, Lee C, Aller JY (2002) Bioturbation in shelf/slope sediments off Cape Hatteras, North Carolina: the use of Th-234, Chl-a, and Br- to evaluate rates of particle and solute transport. *Deep-Sea Res Part II-Top Stud Oceanogr* 49:4627-4644

- Gelman A., Carlin, J. B., Stern, H. S., Rubin, D. B. (2003) Bayesian data analysis. Texts in statistical science series. Chapman and Hall/CRC.
- Lefevre D, Minas HJ, Minas M, Robinson C, Williams PJ LE B, Woodward EMS (1997) Review of gross community production, primary production, net community production and dark community respiration in the Gulf of Lions. *Deep-Sea Res Part I-Oceanogr Res Pap* 44:801-832
- Lohse L, Kloosterhuis RT, de Stigter HC, Helder W, van Raaphorst W, van Weering TCE (2000) Carbonate removal by acidification causes loss of nitrogenous compounds in continental margin sediments. *Mar Chem* 69:193-201
- Mazé JP, Arhan M, Mercier H (1997) Volume budget of the eastern boundary layer off the Iberian Peninsula. *Deep-Sea Res Part I-Oceanogr Res Pap* 44:1543-1574
- McCave IN, Hall IR (2002) Turbidity of waters over the Northwest Iberian continental margin. *Prog Oceanogr* 52:299-313
- Meysman FJR, Boudreau B, Middelburg JJ (2003) Relations between local, nonlocal, discrete and continuous models of bioturbation. *J Mar Res* 61: 391-410
- Millot C (1990) The Gulf of Lions' hydrodynamics. *Cont Shelf Res* 10:885-894
- Monaco A, Biscaye P, Soyer J, Pocklington R, Heussner S (1990) Particle Fluxes and Ecosystem Response on a Continental-Margin - the 1985-1988 Mediterranean Ecomarge Experiment. *Cont Shelf Res* 10:809-839
- Mullenbach BL, Nittrouer CA (2000) Rapid deposition of fluvial sediment in the Eel Canyon, northern California. *Cont Shelf Res* 20:2191-2212
- Oliveira A, Vitorino J, Rodrigues A, Jouanneau JM, Dias JMA, Weber O (2002) Nepheloid layer dynamics in the northern Portuguese shelf. *Prog Oceanogr* 52:195-213

- Palanques A, Martin J, Puig P, Guillen J, Company JB, Sarda F (2006a) Evidence of sediment gravity flows induced by trawling in the Palamos (Fonera) submarine canyon (northwestern Mediterranean). *Deep-Sea Res Part I-Oceanogr Res Pap* 53:201-214
- Palanques A, Durrieu de Madron X, Puig P, Fabres J, Guillén J, Calafat A, Canals M, Heussner S, Bonnin J (2006b) Suspended sediment fluxes and transport processes in the Gulf of Lions submarine canyons. The role of storms and dense water cascading. *Mar Geol* 236:43-61
- R Development Core Team (2005). R: A language and environment for statistical computing. R Foundation for Statistical Computing, Vienna, Austria. ISBN 3-900051-07-0, URL <http://www.R-project.org>.
- Reed DC, Huang K, Boudreau BP, Meysman FJR, 2006. Steady-state tracer dynamics in a lattice-automaton model of bioturbation. *Geochim Cosmochim Acta* 70 (23): 5855-5867.
- Schmidt S, de Stigter HC, van Weering TCE (2001) Enhanced short-term sediment deposition within the Nazaré Canyon, North-East Atlantic. *Mar Geol* 173:55-67
- Shuman FR, Lorenzen CF (1975) Quantitative degradation of chlorophyll by a marine herbivore. *Limnol Oceanogr* 20:580-586
- Smith CR, 1993. Age-dependent mixing of deep-sea sediments. *Geochim Cosmochim Acta* 57:1473-1488.
- Soetaert K, Herman PMJ, Middelburg JJ, Heip C, deStigter HS, vanWeering TCE, Epping E, Helder W (1996a) Modeling Pb-210-derived mixing activity in ocean margin sediments: Diffusive versus nonlocal mixing. *J Mar Res* 54:1207-1227
- Soetaert K, Herman PMJ, Middelburg JJ (1996b) Dynamic response of deep-sea sediments to seasonal variations: A model. *Limnol Oceanogr* 41:1651-1668
- Soetaert K, deClippele V, Herman P (2002) FEMME, a flexible environment for mathematically modelling the environment. *Ecol Mod* 151:177-193

- Sokal, R. R., Rohlf, F. J. (1995) *Biometry, The Principles and Practice of Statistics in Biological Research*, 3rd ed. Freeman, New York, 887 pp.
- Sun MY, Aller RC, Lee C (1991) Early Diagenesis of Chlorophyll-a in Long-Island Sound Sediments - a Measure of Carbon Flux and Particle Reworking. *J Mar Res* 49:379-401
- Sun MY, Lee C, Aller RC (1993) Laboratory Studies of Oxidic and Anoxic Degradation of Chlorophyll-a in Long-Island Sound Sediments. *Geochim Cosmochim Acta* 57:147-157
- Thomsen L, van Weering T, Gust G (2002) Processes in the benthic boundary layer at the Iberian continental margin and their implication for carbon mineralization. *Prog Oceanogr* 52:315-329
- Turnewitsch R, Witte U, Graf G (2000) Bioturbation in the abyssal Arabian Sea: influence of fauna and food supply. *Deep-Sea Res Part II-Top Stud Oceanogr* 47:2877-2911
- van Oevelen D, Middelburg JJ, Soetaert K, Moodley L (2006) The fate of bacterial carbon in an intertidal sediment: Modeling an in situ isotope tracer experiment. *Limnol Oceanogr* 51:1302-1314
- Van Weering TCE, De Stigter HC, Boer W, De Haas H (2002) Recent sediment transport and accumulation on the NW Iberian margin. *Prog Oceanogr* 52:349-371
- Vanney JR, Mougnot D (1981) La plateforme continentale du Portugal et les provinces adjacentes: analyse géomorphologique. *Mem Serv Geol Portug*, 28:1-86
- Vitorino J, Oliveira A, Jouanneau JM, Drago T (2002) Winter dynamics on the northern Portuguese shelf. Part 1: physical processes. *Prog Oceanogr* 52:29-153
- Wheatcroft, R. A., Jumars, P. A., Smith, C. R., Nowell, A. R. M. 1990. A mechanistic view of the particulate biodiffusion coefficient: step length, rest period and transport directions. *J Mar Res* 48:177-207.

Chapter 4

Yentsch CS, Menzel DW (1963) A Method for the Determination of Phytoplankton Chlorophyll and Phaeophytin by Fluorescence. *Deep-Sea Research* 10:221-231

CHAPTER 5

Conclusions and remarks

ORGANIC MATTER AND MEIOBENTHOS IN SUBMARINE CANYONS OF THE IBERIAN CONTINENTAL MARGIN

This thesis investigated gradients of organic matter contents and diagenetic characteristics in two submarine canyons (Nazaré and Cap de Creus canyons) and adjacent open slopes. It also investigated meiofaunal communities in the Nazaré canyon and respective adjacent open slope, and the relationships with the observed organic matter gradients. Furthermore, it assessed the biodeposition by biogenic structures of fresh phytodetritus under high bottom flow conditions at the head of the Nazaré canyon. Finally, differences in sediments biogeochemical characteristics, such as organic matter deposition and bioturbation, were investigated in the Nazaré and Cap de Creus canyons, and respective adjacent open slopes, and linked to the oceanographically different conditions characterizing the study areas.

The results presented in the three manuscripts of this thesis allowed giving answer to the hypothesis formulated in Chapter 1.

Answer H1) Organic matter contents and diagenetic characteristics in submarine canyons can be higher than in the adjacent open slopes, but not always.

Answer H2) Organic matter contents and diagenetic characteristics decrease along a depth gradient in canyon ecosystems and adjacent slopes, but not always.

Answer H3) The composition of meiofaunal assemblages changes significantly along a depth gradient in canyon ecosystems as well as between canyons and slopes at same depths, but the differences in organic matter contents and diagenetic characteristics are not the main ecological drivers. The instability of canyon sediments seems to be an important ecological driver for benthic fauna in these environments.

Answer H4) Benthic biogenic structures are able to deposit fresh phytodetritus under high bottom current conditions in submarine canyons.

Answer H5) Canyons with oceanographically different conditions show differences in terms of organic matter content, diagenetic characteristics, organic matter deposition and bioturbation rates.

The main outcomes of this study are summed up in the next sections.

The Nazaré submarine canyon

The organic carbon, phytopigment and amino acid data in surface sediments and sedimentary record indicated that the Nazaré canyon had higher contents of organic matter than the adjacent open slope at equivalent water depths. The organic matter contents decreased with increasing water depths along the Nazaré canyon and the open slope. Furthermore, the organic matter in the upper area of the canyon was less refractory than in the adjacent open slope or middle and deeper canyon regions. In the middle and deeper regions of the canyon and along the adjacent open slope, organic matter refractory characteristics were similarly low. Across the two canyon cross sections investigated, the organic matter in surface sediments tended to accumulate towards the thalweg of the canyon rather than on the walls. The lability of the organic matter across the canyon section was similar and low. The lability of the bulk organic matter in the canyon and the open slope were similar.

Transport wise, the organic carbon, phytopigment and amino acid data supports the idea that the suspended particulate organic matter from the shelf enters the Nazaré canyon through the upper region and accumulates

there, and that the transport of organic material from the surrounding shelf into the upper and middle canyon areas may also be possible via the lateral walls of the canyon. Then, this organic material is further transported down to the middle and deeper areas by tidal currents. In the middle part of the canyon, the walls widen and the organic material gets dispersed across a larger area, therefore concentrations in sediments become lower because of being dispersed throughout a wider area. The organic material in this larger area is also more refractory due to the degradation processes undergone during transport and deposition processes. The tide circulation also transports upstream refractory organic matter from deeper canyon areas, which may dilute the lability of the bulk organic matter in surface sediments to slope levels.

The higher organic matter contents in the Nazaré canyon and less refractory material in the upper regions indicated higher availability of food for the benthic fauna in this region. However, it appeared that the meiobenthos was unable to fully exploit the food resources in the canyon. This seemed specially the case of the upper canyon area. The metazoan meiofauna was not necessarily more abundant in the canyon than on the adjacent open slope. In the upper canyon region only station S26 at 1000 m depth markedly had the highest abundances of metazoans. The nematode biomass mimicked the pattern observed for the abundances; also recording station S26 the highest biomass. Foraminifera numbers in the canyon were very low when compared to the numbers obtained at the adjacent open slope. The meiobenthos at the open slope was as abundant as the meiobenthos in the canyon, or more, but with less abundant food resources. The local high-velocity bottom currents and unstable sedimentary conditions in the Nazaré canyon may hinder the settlement of abundant and diverse meiobenthic communities. The low diversity values obtained for the nematode assemblages in the upper and middle canyon region, the patchy distribution of the meiofauna abundance and the dominance of two very opportunistic nematode genera (*Sabatieria* sp. and *Metalinhomoeus* sp.) able to withstand great sedimentary disturbance, high organic loads and suboxic conditions may

indicate the Nazaré canyon meiobenthos is under permanent re-colonization process of a disturbed sedimentary habitat.

Different oceanography and sedimentary biogeochemical characteristics in the Nazaré and Cap de Creus submarine canyons

An important driver determining the biogeochemistry in submarine canyon sediments seems to be the oceanography of the surrounding continental margin. The Western Iberian Margin and the Gulf of Lions are characterized by oceanographically different regimes, and the respective Nazaré and Cap de Creus canyons and adjacent open slopes show different biogeochemical sedimentary characteristics. In the Cap de Creus canyon the transport of sedimentary material is triggered by the convergence of the shelf cyclonic circulation of water and the Liguro-Provençal current that cause downwelling of shelf water down-canyon and along the slope. Fine-grained sediment and organic matter may be also spread out evenly over the canyon and adjacent slope by nepheloid layers, without much focusing of deposition in the canyon due to the low primary productivity and lack of tidal transport mechanism. Seasonally, dense shelf water cascading events intensify the downwelling of shelf water along the canyon and slope, that when are large events erode away the canyon sediments. This oceanographic regime explains well the very low and homogenous organic contents and phytodetritus labilities, low organic matter background concentrations, depositions and bioturbation rates in the Cap de Creus canyon. Differently, the tidal circulation of water and the formation of dense nepheloid layers trigger the transport of organic sedimentary material in the Nazaré canyon. The tide driven currents resuspend and deposit sedimentary material in the canyon, and also transport it up and down canyon with the rise and ebb tide, with a net down canyon transport. This oceanographic regime in the Nazaré canyon coupled with the prevailing upwelling regime in the area producing high primary productivities explains well the higher organic matter depositions, higher organic matter contents, background concentrations, and the mixed nature of the sediments

due to sporadic turbidity flows. In addition, in continental slopes and submarine canyons, the chl *a* decay rate as given in Sun et al. (1993) can be used in most of the cases in order to obtain chl *a* depositions and bioturbation rates, using the general diagenetic equation.

PERSPECTIVES

These thesis investigations have contributed to the better understanding of the biogeochemistry, benthic meiofauna and ecological drivers in submarine canyon compared to adjacent open slopes. However, submarine canyons are far too large and complex environments to make generalizations from the data presented here. At present, the meiofauna and organic matter data presented for the Nazaré canyon indicate that despite the high availability of food, the benthic fauna in the canyon is not extremely abundant and is dominated by only few very opportunistic species able to withstand high levels of persistent sediment disturbance. Previous studies on the macrofauna of the canyon also found dominance of very opportunistic macrofaunal species. Therefore, the Nazaré canyon does not seem to be important in terms of biodiversity. Probably the same could be told for the Cap de Creus canyon. The comparatively lower organic matter concentration in the Cap de Creus canyon sediments, and the generally low labilities, indicate the food availability is low. Accordingly, the meiofauna from this canyon is hypothesised to have low abundances and probably also be dominated by only few opportunistic species. The Cap de Creus canyon sediments also may be highly disturbed due to the recurring influence of the dense shelf water cascading. Studies addressing these issues will help to better understand the importance of submarine canyons in terms of biodiversity. Recent camera surveys on the Nazaré canyon have revealed the presence of filter feeding fauna on the walls, and the shallow areas of the Cap de Creus canyon are known to harbour communities of soft and hard corals. Hence, it might well be

that in terms of biodiversity canyon walls are more important, and should be better studied.

This thesis presents biogeochemical and benthic faunal community data in submarine canyons and adjacent slopes during springtime only. Therefore, conducting surveys during summer, autumn and winter would be highly recommended to enlarge our knowledge about seasonal patterns in these environments. The patchiness in faunal distributions and biogeochemical characteristics should also be addressed. Seasonal data and information in how patchy the biologic variables measured in such environments can be would allow making firmer statements about its functioning. Ideally, a grid of stations covering, at best, the full bathymetry along and across these canyons with key stations being repeatedly sampled over time would help to gain this knowledge. However, this is a difficult task in such large environments of difficult access, and can only be achieved improving our cooperation with other researcher.

The subject of food availability is complex to address, as food availability is intrinsic to the capacity of a given organism to digest the food available in the environment. Statistically correlating organic matter quality proxies to faunal abundances and compositions can give valuable information on ecosystem functioning. However, all the other possible factors exerting a control on faunal communities have to be taken into account because they may influence the statistical correlations. If the subject of food availability in deep sea wants to be fully address, experiments must be conducted in situ, and assess, for example, how different compartments in the ecosystems use the available high or low quality organic matter. Marking high and low quality organic matter with stable isotopes and track the isotopes through the different benthic compartments is a good approach, would allow to better assess the rates at which different benthic compartments utilise the available organic carbon. This is a relatively simple experiment in shallow water environments, but becomes a challenge in deep sea due to the technological and physical barriers to overcome.

APPENDIX I

OceanLab flume calibration

Laboratory benthic flumes are experimental units that allow studying multiple natural flow dependent related processes by simulating laminar flow conditions in the laboratory. Benthic flumes have been used to study for instance, erodability of mudflats (Houwing 1999) resuspension of phytodetritus from the sea floor (Beaulieu 2003), aggregation/deposition processes (McAnally & Mehta 2002) or the interaction between organisms and the surrounding flow (Gambi et al. 1990, Willows et al. 1998, Friedrichs et al. 2000, Van Duren et al. 2006).

OCEANLAB FLUME CHARACTERISTICS

The OceanLab flume is a duplicate of the flume developed at the Friday Harbor Laboratories, University of Washington. It consists of a racetrack shaped channel made of stainless steel coated with waterproof paint to avoid corrosion (Fig. 1). The total length of the flume is 10 m, the width 76 cm and the maximum flow depth is 30 cm. The flume has a 6 m straight working area and a test section 60 cm long per 30 cm deep, filled with sand and fitted with a glass at each side of the channel for direct visual observations. The test section is situated at the end of the straight working area, at 4.6 m from the beginning of the working area. At either end of the flume, the bends have an outer diameter of 2.5 m. Within these bends the water flow is guided

through four sub channels of identical volume by partitioning walls. At the start of the working area the water passes through a honeycomb grid to assure a uniform flow pattern. The total water volume of the system is 4 m³. The water flow is generated by a conveyor belt system developed by the NIOO-CEME institute, which acts as paddle wheel and is controlled from a digital unit on the side. Adjacent to the flume there is a 6800 litres container equipped with a water filtration system where seawater is stored. Flow measurements are taken with an Acoustic Doppler Velocimeter (ADV, Nortek A. S., Bruksveien 17, N1390 Vollen, Norway). A 3D positioning system made by ISEL Automation GmbH & Co. KG allows an accurate positioning of the ADV sensor across the total width and depth of the flume and over a maximum length of 110 cm in the direction of the main flow. The flume is electronically controlled via ISEL software and the collection of the data via Collect V from Nortek. The software WinADV is used for data processing.

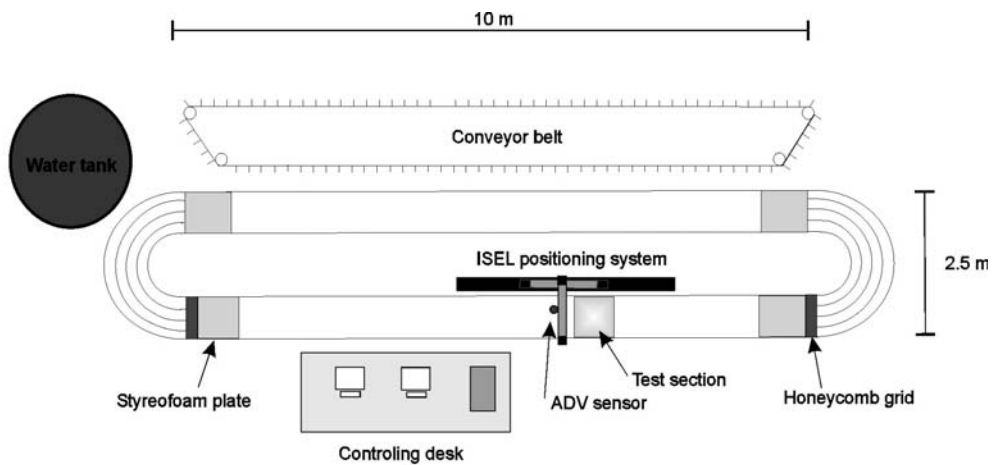


Fig. 1. The benthic flume plant at the OceanLab

HYDRAULIC CALIBRATION TEST

The relation between the conveyor belt motor settings and resulting flow speed, the response time to speed changes, three velocity profiles and the sidewall effects at three different positions in the flume channel were tested. Measurements were done with a water level of 21 cm, and when otherwise noted, measurements were always done at 38 cm from each sidewall and at a height of 11 cm above the bottom of the flume. On average the flume water temperature was 14 °C and the salinity 34 ppt. The flow speed was measured with an ADV velocimeter at a sampling frequency of 25 Hz and at each data point measurements lasted for 30 seconds. A stainless steel plate was used on the test section in order to obtain a hydrodynamically smooth surface.

Relation between belt motor settings and resulting flow speed

Water flow measurements were done some centimetres ahead the test section to avoid the influence of the edge between the flume bottom and of the covering plate on the test section. The belt motor settings were increased at 100 rpm intervals from 300 to 1000 rpm, and at 250 rpm intervals from 1000 to 3000 rpm. The relation between the conveyor belt motor settings and the flow speed measured with the ADV sensor followed a strong linear correlation (Fig. 2)($r^2 = 0,999$). Therefore, it is reliable inferring flow velocities from the conveyor belt motor settings in rpm.

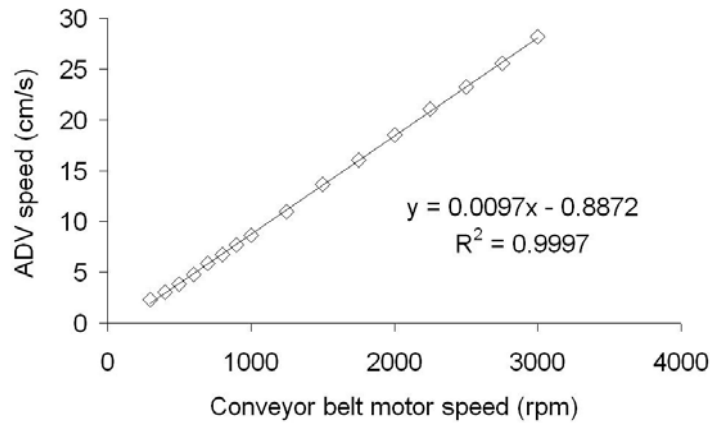


Fig. 2. Relation between belt motor and resulting flow in the centre of the flow and at 11 cm from the flume bottom with a 21 cm depth water column.

The response time to speed changes

The response time to speed changes was monitored during 20 minutes. During these time the speed was increased from 0 to 20 cm s⁻¹ during the first minute and decreased again to zero after nine more minutes. The water column in the flumes took ~2 minutes in reaching the desired speed of 20 cm s⁻¹ (Fig. 3). When the conveyor belt system creating the flow was stopped, the water column in the flume reached still conditions after 10 minutes. Therefore, when increasing flow velocities in the flume we should wait ~2 minutes to ensure the water column reached the desired velocities. When decreasing flow velocities we should wait for at least 10 minutes to ensure the flow reached a constant lower velocity.

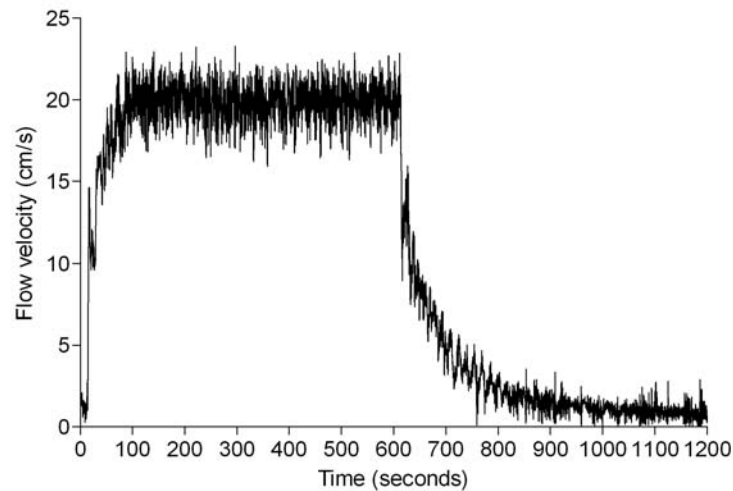


Fig. 3. The response time to speed changes in the centre of the flow at 11 cm from the flume bottom with a 21 cm depth water column.

Velocity profiles

Three vertical velocity profiles were measured at free stream velocities of 5 cm s^{-1} , 12 cm s^{-1} and 25 cm s^{-1} at three different sections of the flume working area. Vertical profiles were measured in the middle of the test section, 60 cm and 230 cm ahead the test section. Flow measurements were taken 0.2 cm apart from 0.4 to 1.8 cm, 0.4 cm apart from 1.8 to 5 cm, and 1 cm apart from 6 to 14 cm in the water column. From these profiles benthic boundary layer height, shear stress (U^*), roughness height (Z_0), turbulence intensity (TI) and Reynolds number (Re) were calculated. The boundary layer is defined as the zone in which the increase of flow speed follows a logarithmic law. Thus, the benthic boundary layer height can be determined graphically from semi-logarithmic plots of the vertical velocity profiles, with height in the logarithmic scale. In this kind of plots, the benthic boundary layer appears as a straight line. An example of the vertical velocity profiles and semi-logarithmic plots obtained for the three different free stream velocities tested in the middle of the test section are given in Fig. 4.

Appendix I

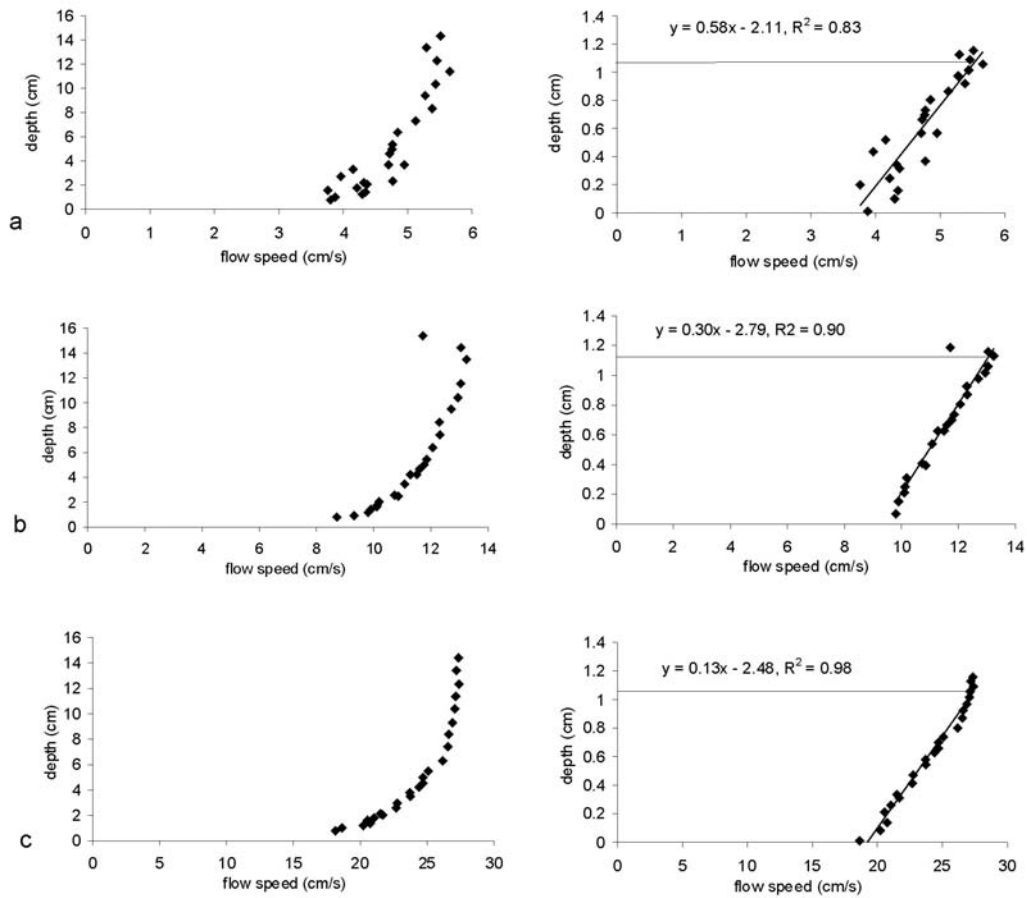


Fig. 4. Velocity profiles (left: linear scale plot, right: semi-logarithmic scale plot) measured in the middle of the test section at three different free stream velocities (a: 5 cm s^{-1} , b: 12 cm s^{-1} and c: 25 cm s^{-1}).

The heights of the boundary layer obtained at the three different free stream velocities in the three different sections of the flume working area are given in Table 1.

Table 1. Benthic boundary layer height at 5 cm s^{-1} , 12 cm s^{-1} and 25 cm s^{-1} free stream velocities, in three different sections of the flume working area.

BBL height (cm)	Free stream velocities		
	5 cm s^{-1}	12 cm s^{-1}	25 cm s^{-1}
Test Section	13.9	15.1	10.5
60 cm ahead Test Section	16.7	14	11
230 cm ahead Test Section	15.2	9.5	7.4

The heights of the boundary layer decreased with increasing flow velocities in the different sections of the flume working area. Further, at 12 cm s⁻¹ and 25 cm s⁻¹, the heights of the boundary layer rose toward the middle of the test section. However, at 5 cm s⁻¹ the height of the boundary layer in the middle of the test section was smaller than at 60 cm and 230 cm ahead of the middle of the test section. In figure 4a, it can be observed that the vertical velocity profile at 5 cm s⁻¹ was more irregular than at higher velocities. Furthermore, the vertical velocity profiles at 5 cm s⁻¹ at 60 cm and 230 cm ahead of the middle of the test section appeared more regular than in the middle of the test section (Fig. 5). The disturbance of the velocity measurements at low flow velocities might be produced by backward reflections of the water column against the flume walls before entering the bends of the flume. These disturbances are responsible for more irregular heights of the benthic boundary layer.

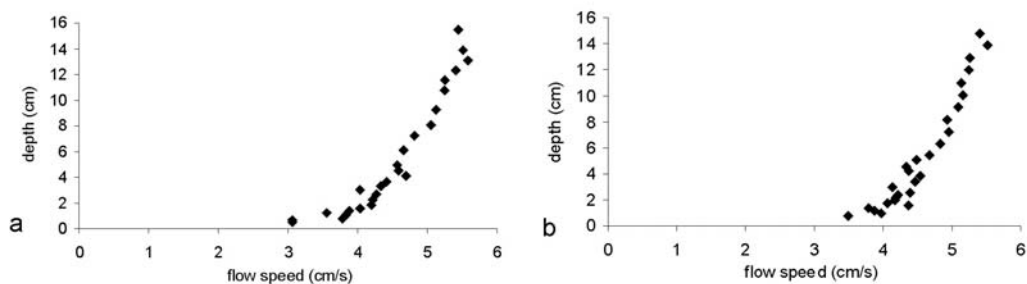


Fig. 5. Velocity profiles measured at a) 60 cm and b) 230 cm ahead the middle of the test section at 5 cm s⁻¹ free stream flow velocity.

This disturbance specially affecting the test section was minimised by installing a Styrofoam plate and a honeycomb grid before the entrance to the bend of the flume located after the test section. Styrofoam plates are used to smooth the undulations of the water surface, and honeycomb grids help to obtain a uniform flow pattern. The vertical velocity profiles measured in the middle of the test section with the Styrofoam plate and honeycomb grid showed reduced disturbance (Fig. 6) when compared with the velocity profile measured with no Styrofoam plate and honeycomb grid (Fig. 4a).

Appendix I

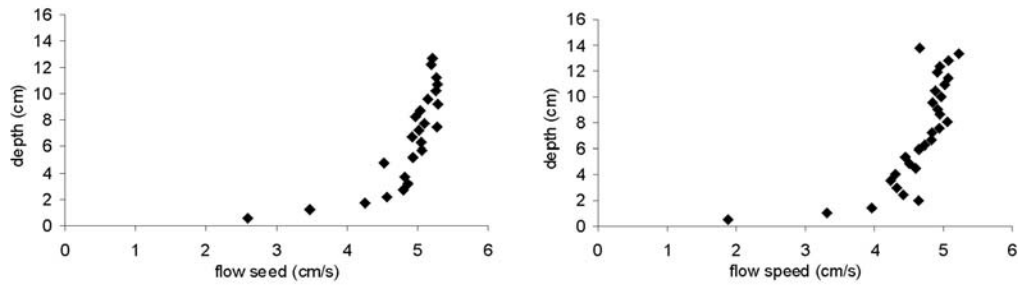


Fig. 6. Velocity profiles measured in the middle of the test section at 5 cm s⁻¹ free stream flow velocity, with a Styrofoam plate and a honeycomb grid located before the entrance of the bend of the flume to reduce disturbance.

The von Karman-Prandtl equation, as the “law of the wall”, describes the decrease of the flow velocity in a logarithmic fashion near boundaries due to friction retardation,

$$U_z = \frac{U_*}{\kappa} \ln \frac{z}{z_0}$$

where U_z is the flow speed at height z above the boundary, U_* is the shear velocity, κ is the von Karman constant ($\kappa = 0.41$), z is the height above the boundary, and z_0 is the roughness height or height at which the flow velocity is zero.

This equation was used to calculate the shear velocities produced in the different sections of the flume at the tested flow stream velocities. The heights of the benthic boundary layer (z) were derived from the semi-logarithmic plots of the vertical velocity profiles (Table 1). The roughness heights (z_0) were also derived from the same semi-logarithmic plots (Table 2).

Table 2. Roughness height at 5 cm s⁻¹, 12 cm s⁻¹ and 25 cm s⁻¹ free stream velocities, in three different sections of the flume working area.

Zo (cm)	Free stream velocities		
	5 cm s ⁻¹	12 cm s ⁻¹	25 cm s ⁻¹
Test Section	0.008	0.002	0.003
60 cm ahead Test Section	0.007	0.004	0.002
230 cm ahead Test Section	0.003	0.0001	0.00003

The shear velocities increased with increasing flow velocities (Table 3). For a given flow velocity the shear velocities did not show strong variation along the working section of the flume.

Table 3. Shear velocities created at 5 cm s⁻¹, 12 cm s⁻¹ and 25 cm s⁻¹ free stream velocities, in three different sections of the flume working area.

U*	Free stream velocities		
	5 cm s ⁻¹	12 cm s ⁻¹	25 cm s ⁻¹
Test Section	0.31	0.59	1.38
60 cm ahead Test Section	0.29	0.65	1.21
230 cm ahead Test Section	0.26	0.46	0.83

The turbulence intensity (T.I.) is a scale for the relative importance of cross-stream fluctuations. Values of T.I. = 100% would indicate that fluctuations are as strong as the main flow, which would mean a fully developed turbulent flow. As the ADV velocimeter measures the three orthogonal components of the flow vector simultaneously, the turbulence intensity can be calculated by means of a simple mathematical approach that divides the vector sum of the standard deviations by the vector sum of the average flow (modified after Gambi et al 1990).

$$T.I. = \frac{100 \times \sqrt{s_u^2 + s_v^2 + s_w^2}}{\sqrt{U^2 + V^2 + W^2}}$$

The turbulence intensity is normally calculated at 5 cm above the bottom and at 20% of the water column height (Jonsson et al. 2006).

Turbulence intensity decreased with increasing free stream velocity and had slight changes with distance from the grid (Table 4). No significant differences in turbulence intensity were observed when comparing the values at 5 cm above the bottom with the values at 20% of the water column height (Table 5).

Appendix I

Table 4. Turbulence intensity at 5 cm above the bottom, at 5 cm s⁻¹, 12 cm s⁻¹ and 25 cm s⁻¹ free stream velocities, in three different sections of the flume working area .

T.I. (%)	Free stream velocities		
	5 cm s ⁻¹	12 cm s ⁻¹	25 cm s ⁻¹
Test Section	25.8	10.3	8.8
60 cm ahead Test Section	18.2	11.9	8.7
230 cm ahead Test Section	23.2	7.9	6.1

Table 5. Turbulence intensity at 20% of the water column height, at 5 cm s⁻¹, 12 cm s⁻¹ and 25 cm s⁻¹ free stream velocities, in three different sections of the flume working area .

T.I. (%)	Free stream velocities		
	5 cm s ⁻¹	12 cm s ⁻¹	25 cm s ⁻¹
Test Section	35.2	13.2	9.4
60 cm ahead Test Section	17.0	12.3	9.0
230 cm ahead Test Section	18.7	9.0	7.0

To determine the turbulent conditions of the flow in flumes, three different Reynolds numbers can be calculated using the formula from Osborne's Reynolds work about the flow in pipes,

$$Re = \frac{\text{characteristic length} \times \text{flow speed}}{\text{kinematic viscosity of the fluid}}$$

where the unit of the characteristic length is in meters, flow speed is in m s⁻¹ and the kinematic viscosity of water is 1.047·10⁻⁶ m² s⁻¹.

When applying the flume channel width the channel Reynolds number is obtained (Re_c), where values bellow 40 indicate the flow is laminar, between 40 and 200 000 indicate it is transitional, and above 200 000 is fully turbulent (Vogel 1989). When applying the distance taken from the entrance of the straight working section until the ADV velocity sensor the local Reynolds number is obtained (Re_x), which give an idea of the turbulent conditions

within the boundary layer. Values of more than 500 000 mark the transition to turbulent flow. When applying the height of the benthic boundary layer the Reynolds number of the boundary layer is obtained (Re_δ). According to Nowell and Jumars (1987), values above 3000 (values good to a factor 5) express turbulent conditions within the boundary layer. The Reynolds number obtained for the OceanLab flume indicated that the main flow stays below turbulent conditions, with flow developing turbulent conditions at high velocities (Table 6).

Table 6. Channel Reynolds numbers (Re_c), local Reynolds number (Re_x) and Reynolds number of the benthic boundary layer (Re_δ) in the middle of the test section at 5 cm s⁻¹, 12 cm s⁻¹ and 25 cm s⁻¹ free stream velocities.

Re	Free stream velocities		
	5 cm s ⁻¹	12 cm s ⁻¹	25 cm s ⁻¹
Re_c	36 294	87 106	181 471
Re_x	214 900	515 759	1 074 499
Re_δ	6 638	1 7 307	2 5 072

Sidewalls effect

The boundary layer on the sidewalls is an intrinsic effect of a flume that does not exist in nature, and can produce unwanted artefacts on the measurements. Hence, the sidewall effect should be kept as small as possible. In order to assess the sidewall effect in the OceanLab flume, horizontal velocity profiles were measured at the free stream velocities used for the previous calibrations in the middle of the test section and 230 cm ahead the test section. Flow measurements were taken at 1 cm intervals across the width of the flume channel and at a height of 11 cm above the bottom of the flume.

The results showed that the sidewall effects at the different flow velocities tested were lower in the test section that closer to the entrance of the straight working area of the flume (Fig. 7). The wall layer in the middle of the test section appeared with less undulation than the profiles at the entrance of the straight working area.

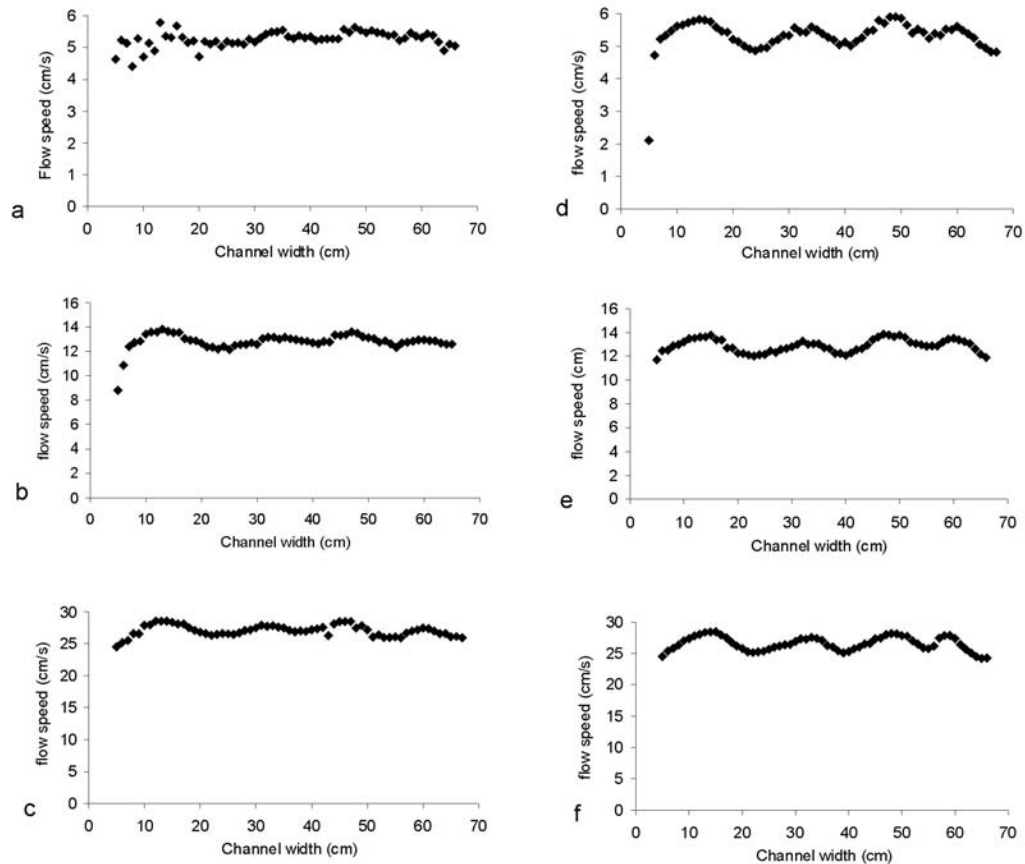


Fig. 7. The wall layer in the middle of the test section at the three stream velocities of a) 5 cm s⁻¹, b) 12 cm s⁻¹ and c) 25 cm s⁻¹, and sidewall effect at 230 cm ahead of the test section at stream velocities d) 5 cm s⁻¹, b) 12 cm s⁻¹ and c) 25 cm s⁻¹. The measurements started on the inner wall and moved towards the outside wall of the flume.

In addition, the wall layer in the test section appeared straighter in the centre of the profiles than on the edges (Fig. 7a,b,c). Therefore, to avoid possible artefacts in the measurements, experiments should be carried out closer to the centre of the flume channel than to the walls.

LITERATURE CITED

Beaulieu SE (2003) Resuspension of phytodetritus from the sea floor: A laboratory flume study. *Limnology and Oceanography* 48: 1235-1244

- Friedrichs M, Graf G, Springer B (2000). Skimming flow induced over a simulated polychaete tube lawn at low population densities. *Mar Ecol Prog Ser* 192:219-228
- Gambi MC, Nowell ARM, Jumars PA (1990). Flume observations on flow dynamics in *Zoostera marina* (eelgrass) beds. *Mar Ecol Prog Ser* 61:159-169
- Houwing EJ (1999) Determination of the critical erosion threshold of cohesive sediments on intertidal mudflats along the Dutch Wadden Sea Coast. *Estuarine Coastal and Shelf Science* 49: 545-555
- Jonsson, P.R., van Duren, L.A., Amielh, M., Asmus, R., Aspden, R.J., Daunys, D., Friedrichs, M., Friend, P.L., Olivier, F., Pope, N., Precht, E., Sauriau, P-G. and Schaaff, E. (2006) Making water flow: a comparison of the hydrodynamic characteristics of 12 different benthic biological flumes. *Aquat Ecol*, 40:409-438
- McAnally WH, Mehta AJ (2002) Significance of aggregation of fine sediment particles in their deposition. *Estuarine Coastal and Shelf Science* 54: 643-653
- Nowell ARM, Jumars PA (1987) Flumes: theoretical and experimental considerations for simulation of benthic environments. *Oceanographical Mar Biol Ann Rev* 25:91-112
- Van Duren LA, Herman PMJ, Sandee AJJ, Heip CHR (2006) Effects of mussel filtering activity on boundary layer structure *J Sea Res* 55:3-14
- Willows RI, Widdows J, Wood RG (1998) Influence of an infaunal bivalve on the erosion of an intertidal cohesive sediment: A flume and modelling study. *Limnology and Oceanography* 43: 1332-1343

Appendix I

APPENDIX II

Degradation index calculation

The degradation index (DI) is based on the distribution of the 14 commonly analysed protein amino acids in the organic matter (Dauwe and Middelburg 1998, Dauwe et al. 1999). This index summarizes into a value the subtle changes in the amino acids distribution. The index varies from -2.2 to 1.5, with sources such as phytoplankton, bacteria, and sediment trap organic matter having DI's between 1 and 1.5, which are higher than those of POM in coastal and ocean margin sediments (-0.3 to 1) and of refractory POM from pelagic deep sea sediments (<-1) (Dauwe et al. 1999).

The degradation index is calculated using the formula:

$$DI = \sum_i \left[\frac{\text{var}_i - \text{AVG var}_i}{\text{STD var}_i} \right] \cdot \text{fac.coef.}_i$$

where var_i is the original (nonstandardized) mole percentage of amino acid i , AVG var_i and STD var_i are its mean and standard deviation as given by the data set in Table 1 in Dauwe et al. (1999), and fac.coef._i the factor coefficient for amino acid i , also given in the same table in Dauwe et al (1999).

The amino acids data set used to calculate the degradation index shown in Chapter 2 is presented in Table 1 of this appendix. Only the first 14 amino acids (from Asp to Leu) in the table are used for the DI calculations.

Table 7. Protein and non-protein amino acids analysed in aggregates from sediments from the stations sampled during May 2004 along a bathymetric gradient in the Nazaré canyon and adjacent slope, and from the stations sampled along two cross sections in the Nazaré canyon during May 2005. The amino acids used to calculate the DI are the first 14 amino acids of the table.

Station	Asp	Glu	Ser	His	Gly	Thr	Arg	Ala	Tyr	Met	Val	Phe	Ile	Leu	Lys	b-ala	gaba	aba	orn
Transect along open slope May 2004																			
S39	10.71	8.68	10.19	0.00	15.18	5.96	4.72	9.33	1.72	4.07	5.81	2.64	3.14	4.55	4.87	3.14	2.43	2.58	0.29
S27	10.55	8.92	9.34	0.32	17.83	6.03	4.92	9.29	1.76	1.59	5.20	2.45	3.03	4.64	5.41	4.07	3.84	0.82	0.00
S25	9.69	7.78	8.22	0.35	18.45	6.10	4.64	8.58	1.10	1.43	5.17	3.29	2.78	4.26	4.13	5.47	4.58	3.83	0.16
Transect along Nazaré canyon May 2004																			
S41	10.22	8.77	9.86	0.68	17.17	5.98	4.26	9.74	2.25	1.68	6.07	2.96	3.21	5.76	4.27	2.21	2.08	2.40	0.43
S26	11.03	11.03	8.98	0.62	14.60	6.25	5.40	9.58	2.45	1.00	5.27	3.22	3.61	5.97	6.48	2.20	1.55	0.53	0.25
S34	10.23	7.88	9.64	0.58	18.06	6.87	4.42	9.98	2.16	1.73	5.66	2.72	3.09	4.69	5.12	3.21	2.93	0.42	0.61
S24	10.11	8.16	8.58	0.52	17.30	6.75	4.55	9.41	1.85	1.36	5.42	2.60	2.96	4.50	4.32	4.65	3.74	3.08	0.13
S22	10.62	8.23	8.51	0.11	17.89	6.21	4.85	9.38	1.22	1.85	5.41	2.18	2.59	4.24	5.18	5.70	4.28	0.93	0.65
Transect A (upper Nazaré canyon) May 2005																			
S21	10.26	8.58	9.51	0.00	16.59	6.84	6.53	10.04	1.96	1.01	6.01	3.22	3.30	5.08	5.21	2.85	0.97	2.06	0.00
S13	11.63	8.78	9.15	0.37	15.32	7.17	5.59	10.23	2.03	1.14	5.58	2.89	3.17	4.97	5.78	2.76	2.25	1.18	0.00
S07	11.42	8.54	8.88	0.07	17.81	6.93	4.34	9.99	1.94	0.61	5.42	3.41	3.01	4.78	5.67	3.66	2.33	0.97	0.23
Transect B (middle Nazaré canyon) May 2005																			
S20	9.71	8.54	8.41	0.23	18.98	6.88	4.35	9.35	1.74	0.41	5.43	2.67	3.15	4.86	5.65	3.85	2.63	2.60	0.57
S14	10.60	7.75	8.27	0.36	21.69	6.73	3.47	9.27	1.30	0.38	5.53	2.82	2.91	4.40	5.31	3.30	1.98	3.91	0.00
S15	10.89	8.42	8.40	0.08	16.55	6.79	5.48	10.01	1.95	0.82	6.09	3.40	3.32	5.10	5.83	2.72	1.97	2.00	0.21
S24*	9.44	8.79	8.42	0.52	19.97	6.49	5.27	9.83	1.63	0.46	5.27	3.11	3.29	5.13	5.17	2.82	2.07	2.32	0.00
S23	11.02	8.52	10.11	0.28	16.42	6.40	8.14	9.95	1.14	2.20	5.61	0.70	3.07	4.69	6.59	1.38	0.92	2.87	0.00

LITERATURE CITED

Dauwe B, Middelburg JJ (1998) Amino acids and hexosamines as indicators of organic matter degradation state in North Sea sediments. *Limnol Oceanogr* 43:782-798

Dauwe B, Middelburg JJ, Herman PMJ, Heip CHR (1999) Linking diagenetic alteration of amino acids and bulk organic matter reactivity. *Limnol Oceanogr* 44:1809-1814

